Key Points:
- The Arctic Ocean Freshwater System has major intra-Arctic and extra-Arctic effects
- The Arctic Ocean Freshwater System regulates and constrains physical and biogeochemical processes
- Changes in the Arctic Ocean Freshwater System are expected in the future with substantial impacts

Correspondence to:
E. C. Carmack,
carmacke@dfo-mpo.gc.ca

Freshwater and its role in the Arctic Marine System: Sources, disposition, storage, export, and physical and biogeochemical consequences in the Arctic and global oceans

E. C. Carmack[1], M. Yamamoto-Kawai[2], T. W. N. Haine[3], S. Bacon[4], B. A. Bluhm[5], C. Lique[6,7], H. Melling[1], I. V. Polyakov[8], F. Straneo[9], M.-L. Timmermans[10], and W. J. Williams[1]

[1]Fisheries and Oceans Canada, Sidney, British Columbia, Canada, [2]Tokyo University of Marine Science and Technology, Tokyo, Japan, [3]Earth and Planetary Sciences, The Johns Hopkins University, Baltimore, Maryland, USA, [4]National Oceanography Centre, Southampton, UK, [5]Department of Marine and Arctic Biology, UiT The Arctic University of Norway, Tromsø, Norway, [6]Department of Earth Sciences, University of Oxford, Oxford, UK, [7]Now at Laboratoire de Physique des Océans, Ifremer, Plouzané, France, [8]International Arctic Research Center, University of Alaska Fairbanks, Fairbanks, Alaska, USA, [9]Woods Hole Oceanographic Institution, Woods Hole, Massachusetts, USA, [10]Department of Geology and Geophysics, Yale University, New Haven, Connecticut, USA

Abstract The Arctic Ocean is a fundamental node in the global hydrological cycle and the ocean's thermohaline circulation. We here assess the system's key functions and processes: (1) the delivery of fresh and low-salinity waters to the Arctic Ocean by river inflow, net precipitation, distillation during the freeze/thaw cycle, and Pacific Ocean inflows; (2) the disposition (e.g., sources, pathways, and storage) of freshwater components within the Arctic Ocean; and (3) the release and export of freshwater components into the bordering convective domains of the North Atlantic. We then examine physical, chemical, or biological processes which are influenced or constrained by the local quantities and geochemical qualities of freshwater; these include stratification and vertical mixing, ocean heat flux, nutrient supply, primary production, ocean acidification, and biogeochemical cycling. Internal to the Arctic the joint effects of sea ice decline and hydrological cycle intensification have strengthened coupling between the ocean and the atmosphere (e.g., wind and ice drift stresses, solar radiation, and heat and moisture exchange), the bordering drainage basins (e.g., river discharge, sediment transport, and erosion), and terrestrial ecosystems (e.g., Arctic greening, dissolved and particulate carbon loading, and altered phenology of biotic components). External to the Arctic freshwater export acts as both a constraint to and a necessary ingredient for deep convection in the bordering subarctic gyres and thus affects the global thermohaline circulation. Geochemical fingerprints attained within the Arctic Ocean are likewise exported into the neighboring subarctic systems and beyond. Finally, we discuss observed and modeled functions and changes in this system on seasonal, annual, and decadal time scales and discuss mechanisms that link the marine system to atmospheric, terrestrial, and cryospheric systems.

1. Introduction

1.1. Rationale

The cycling of freshwater through Earth's atmospheric, terrestrial, and oceanic components is a central element in climate and life systems, of which the Arctic is a major player. Currently, the Arctic Ocean is freshening [*Proshutinsky et al.*, 2009; *McPhee et al.*, 2009; *Rabe et al.*, 2011; *Haine et al.*, 2015], warming [*Polyakov et al.*, 2005, 2012; *McLaughlin et al.*, 2009], losing sea ice [*Kwok et al.*, 2009; *Stroeve et al.*, 2012a, 2012b; *Cavalieri and Parkinson*, 2012; *Comiso*, 2012], and its ice cover is changing properties and moving faster [*Barber et al.*, 2009; *Rampal et al.*, 2009, 2011; *Kwok et al.*, 2013; *McPhee*, 2013]. Internal to the Arctic Ocean the distribution and spreading pathways of stored freshwater (FW) are shifting on a variety of time scales from annual to multidecadal [*McPhee et al.*, 2009; *Timmermans et al.*, 2011; *Morison et al.*, 2012; *Giles et al.*, 2012; *Mauritzen*, 2012; *Proshutinsky et al.*, 2015]. External to the Arctic Ocean the exchanges of heat, salt, and biogeochemical properties with the bordering subarctic oceans are undergoing substantial change [*Curry and Maurizen*, 2005; *Carmack and McLaughlin*, 2011; *Beszczynska-Möller et al.*, 2011; *Woodgate et al.*, 2012], and as the physical attributes of the Arctic FW System undergo change so do its geochemical [*Yamamoto-Kawai et al.*, 2009, 2013; *McLaughlin and Carmack*, 2010] and biological [*Pabi et al.*, 2008; *Arrigo and van Dijken*, 2011; *Li et al.*, 2009; *Tremblay and Gagnon*, 2009; *Petrenko et al.*, 2013] components. Linkages and feedbacks then create strong
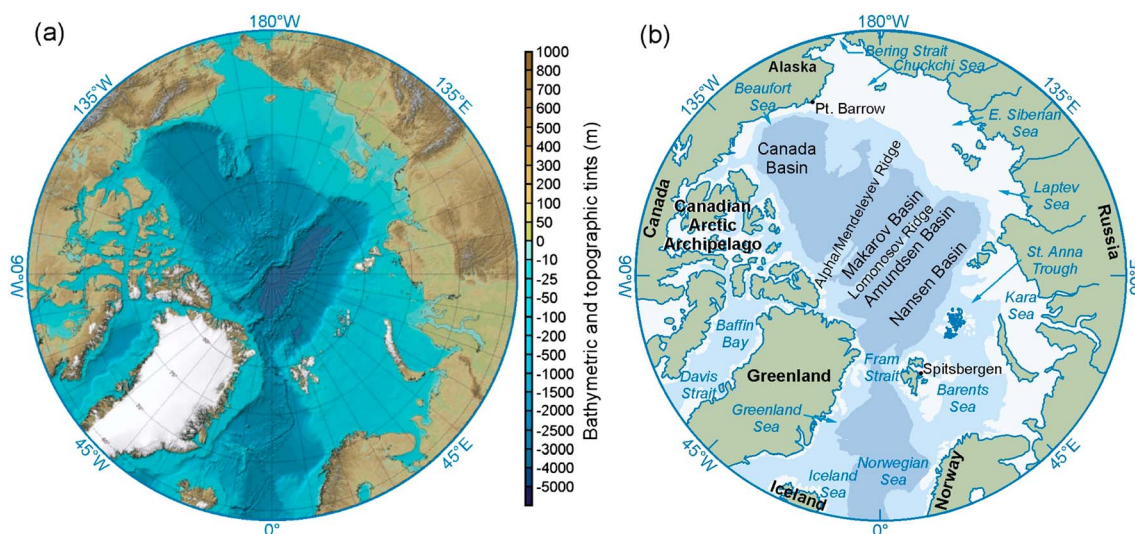
Figure 1. Maps showing (a) bathymetry of the Arctic Ocean from the International Bathymetric Chart of the Arctic Ocean [*Jakobsson et al.*, 2012] and (b) place names of the major basins, ridges, shelf seas, and gateway straits.

two-way ties among the Arctic Ocean and atmospheric and terrestrial components of the system [*White et al.*, 2007; *Francis et al.*, 2009; *Vösömarty et al.*, 2011; *Bhatt et al.*, 2014]. The rate at which such changes within individual systems are occurring is further accelerated by cross-system a class of processes termed Arctic amplification [*Serreze and Francis*, 2006; *Bekryaev et al.*, 2010; *Serreze et al.*, 2009; *Serreze and Barry*, 2011; *Barnes*, 2013; *Alexeev and Jackson*, 2013]. The rapid cascading of linkages through multiple system components in recent years has led to the dramatic but observationally correct term "New Arctic" [*Jeffries et al.*, 2013; *Wood et al.*, 2013] and the possibility of new trajectories within the Arctic system [*Overpeck et al.*, 2005; *Francis et al.*, 2009; *Wassmann and Lenton*, 2012; *Hinzman et al.*, 2013]. And essential to all, the above is evidence of an accelerating hydrological cycle, both globally [*Huntington*, 2006; *Milliman et al.*, 2008; *Durack and Wijffels*, 2010; *Syed et al.*, 2010] and within the Arctic [*Peterson et al.*, 2006; *McClelland et al.*, 2006; *Déry et al.*, 2009]; indeed, the acceleration of the Arctic hydrological cycle in the twentieth century is without precedence in the Holocene [*Wagner et al.*, 2011].

1.2. Role in Regulating Physical Processes

In contrast to the Southern Hemisphere, the configuration of continents in the Northern Hemisphere is such that they capture moisture from the atmospheric Westerlies and redirect in north flowing drainage basins disproportionate quantities of freshwater (FW) into the Mediterranean configuration of the Arctic Ocean (Figure 1) [*Aagaard et al.*, 1985; *Bring et al.*, 2016; *Vihma et al.*, 2016]. Hence, while the Arctic Ocean is only 1% and 3% of the global ocean in terms of volume and surface area, it collects over 11% of the global river discharge [*Gleick*, 2000; *Dai and Trenberth*, 2002]. The resulting salt stratification (e.g., a freshened upper ocean and salinity increasing with depth) is a dominant characteristic of high-latitude seas in general and the Arctic Ocean in particular [*Aagaard et al.*, 1981; *Carmack*, 2007]. A fundamental fact is that in the deep ocean, sea ice can only form over oceans where a permanent halocline limits deep, thermally driven convection [*Bulgakov*, 1962]. As such, salt stratification plays an indirect but key role in determining the planetary albedo and ice/albedo feedback effects [*Aagaard and Carmack*, 1994]. As well, salt stratification constrains the upward diffusive flux of heat from the underlying and warmer inflows from the Atlantic and Pacific Oceans, thus also allowing persistence of ice cover [*Polyakov et al.*, 2013b; *Carmack et al.*, 2015a]. But the distribution of FW within the Arctic Ocean is not uniform, with salinities ranging from about 35 where the Atlantic water enters the basin to near 0 near river mouths and along the coast [*Carmack et al.*, 2015b]. This huge range of salinity, the main parameter that determines seawater density at high latitudes, affects almost every aspect of circulation and mixing within the Arctic Ocean and yet remains poorly understood and modeled [*Carmack*, 2007].

1.3. Role in Regulating Biogeochemical Processes

The FW cycle in the Arctic Ocean regulates biological and geochemical processes, and each source of FW has a different biogeochemical role. FW derived from terrestrial sources transports dissolved and particulate materials and plays a major role in setting rates of geochemical transformations in coastal regions [e.g., *Dittmar and Kattner*, 2003; *Bhatia et al.*, 2013]. Along with their freshwater anomaly and effects on stratification, Pacific origin waters (PW) advect heat and nutrients [e.g., *Codispoti et al.*, 2013] and are preconditioned for low calcium carbonate saturation state (Ω)[*Yamamoto-Kawai et al.*, 2013]. Furthermore, the PW through-flow transports excess phosphate (relative to nitrate) to the North Atlantic where it contributes to the nitrogen fixation [*Yamamoto-Kawai et al.*, 2006]. Mixing with FW decreases Ω and accelerates ocean acidification, but the local degree of acidification depends on the chemical properties of the FW source [*Yamamoto-Kawai et al.*, 2009; *Arctic Monitoring and Assessment Program* (*AMAP*), 2013]. Surface freshening suppresses the supply of nutrients from depths, decreases primary production, and changes plankton size structure in the euphotic zone [*Tremblay and Gagnon*, 2009; *Li et al.*, 2009; *McLaughlin and Carmack*, 2010]. On shelves, salt stratification obstructs bottom water from contacting with the atmosphere and results in a decrease of oxygen content, an accumulation of CO_2, and can have negative impacts on benthic communities [*Bates et al.*, 2013]. Formation of sea ice and associated brine release redistributes FW and materials from the surface to depths by convection. Drifting sea ice transports FW and sediments from shelves to deep basins [e.g., *Nürnberg et al.*, 1994]. The formation and outflow of brine-enriched shelf water also transports terrestrial and remineralized materials to intermediate and deep layers [*Guéguen et al.*, 2007; *Nakayama et al.*, 2011] and changes the residence times of these materials in the ocean, although this process has not been well quantified. Arctic outflows into the Labrador Sea and subarctic North Atlantic have clear biological consequences [cf. *Drinkwater and Harding*, 2001; *Greene and Pershing*, 2007].

1.4. Role in Terrestrial and Atmospheric Processes

The net poleward atmospheric moisture flux is largely compensated by the net oceanic export of freshened seawater and sea ice to lower latitudes. These FW exports also carry large amounts of carbon [*MacGilchrist et al.*, 2014] and nutrients [*Torres-Valdés et al.*, 2013]. When FW exports reach the subarctic Nordic Seas, they influence the surface salinity [e.g., *Haak et al.*, 2003; *Dickson et al.*, 1988] and the rate of dense water formation, with potential feedbacks on Arctic climate [e.g., *Dukhovskoy et al.*, 2004] and implications for the strength of the Atlantic meridional overturning circulation (AMOC) [e.g., *Rennermalm et al.*, 2007; *Arzel et al.*, 2007; *Jahn and Holland*, 2013; *Rahmstorf et al.*, 2015]. Through its associated transport of heat, the AMOC plays a key role for the global climate regulation [*Vellinga and Wood*, 2002] as well as for the weather in Western Europe through a strong modulation of the storm track [e.g., *Woollings et al.*, 2012]. The sea ice cover decrease in the Arctic Basin, through its feedback to the atmosphere, may also influence the position of the jet stream and storm tracks over the North American and Eurasian continents [e.g., *Deser et al.*, 2010; *Overland et al.*, 2011; *Francis and Vavrus*, 2012; *Screen et al.*, 2013; *Francis and Skific*, 2015; *Barnes and Screen*, 2015].

1.5. Objective

This paper aims to provide a synthesis on the Arctic Ocean's FW system, specifically to assess its basic sources and regulating processes, to discuss the importance of variability and regionality, to examine the consequences of salt stratification and material inputs on physical and biogeochemical processes, to document recently observed and modeled changes, and to relate the above to atmospheric and terrestrial and cryospheric systems. In this synthesis no claim is made to provide a complete review of the subjects that comprise the Arctic Ocean FW system and its consequences [see, for example, *Arctic Climate Impact Assessment*, 2005] but rather to provide a perspective and framework upon which future process and cross-disciplinary investigations can be based. Throughout an effort is made to link to other components in the Arctic Freshwater Synthesis (AFS) as presented in this volume.

2. System Function, Basic State, and Key Processes

2.1. Boundaries and Regional Domains

Budget formulations require clear definitions of the regions under consideration [cf. *Prowse and Flegg*, 2000; *Prowse et al.*, 2015a, 2015b]. Following earlier work, we define the Arctic Marine System (AMS) as the pan-Arctic domain north of Bering Strait in the Pacific and Greenland-Scotland Ridge in the Atlantic (Figures 1a and 1b).
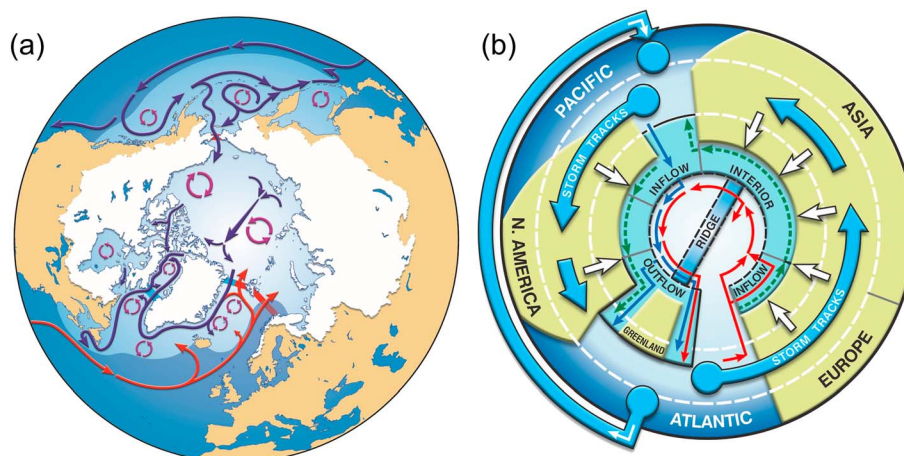
Figure 2. Schematic maps of (a) the major ocean currents (long arrows), the four Arctic Ocean gateways in Fram Strait, the Barents Sea Opening, Davis Strait, and Bering Strait (thick bars with red denoting inflow and blue denoting outflow), the gyral circulation patterns (circular arrows), the salt-stratified ocean domains are shown in light blue, and the All Arctic Regions definition of the terrestrial contributing areas shown in white and (b) summary of components of the high-latitude freshwater system as introduced in *Prowse et al.* [2015a, 2015b]. Here moisture is transported from the subtropical and tropical Atlantic Ocean to the Pacific Ocean via the Trade Winds over Central America (thick blue arrow). The subarctic front separates the thermally stratified subarctic oceans (darker blue) from the salt-stratified Northern Ocean (lighter blue) in both the Atlantic and Pacific Oceans. Moisture is transported from the Pacific and Atlantic Oceans to the Arctic catchment basins by the midlatitude (Westerlies) storm tracks (thick blue arrows), which subsequently drains into the Arctic Ocean (thick white arrows) where it spreads initially within the Riverine Coastal Domain (dashed green arrows). Warm, salty Atlantic origin waters (thin red arrows) enter the Arctic Ocean through Fram Strait (the Fram Strait Branch) and through the Barents Sea Opening (the Barents Sea Branch) and circulate within the Arctic Basins as subsurface, cyclonic, topographically steered boundary currents along the continental margin and ridge system. Internally modified Atlantic waters exit the Arctic Ocean southward through Fram Strait along eastern Greenland. Cooler and fresher Pacific origin waters (thin blue arrows) enter the Arctic Ocean through Bering Strait and exits through the Canadian Arctic Archipelago and Fram Strait along eastern Greenland. Within the Arctic Ocean a topological distinction is made between inflow, interior, and outflow shelves [cf. *Carmack and Wassmann*, 2006; *Bluhm et al.*, 2015].

We take the Norwegian, Iceland, and Greenland seas south of Fram Strait and west of the Barents Sea Opening as the Nordic Seas, and the remainder, bounded by Fram Strait, the Barents Sea Opening, Bering Strait, and Davis Strait (the so-called gateways) as the Arctic Ocean. In this classification we also recognize the subarctic Labrador and Irminger seas south of Davis Strait and later include a discussion of the role of FW inputs from more southerly watersheds, such as those that drain into Hudson Bay and the St. Lawrence Seaway and subsequently enter the subarctic North Atlantic where they may influence the convective gyres or recirculate back into the Arctic Ocean through the Fram Strait and Barents Sea Opening gateways [cf. *Isachsen et al.*, 2003]. The main ocean currents, the oceanic gateways into and out of the Arctic Ocean, and the watersheds bordering the Arctic Ocean are shown in Figure 2a, and a schematic of the AFS including atmospheric, terrestrial, and marine components is shown in Figure 2b. It is within this interconnected and salt-stratified marine system—or Northern Ocean [*Carmack*, 2007]—that FW components are supplied by river discharge from subarctic and Arctic river basins, by net precipitation over the ocean, by distillation during the freeze/thaw sea ice cycle, and by inflows of freshened waters from the Pacific Ocean.

As defined, the Arctic Ocean is a mediterranean sea that is roughly half continental shelf and half basin and ridge complex. To simplify the complicated bathymetry of the Arctic Ocean for the purposes of this paper and to link physical and morphometric properties with biological distributions and functions, we divide the Arctic Ocean into fundamental hydromorphological domains (Figure 2b) [*Carmack and Wassmann*, 2006; *Bluhm et al.*, 2015]. These are the inflow shelves (the Barents and Chukchi shelves, through which flow the incoming Atlantic and Pacific waters, respectively), the interior shelves (the Kara, Laptev, East Siberian, and Beaufort shelves, into which enter approximately 80% of the river discharge), the outflow shelves (e.g., the Canadian Arctic Archipelago (CAA) and East Greenland shelves) through which pass Arctic-modified waters back into the subarctic Atlantic, the two main basins (Eurasian and Amerasian), and the ridge and borderland features
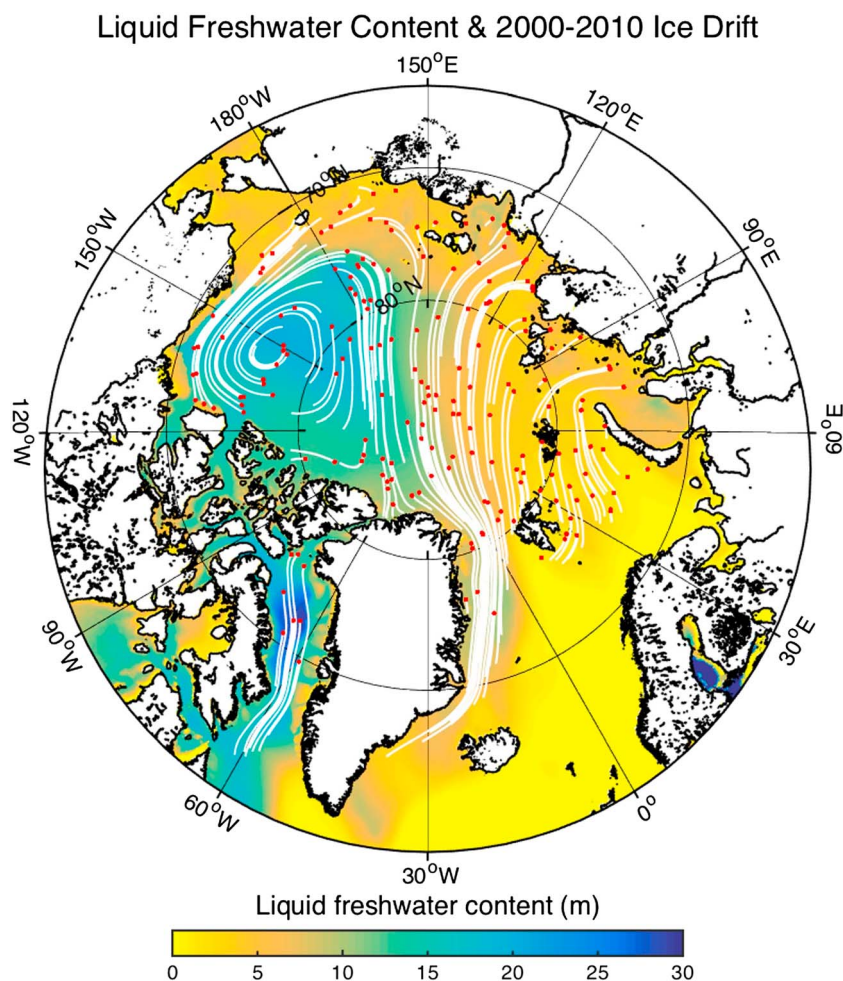
Figure 3. Liquid freshwater content (m) from the PHC (Polar Science Center Hydrographic Climatology) 3.0 climatology [*Steele et al.*, 2001] and trajectories of sea ice computed using 2000–2010 satellite ice velocities from the Polar Pathfinder Sea Ice Motion data [*Fowler et al.*, 2013]. The small red dots indicate the starting points of the trajectories, which last 2 years.

[*Jakobsson et al.*, 2012]. Liquid FW on the shelves is concentrated near coasts downstream of rivers, typically as plumes extending outward across the shelves or as narrow (1–20 km), shallow (10–20 m) surface-trapped buoyancy boundary currents, which *Carmack et al.* [2015b] term the Riverine Coastal Domain (RCD; section 2.5.6). The two main basins, Eurasian and Amerasian, are separated by the Lomonosov Ridge; the Eurasian basin is further separated into the Nansen and Amundsen basins by the Gakkel Ridge and the Amerasian Basin into the Makarov and Canada basins by the Alpha-Mendeleyev Ridge. This geomorphological distinction is critical to the understanding of FW partitioning and dynamics owing to the importance of interdomain storage and advection.

2.2. Arctic Ocean Hydrography
2.2.1. Circulation, Water Masses, and Stratification

Near-freezing surface waters, driven by winds and moving ice, form an anticyclonic circulation (Beaufort Gyre) in the Amerasian Basin and a cyclonic circulation in the Siberian Arctic which converge off Siberia to form the Trans-Polar Drift directed toward Fram Strait [*Rudels et al.*, 2012] (Figure 3). Northward of the Siberian shelves the surface flow merges with several branches coming from the marginal shelves [*Aksenov et al.*, 2011]. Below the surface cap of cold, freshwaters involved in this motion lies the halocline complex, composed largely of waters of Atlantic and Pacific origin that are modified during passage over the Barents /Siberian shelves and Bering/Chukchi shelves, respectively [*Jones and Anderson*, 1986; *Pivovarov et al.*, 2003; *Yamamoto-Kawai et al.*, 2005; *Dmitrenko et al.*, 2011, 2015; *Aksenov et al.*, 2011; *Bluhm et al.*, 2015], as well as halocline waters formed over the deep basins [*Rudels et al.*, 1996]. Halocline

stratification is much stronger in the Amerasian Basin than in the Eurasian Basin, owing to additional inputs of low-salinity water from the Pacific to Bering Strait [*Aagaard et al.*, 2006], and surface flow convergence under the atmospheric Beaufort High. Below the halocline lies the warm, intermediate depth (150–800 m) Atlantic Water (AW), in which salinities increase to ~34.8 practical salinity unit (psu) [e.g., *Pfirman et al.*, 1994; *Schauer et al.*, 2008]. Stratification within the halocline—strong vertical gradients of salinity and potential density but a negligible gradient of potential temperature—impedes vertical mixing and the upward transport of heat from the ocean interior [e.g., *Aagaard et al.*, 1981; *Rudels et al.*, 1996].

Below the halocline complex the general circulation of the underlying Atlantic layer is dominated by narrow, topographically steered, pan-Arctic boundary currents along the continental slope and mid-ocean ridges, forming cyclonic gyres within the deep basins [e.g., *Aagaard*, 1989; *Rudels et al.*, 1994]. These waters are supplied to the Eurasian continental slope by two branches of the pan-Arctic boundary current. One branch enters the Eurasian Basin through Fram Strait. The second branch flows into the Barents Sea and enters the Arctic Ocean through the St. Anna Trough, a ~600 m deep trench in the northern Kara Sea [*Dmitrenko et al.*, 2015]. North of the Kara Sea, the warmer Fram Strait branch and colder Barents Sea branch converge and continue eastward along the Eurasian slope as two separate flows. After passing the Laptev Sea slope, the boundary current bifurcates into branches over the Lomonosov Ridge and along the Eurasian slope [*Woodgate et al.*, 2001]. Part of the AW flow continues into the Makarov Basin, while another branch continues along the Lomonosov Ridge toward Fram Strait. Limited mooring observations in the eastern Eurasian Basin suggest that halocline and Atlantic waters circulate roughly in the same direction there [*Pnyushkov et al.*, 2015]. Enhanced inflow of AW heat was observed in the 2000s, resulting in an exceptionally warm AW layer with no precedent since the 1950s [*Polyakov et al.*, 2013a]; moreover, based on paleoclimate evidence, *Spielhagen et al.* [2011] concluded that the early 21st century AW temperatures are unprecedented over the past 2000 years. It has been put forward that this relates to sea ice losses of recent declines, which appear to be unprecedented over the past 1450 years [*Kinnard et al.*, 2011].

Pacific Water (PW) enters the Arctic Ocean through Bering Strait, crosses the Chukchi Sea and spreads into the deep basin, in the depth range of 60–220 m [*Watanabe and Hasumi*, 2009; *Steele et al.*, 2004]. There is a tendency for this water to flow as a cyclonic boundary current. Indeed, observations of near-slope circulation in the Canada Basin demonstrate the presence of a narrow (~20 km) boundary current transporting AW and PW into the Beaufort Sea; see, for example, *von Appen and Pickart* [2012] for details. However, the overlying anticyclonic Beaufort Gyre and the generation of mesoscale eddies off Point Barrow act to weaken this boundary current and move PW into the interior halocline of the Canada Basin [*Pickart et al.*, 2005]. Further, Ekman convergence where PW outcrops the surface in the Chukchi Sea drives subduction of PW into the interior Beaufort Gyre, where PW is swept along geostrophic contours [*Timmermans et al.*, 2014]. As such, the influence of Pacific inflow is mostly confined to the Amerasian Basin [*Bluhm et al.*, 2015]. The frontal boundary between AW and PW is an important element of water column structure and freshwater storage (section 2.5.3) [e.g., *McLaughlin et al.*, 1996]; it is roughly aligned with the Trans-Polar Drift although its position changes with time [*Steele and Boyd*, 1998; *Alkire et al.*, 2007; W. J. Williams et al., The shifting Atlantic/Pacific Halocline Front of the Arctic Ocean: Observations from Ice Camps and Trans-Arctic cruises, *Geophys Research Letters*, manuscript in preparation, 2015].

2.2.2. Stratification as a Barrier to Vertical Heat Flux and Ice Melt

FW cycled through the Arctic Ocean keeps Arctic surface salinities low relative to waters entering from the Pacific and Atlantic Oceans. Low surface salinities cause the inflows to subduct on entering the Arctic and interflow at depths largely determined mainly by their salinity. The result is a layered halocline with strength and thickness lowest in the Eurasian Basin where AW enters and greatest in the Amerasian Basin. Arctic surface water at western longitudes is underlain sequentially by Alaskan Coastal Water, Pacific Summer Water, and Pacific Winter Water in addition to the layers of Barents Cold Halocline Water and Atlantic Water found at east longitudes [e.g., *Rudels et al.*, 1991]. Warm intrusive AW resides at 150–800 m depth throughout the Arctic, whereas warm PW at 60–220 m depth is generally confined to west longitudes [*Carmack et al.*, 1997]. Local insolation in summer creates additional thermal stratification by warming thin surface and subsurface layers over ice-free areas which may affect the seasonal freeze/melt cycle [*Jackson et al.*, 2010, 2012].

Any upward flux of heat to the surface from the warm subsurface water has the potential to reduce the growth of sea ice. The only viable mechanism to drive such flux over much of the Arctic Ocean is turbulent diffusion, which is driven by kinetic energy extracted from shear in velocity and suppressed by the stable

Table 1. Freshwater Budgets for the Arctic Ocean From Selected Published Sources[a]

Source	Aagaard and Carmack [1989]	Serreze et al. [2006]	Haine et al. [2015]	Haine et al. [2015]
Period	Prior to 1989	~1979–2001	1980–2000	2000–2010
Reservoirs (km^3)				
Liquid freshwater	80,000	74,000 ± 7,400	93,000	101,000
Sea ice	17,300	10,000	17,800	14,300
Total freshwater	97,300	84,000	110,800	115,300
Fluxes ($km^3 yr^{-1}$)				
Runoff	3,300	3,200 ± 110	3,900 ± 390	4,200 ± 420
P-E	900	2,000 ± 200	2,000 ± 200	2,200 ± 220
Bering Strait (total)	1,670	2,500 ± 300	2,540? ± 300	2,640 ± 100
Fram Strait liquid	−980	−2,700 ± 530	−2,700 ± 530	−2,800 ± 420
Fram Strait ice	−2,790	−2,300 ± 340	−2,300 ± 340	−1,900 ± 280
Davis Strait (total)	−920	−3,380 ± 320	−3,360 ± 320?	−3,220 ± 190
Miscellaneous	−290	−90 ± 90	40 ± 90?	80 ± 90?
Total inflow	6,120	7,950 ± 400	8,800 ± 530?	9,400 ± 490
Total outflow	−5,520	−8,720 ± 700	−8,700 ± 700	−8,250 ± 550
Residual	890	−770 ± 800	100 ± 900?	1,200 ± 730

[a]Positive fluxes indicate freshwater sources to the Arctic Ocean. Miscellaneous fluxes include Barents Sea Opening, Fury and Hecla Straits, and the freshwater flux from Greenland. They are included separately in the total inflow and outflow fluxes, where possible. Aagaard and Carmack [1989] and Serreze et al. [2006] consider the Arctic Ocean to exclude the CAA and Baffin Bay, whereas Haine et al. [2015] include them. The Fram Strait liquid flux includes the East Greenland Current, the deep outflow, and the West Spitsbergen Current. Uncertainties (on the mean values) are given where available. In the above table P is precipitation and E is evaporation.

vertical gradient of density [McPhee, 2008]. Observations reveal that the diapycnal heat flux through the Arctic halocline varies locally but generally is very weak [e.g., Toole et al., 2010; Rainville et al., 2011], at most a few watts per square meters [Carmack et al., 2015a]. Indeed, only 1 W/m^2 is required to explain the observed ice loss [Kwok and Untersteiner, 2011].

However, the combined influence of wind and steep seafloor topography does force warm water from both Pacific and Atlantic intrusions upward onto the continental shelves at some locations along the Arctic perimeter [Carmack and Kulikov, 1998; Williams et al., 2008; Pickart et al., 2009; Williams and Carmack, 2014]. This upwelling can bring heat from several hundred meters depth into close proximity with growing or preexisting sea ice; tides can achieve the same result where currents are strong. Ocean influence in the range of 5–15 W m^{-2} is commonly determined in such areas [cf. Rippeth et al., 2015], and much larger values occur from time to time in dynamic environments such as the North Water Polynya situated north of Baffin Bay [Melling et al., 2001].

2.3. Freshwater Sources and Delivery to the Arctic Ocean

Conceptually, the atmospheric convergence of water over the Arctic is the starting point to consider the Arctic Ocean FW budget and is the main driver of variability in it. FW components enter the Arctic Ocean as net precipitation, as river discharge drawn from the large subarctic and Arctic drainage basins, and as the estuarine component of the Pacific inflow through Bering Strait [Aagaard and Carmack, 1989]. Additional distillation by the seasonal ice cycle of freezing and thawing, accompanied by disproportionate transport of solid and liquid components (including shelf-basin interaction), contributes to the separation of fresh and saline components. Various budget calculations for full-system inflow, storage, and outflow have been published by Aagaard and Carmack [1989], Carmack [2000], Serreze et al. [2006], Dickson et al. [2008], and Haine et al. [2015] and are summarized in Table 1. Overall, a balance is (nearly) reached between these different fluxes whereby the FW added from the atmosphere and land drains as liquid FW and sea ice to the Atlantic Ocean.

For the purpose of budget calculations the above groupings of FW distinction rely on the practical but nonrigorous concept of a FW anomaly, calculated relative to a reference salinity that is user specified (but see Appendix A). That is, FW storage and transport is quantified by the amount of zero-salinity water required to attain the observed salinity of a seawater sample starting from a given reference salinity. Most Arctic FW budget and flux calculations follow the original suggestion of Aagaard and Carmack [1989] and use 34.8 as

the reference salinity, which is roughly the mean salinity of the Arctic Ocean. This concept has both positive and negative attributes (see Appendix A, *Carmack et al.* [2008], *Tsubouchi et al.* [2012], and *Bacon et al.* [2015] for discussions).

Discharge from land, as FW in rivers and streams and as groundwater, amounts to $4200 \pm 420\,\text{km}^3\,\text{yr}^{-1}$ (from data representing the period 2000–2010, with the uncertainty on the mean quoted) [*Haine et al.*, 2015]. This estimate is dominated by large rivers, mainly on the Eurasian side. For example, the total discharge from the six largest Eurasian rivers (Northern Dvina, Pechora, Ob, Yenisey, Lena, and Kolyma) is estimated to have been $1813\,\text{km}^3\,\text{yr}^{-1}$ in 2010 [*Shiklomanov and Lammers*, 2011]. The drainage area that is covered by gauged rivers accounts for 61–81% of the total area draining into the Arctic Ocean (excluding the CAA) [*Serreze et al.*, 2006]. Therefore, about a third of the FW discharge from land to the Arctic Ocean is not directly measured. Moreover, observations from those rivers that are gauged are not available in real time [*Shiklomanov and Lammers*, 2011]. Further, as noted in *Prowse et al.* [2015a, 2015b], the largest rivers entering the Arctic Ocean derive from drainage systems originating in the midlatitudes, with hydrologic characteristics distinct from true (albeit smaller) Arctic rivers. These factors lead to substantial uncertainty in the total flux of FW from land to the Arctic Ocean.

PW inflow through Bering Strait is the second main source of FW to the Arctic Ocean. It supplies, relative to a reference salinity of 34.8 psu, $2640 \pm 100\,\text{km}^3\,\text{yr}^{-1}$ (the average for 2000–2010) [*Woodgate et al.*, 2006; *Haine et al.*, 2015]. This flow is forced by the steric height difference between the Pacific and Arctic Oceans (~0.7 m) and includes contributions from additional rivers entering the Bering Sea [*Stigebrandt*, 1981; *Aagaard et al.*, 2006]. This inflow is about 95% liquid FW, the remainder being sea ice exported from the Bering Sea. Bering Strait inflow is relatively well monitored with oceanographic moorings since 1998.

Precipitation minus evaporation is the third major net source of FW to the Arctic Ocean, delivering about $2200 \pm 220\,\text{km}^3\,\text{yr}^{-1}$ (for 2000–2010) [from *Haine et al.*, 2015; also see *Vihma et al.*, 2016]. This net exchange with the atmosphere is the difference between precipitation (as liquid water and ice), which is about five thirds of the net flux, and evaporation, which is about two thirds of the net flux [*Serreze et al.*, 2006]. In other words, about 40% of precipitation is recycled water from the Arctic Ocean, rather than imported by the atmosphere. The main challenge in estimating precipitation minus evaporation is to estimate precipitation accurately. Measuring Arctic precipitation is difficult, especially frozen precipitation over the ocean, and estimating precipitation from atmospheric reanalysis products is also hard because among other reasons, reanalysis models do not conserve water during their data assimilation process (see *Lindsay et al.* [2014] for a comparison of Arctic atmospheric reanalyses).

In addition to the primary sources of FW to the Arctic Ocean, sources considered minor today may gain in quantity and biogeochemical importance in the future; these include glacial melt, thawing permafrost, and groundwater discharges. Also, the discharge of FW into the adjacent subarctic North Atlantic by large rivers south of the conventional Arctic Ocean gateways must be taken into account, as it is in these seas that deep convection occurs. These issues are discussed in section 2.6 below.

2.4. Freshwater Storage, Redistribution, and Release

The upper layers of the Arctic Ocean are formed from the sources of FW described in section 2.3. Relative to a salinity of 34.8 about 101,000 km³ of FW is stored in this fresh lens (this is an estimate of the 2000–2010 annual average volume by *Haine et al.* [2015]. The distribution of liquid FW is not uniform, however, across the Arctic. Instead, most FW exists in the Amerasian Basin, and specifically in the Beaufort Gyre above the Canada Basin, where about 23,500 km³ FW are stored, and the accumulated FW anomaly diluting the upper ocean above the 34.8 isohaline surface is about 20 m thick [*Haine et al.*, 2015]. In the Eurasian Basin, typical liquid FW thicknesses are 5–10 m. This pattern of liquid FW storage reflects the dominant surface circulation (section 2.2 and Figure 3): Eurasian Basin surface water flows toward the Trans-Polar Drift and hence leaves via Fram Strait. In contrast, Amerasian Basin surface water circulates anticyclonically in the Beaufort Gyre leaking into the Trans-Polar Drift, or the CAA, at the edges. The Beaufort Gyre is driven by the Beaufort high in atmospheric pressure [*Serreze and Barrett*, 2011] and the associated anticyclonic surface winds (*Vihma et al.*, 2016). Collectively, the Beaufort Sea High, the Beaufort Gyre, and the associated deep layer of liquid FW comprise the so-called "dynamical pole" in the ocean/atmosphere system, which is displaced from the geographic North Pole due to asymmetry in the continental topography and ocean bathymetry.

FW in the solid phase, as sea ice (frozen sea water) is another important reservoir in the Arctic [see *Krishfield et al.*, 2014]. There are about 14,300 km^3 FW stored in sea ice (2000–2010 average from *Haine et al.* [2015]). Sea ice has an average salinity of about 4 [*Aagaard and Carmack*, 1989] and a smaller density than FW, so the corresponding volume of sea ice is about 26% larger. As with liquid FW, the sea ice is not distributed uniformly over the Arctic Ocean. The largest sea ice volumes are north of the CAA and Greenland and across the pole, where the ice is still thick and old [e.g., *Kwok et al.*, 2009].

The seasonal freeze-thaw cycle acts to exchange FW between the liquid and solid phases. Its amplitude is about 13,400 km^3 (averaged over the decade of the 2000s) [*Haine et al.*, 2015], close to the annual average FW volume stored in sea ice. Under current conditions only about 35% of the sea ice present at the end of winter, when the ice volume peaks, survives the summer to become multiyear ice. Of the remaining 65%, the great majority melts within the Arctic, although some is exported to the south, mainly through Fram Strait (see below). Like liquid FW, sea ice is redistributed within the Arctic. Sea ice moves under the influence of wind, the surface ocean current, and responds to internal dynamic stresses within the pack. Sea ice formation in winter occurs throughout the Arctic Ocean, but the prevailing currents tend to export ice frozen over the Eurasian shelves toward the central Arctic and the Trans-Polar Drift (Figure 3).

Arctic FW is released to lower latitudes via two marine export pathways. First, and largest, is the pathway east of Greenland through Fram Strait. Oceanographic moorings, ocean models, and satellite observations are used to estimate the flux of liquid and solid FW through this gateway. The 2000–2010 average estimates are 2800 ± 420 km^3 yr^{-1} as liquid and 1900 ± 280 km^3 yr^{-1} as ice [*Haine et al.*, 2015]. These fluxes drain the central Arctic Ocean via the Trans-Polar Drift. The second pathway is through Davis Strait which carries about 2900 ± 190 km^3 yr^{-1} as liquid FW and $320 \pm$ km^3 yr^{-1} as ice, respectively [*Curry et al.*, 2011, 2015]. These estimates are based on oceanographic measurements that span the period 2004–2010. The Davis Strait fluxes [*Curry et al.*, 2011, 2015] include almost all of the flow through the CAA; the flux through Fury and Hecla Straits which enters the North Atlantic via Hudson Strait is only about 200 km^3 yr^{-1}. In sum, about 5700 ± 460 km^3 yr^{-1} leaves the Arctic Ocean as liquid FW, split evenly between Fram and Davis Straits. In sea ice, about 2200 ± 280 km^{3}yr^{-1} FW leaves, with 85% passing through Fram Strait. From the total average volume in liquid and ice (115,300 km^3, see above), we infer a *bulk* FW residence time of about 14 years (recognizing that in reality, a broad range of residence times exist). Although 88% of Arctic FW is in liquid form, only about 73% leaves in that phase; as such, export as ice is disproportionately important.

The sources, sinks, and storage reservoirs for FW in the Arctic Ocean are summarized in Figure 4. The period discussed here is the decade of the 2000s (Figure 4, middle); see section 3 for estimates of past FW reservoir volumes and fluxes (Figure 4 (left); nominally for the period 1980–2000). For the 2000s, the total inflow FW sources sum to 9000 ± 490 km^3 yr^{-1} and the total outflow sinks sum to -8250 ± 550 km^3 yr^{-1} meaning that there was a net freshening of the Arctic Ocean at about 1200 ± 730 km^3 yr^{-1} for the decade of the 2000s [*Haine et al.*, 2015]. This freshening estimate is (marginally) greater than the associated uncertainty indicating, for the first time, that the Arctic FW budget is not balanced over this time scale. We continue discussion of this issue in section 3.

2.5. Spatial and Temporal Disposition and Storage of Freshwater
2.5.1. Volumetric *T/S* Census by Water Mass
Volumetric θ-*S* plots (θ is potential temperature, *S* is salinity, Figure 5) show the height of water column occupied by narrow θ-*S* bins 0.1°C × 0.1 in size. Given multiyear bin average values, the histograms illustrate mean water mass constituents of the Amerasian and Eurasian basins (roughly separated by the Lomonosov Ridge) where the dominant water masses are the cold surface waters with temperatures near the freezing point ($\theta < -1.5$°C), the halocline waters of different origins, including Pacific waters, characterized by -1.5°C $< \theta < 0$°C and $S > 34$, and AW. The water mass census shows strong regional contrasts. The Eurasian Basin water mass structure, for example, is relatively simple, with near-freezing fresh surface mixed layer (SML), cold halocline layer (CHL), and warm (0–4°C) AW layer. In the Amerasian Basin the structure is far richer, with a variety of SML waters fed by river run-off, precipitation, and halocline waters formed by winter convection and by summer and winter PW mixed with shelf waters overlying AW. The two halocline structures merge near the 34.45 isohaline, below which Atlantic origin waters circulate within both basins (cf. Figure 6a and section 2.5.4).
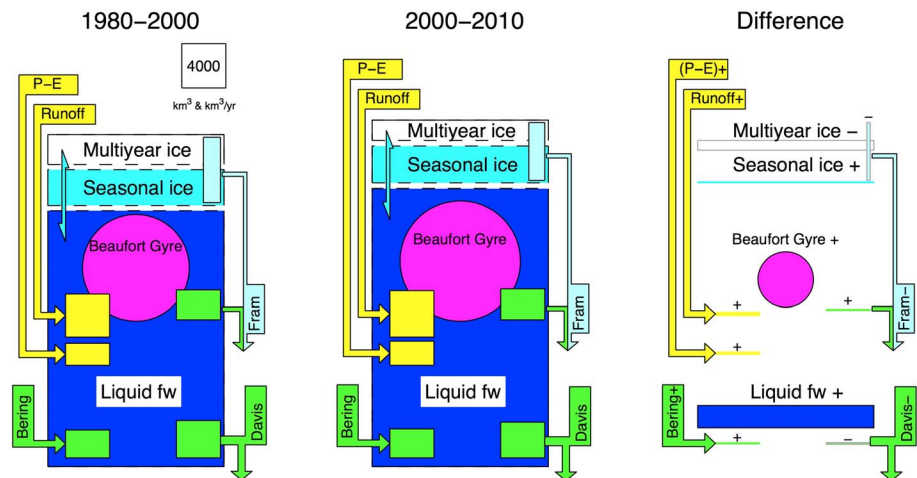
Figure 4. Schematic diagram of the freshwater (FW) budget for the Arctic Ocean. (left) The period (nominally) 1980–2000, (middle) the decade of the 2000s, and (right) the difference between them. In each diagram, the principal freshwater sources are in Figure 4 (left), namely, precipitation minus evaporation (*P-E*), runoff, and flow through Bering Strait. The principal sinks are in Figure 4 (right), namely, outflow through Davis and Fram Straits. The freshwater reservoirs are in Figure 4 (middle), split between liquid freshwater (with the Beaufort Gyre shown in the circle) and sea ice (seasonal and multiyear). The area of each shape is proportional to the corresponding freshwater flux or reservoir volume (see the white box for scale). Reprinted from Global Planetary Change, Volume 125, Thomas W. N. Haine, Beth Curry, Rüdiger Gerdes, Edmond Hansen, Michael Karcher, Craig Lee, Bert Rudels, Gunnar Spreen, Laura de Steur, Kial D. Stewart, Rebecca Woodgate, Arctic freshwater export: Status, mechanisms, and prospects, 13–35, copyright 2015, with permission from Elsevier.

2.5.2. Use of Geochemical Tracers to Identify Source Waters

The distribution of FW is neither spatially nor temporally uniform. Each source of FW has a unique geochemical composition and will thus influence different regions of the Arctic Ocean in different ways. In a changing climate each individual FW source will likely change disproportionately to one another in both volume and phenology. Distillation and export associated with the seasonal sea ice cycle will certainly change in ways that are poorly understood as will the flux and distribution of FW from net precipitation across the basin. The use of geochemical tracers is, therefore, an essential and effective way to understand spatial and temporal disposition and storage of FW in the Arctic Ocean. For example, PW can be distinguished from AW by using nutrient characteristics: dissolved inorganic nitrate/phosphate, silicate concentration, or PO_4^*
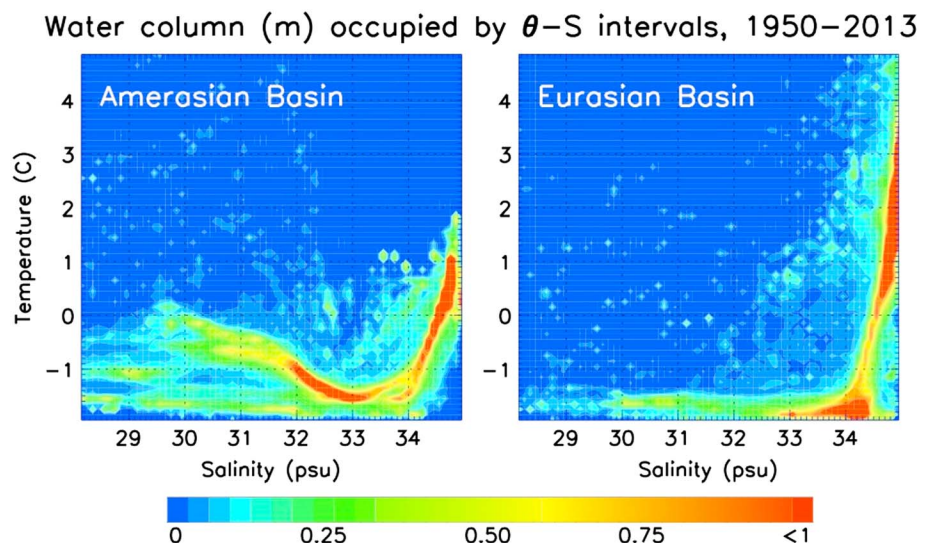

Figure 5. Volumetric θ-S plot of the data averaged over 1950–2013. The color bar shows the water mass segments (m) of water column occupied by θ-S bins in the upper 400 m within the two Arctic Ocean basins.
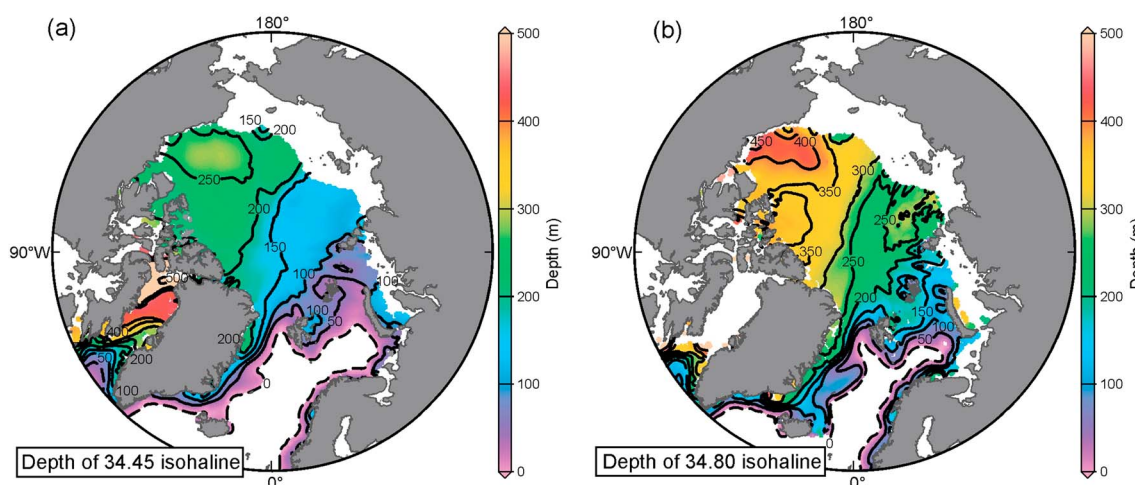
Figure 6. Maps showing (a) the depth of the 34.45 isohaline, which roughly defines the base depth of the halocline complex composed of Atlantic and Pacific origin waters, and (b) the depth of the 34.80 isohaline, which is typically used as the reference salinity for freshwater budget calculations.

[e.g., *Jones et al.*, 2003; *Ekwurzel et al.*, 2001]. Oxygen isotope ratio of water ($\delta^{18}O$) and alkalinity has been used to differentiate meteoric water (river runoff plus precipitation) from sea ice meltwater [e.g., *Macdonald et al.*, 1999; *Schlosser et al.*, 2002; *Anderson et al.*, 2004; *Yamamoto-Kawai et al.*, 2005]. Also, alkalinity and barium concentrations reflect the source of meteoric water as they are in high concentrations in North American rivers and low in Eurasian runoff and are absent in precipitation [e.g., *Yamamoto-Kawai et al.*, 2005; *Guay and Falkner*, 1997; *Guay et al.*, 2009]. A recently developed satellite observation of CDOM enabled a real-time, synoptic monitoring of river runoff spreading in open water areas [*Fichot et al.*, 2013].

From observations of these geochemical tracers, the spatial distribution of each FW source has been determined. PW spreads within the Amerasian Basin (section 2.5.3) and flows out through Fram Strait and CAA with decadal-scale variability [*McLaughlin et al.*, 2002; *Falck et al.*, 2005; W. J. Williams et al., manuscript in preparation, 2015]. PW is traceable as far south as the Grand Banks near 42°N [*Jones et al.*, 2003]. A high concentration of sea ice meltwater is found in summer surface waters of the inflow shelves (Barents and Chukchi shelves), whereas the central Arctic is the region of net ice formation [*Yamamoto-Kawai et al.*, 2005]. The Beaufort Gyre accumulates not only FW from PW, runoff, and precipitation but also salt (brine) rejected during sea ice formation on shelves surrounding the Canada Basin [*Yamamoto-Kawai et al.*, 2005]. Runoff from Eurasian rivers flows toward the Trans-Polar Drift and Fram Strait, but a significant portion also enters the Amerasian Basin [*Carmack et al.*, 2008; *Morison et al.*, 2012]. In fact, the Eurasian runoff is the major source of meteoric water found in the Canada Basin and in the Beaufort Gyre [*Carmack et al.*, 2008; *Guay et al.*, 2009]. Runoff from Mackenzie River flows northwestward into the Canada Basin or eastward toward the CAA. The routing of river runoff varies with local winds as well with larger-scale atmospheric circulation pattern [e.g., *Guay et al.*, 2001; *Anderson et al.*, 2004; *Fichot et al.*, 2013; *Morison et al.*, 2012].

2.5.3. Freshwater Storage in the Upper Mixed Layer and the Freeze/Melt Annual Cycle

Storage of FW varies seasonally with FW removal (and storage in sea ice) taking place during fall and winter and FW addition during the summer melt period. The seasonal cycle of river input (and net precipitation) further modifies liquid FW content of the surface layer. Superimposed on this predominantly solar-forced variability are dynamical processes that redistribute FW laterally as well as vertically within the water column (section 2.5.4).

Temperature and salinity measurements from Ice-Tethered Profilers (ITPs) [*Krishfield et al.*, 2008; *Toole et al.*, 2011] allow for an assessment of FW seasonality in the surface layer beneath the sea ice cover over a full annual cycle (Figure 7). The general seasonal cycle resulting from solar forcing of the upper ocean and sea ice thermodynamics is as follows: beginning around May–June each year, the ocean surface layer warms due to absorption of solar radiation through open water and areas of thin ice. The resulting structure is a relatively fresh, thin (a few meters to ~20 m) surface layer. Beginning in September, penetrative convection
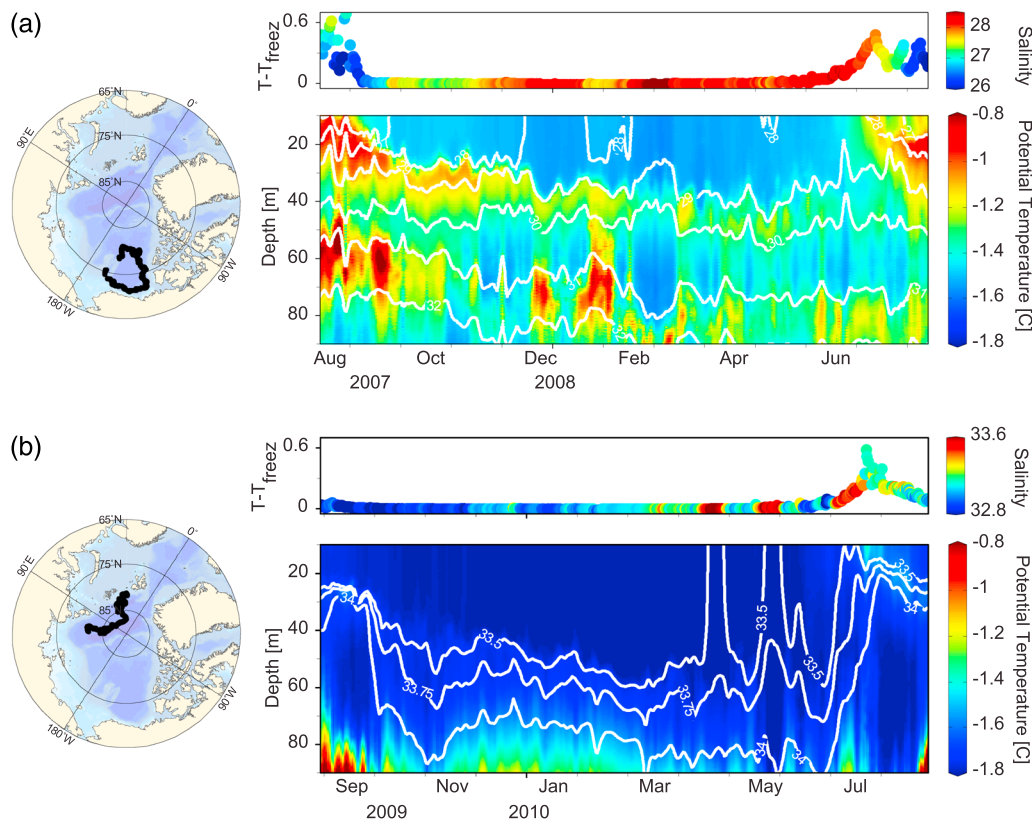
Figure 7. Times series of upper ocean temperature and salinity through an annual cycle in the (a) Amerasian and (b) Eurasian basins as observed from Ice-Tethered Profilers. The top panels in both Figures 7a and 7b show temperature above freezing and salinity at 10 m depth. The Ice-Tethered Profiler data were collected and made available by the Ice-Tethered Profiler Program [*Toole et al.*, 2011; *Krishfield et al.*, 2008] based at the Woods Hole Oceanographic Institution (http://www.whoi.edu/itp).

occurs as a result of sea ice growth and brine rejection; the summer-generated mixed layer becomes saltier and deepens through the month of April. In a closed, one-dimensional system, the net change in FW content integrated over the surface layer would equal that estimated from the net change in sea ice volume (provided winter convective deepening of the surface layer does not exceed the depth of the surface layer at the start of the melt season). However, concurrently with FW exchange associated with sea ice growth and melt cycles, sea ice export, river discharge, net precipitation, and dynamical redistribution processes all influence the FW mass balance in the surface ocean layers.

Ocean and sea ice measurements from ice-based observatories (IBOs) allow for bounds to be placed on freshening due to local ice and snow melt. Measurements from an IBO drifting in the Eurasian Basin in 2010, for example, indicated that the change in FW content of the surface ocean layer over the melt season was about 30% more than could be attributed to melt [*Timmermans et al.*, 2011]. The cause of the freshening appeared to be a redistribution of FW forced by changes in the prevailing winds that allowed fresh surface water to escape the Beaufort Gyre region and penetrate the Eurasian Basin. This wind forcing is always superimposed on the thermodynamic forcing described above and plays a major role in setting upper ocean FW content. The intensity of the Arctic high has been found to be directly correlated to FW content in the Beaufort Gyre surface layer and inversely to upper ocean FW in the Eurasian Basin [e.g., *Proshutinsky et al.*, 2009; *McPhee et al.*, 2009]. Locally, wind-driven variability in FW content can be 20 to 30 times larger than river influx anomalies [*Dmitrenko et al.*, 2008]. For this reason, it is challenging to evaluate FW content variability from river influxes, which peak with snowmelt with a timing that varies significantly across the Arctic; river runoff peaks between March and May in the Barents Sea and between April and June in the Kara, Laptev, East Siberian, and Beaufort seas [*McClelland et al.*, 2012].

Proshutinsky et al. [2009] showed that the mean seasonal cycle of ocean FW in the Beaufort Gyre has two peaks: one in late fall-early winter when the anticyclonic wind stress curl (and therefore Ekman convergence)

is strongest (while salt influxes from sea ice growth are not yet maximal) and another peak in summer associated with maximum ice melt. This can be seen in the seasonal deepening of the surface layer in the Canada Basin, which has a component due to deepening isopycnals (Ekman convergence and downwelling), and one due to convective mixing (Figure 7).

Pervasive upper ocean eddies [e.g., *Zhao et al.*, 2014] and other mesoscale motions (evidenced by isopycnal displacements in the upper water column, Figure 7) further complicate integrated FW content. The mechanisms by which FW is distributed laterally in the surface layer (via small-scale submesoscale instabilities) in the ocean surface under sea ice are not well understood [see *Timmermans et al.*, 2012]. Shear-driven mixing and other mixing processes lead to vertical redistributions of FW components so that analysis of conservative geochemical tracers is required to determine local composition and to place bounds on the evolution of FW.

2.5.4. Extent of Pacific Water in the Arctic Ocean

Water from the Pacific Ocean flows through Bering Strait across the Chukchi Sea shelf, crosses the shelf break into the Canada Basin or is advected along-slope to the east or to the west. On flowing into the basin, it intrudes between the fresh surface waters and the saltier Atlantic origin waters to form a distinctive halocline that contains the temperature maximum of the Pacific Summer Water and the temperature minimum of the Pacific Winter Water and [e.g., *McLaughlin et al.*, 2011]. These Pacific origin waters are uniquely identified via their dissolved nutrients, as they are (1) higher in silicate than inflowing Arctic rivers and Atlantic origin water and (2) deficient in nitrate relative to phosphate when compared to Atlantic origin water [e.g., *Yamamoto-Kawai et al.*, 2008].

Both Pacific Winter Water and Pacific Summer Water are evident throughout the well-sampled Beaufort Gyre Region and extend westward over the Northwind Ridge and Chukchi Abyssal Plain and eastward to the CAA. The northward extent of these water masses is marked by the Pacific/Atlantic halocline front [*McLaughlin et al.*, 1996; *Carmack et al.*, 1997], which can be identified either from dissolved nutrient samples or from the disappearance of the temperature maxima and minimum associated with the Pacific Summer and Winter Waters. An example of this front is shown in Figure 8 using data from the crossing of the Arctic Ocean by the *CCGS Louis S. St-Laurent* in summer 2014. On this crossing, the Pacific-Atlantic front was located over the Alpha-Mendeleev Ridge between the Canada and Alpha-Makarov basins, where isohalines slope upward more steeply toward the north and the temperature and salinity features of the Pacific Summer Water and Pacific Winter water rapidly diminish.

The Atlantic/Pacific halocline front has been found over the last three decades at ice camp stations and by infrequent trans-Arctic sections. Measurements at the North Pole, as part of the LOREX expedition in 1979, show the subsurface signature of Pacific origin water masses from nutrient data, indicating that they had spread across the Makarov basin to the Lomonosov Ridge at that time. Subsequent trans-Arctic sections, in 1994 [e.g., *Swift et al.*, 1997], 2005 [e.g., *Rainville and Winsor*, 2008], and in 2011 and 2014 (W. J. Williams et al., manuscript in preparation, 2015), all show the Pacific-Atlantic front roughly along the Alpha-Mendeleev Ridge rather than the Lomonosov Ridge, suggesting a reduced extent of Pacific origin water masses in the Arctic Ocean basins (W. J. Williams et al., manuscript in preparation, 2015).

While the largest FW storage in the Arctic Ocean basins is within the Beaufort Gyre, changes in the extent of Pacific Water around the northern edge of the Beaufort Gyre represent a source of variability in FW storage due to changes in circulation in the Arctic Basins. In Figure 8, FW content decreases by about 3 m across the Pacific-Atlantic front. If circulation changed, and the Pacific origin water masses extended to the Lomonosov Ridge again, they might cover 400,000 km^2 of the Makarov Basin and, if we use the 2014 decrease in FW content across the front, would increase the FW storage in the Arctic Ocean basins by ~1000 km^3.

2.5.5. Ice-Ocean Interaction and Differential Sea Ice Drift Across Boundaries

Freezing in winter separates FW within a thin ice layer at the surface from brine which mixes via convection into the upper 30–50 m of the ocean. Meanwhile, surface stress (and to a lesser extent baroclinicity) establishes a velocity gradient near the surface that causes the drift trajectories of ice and of underlying water to differ; in consequence, the solid and liquid components of the original source water become widely separated by winter's end. FW from ice formed in the basin may ultimately be released on a shelf in some areas [e.g., *Steele et al.*, 1995], and FW from ice formed on the shelf may be released into a basin in others [e.g., *Melling and Riedel*, 1996; *Melling and Lewis*, 1982]. The net budget of freezing and melting in a given area can be revealed via $\delta^{18}O$ analysis. *Melling and Moore* [1995] used this method to show that annual ice growth
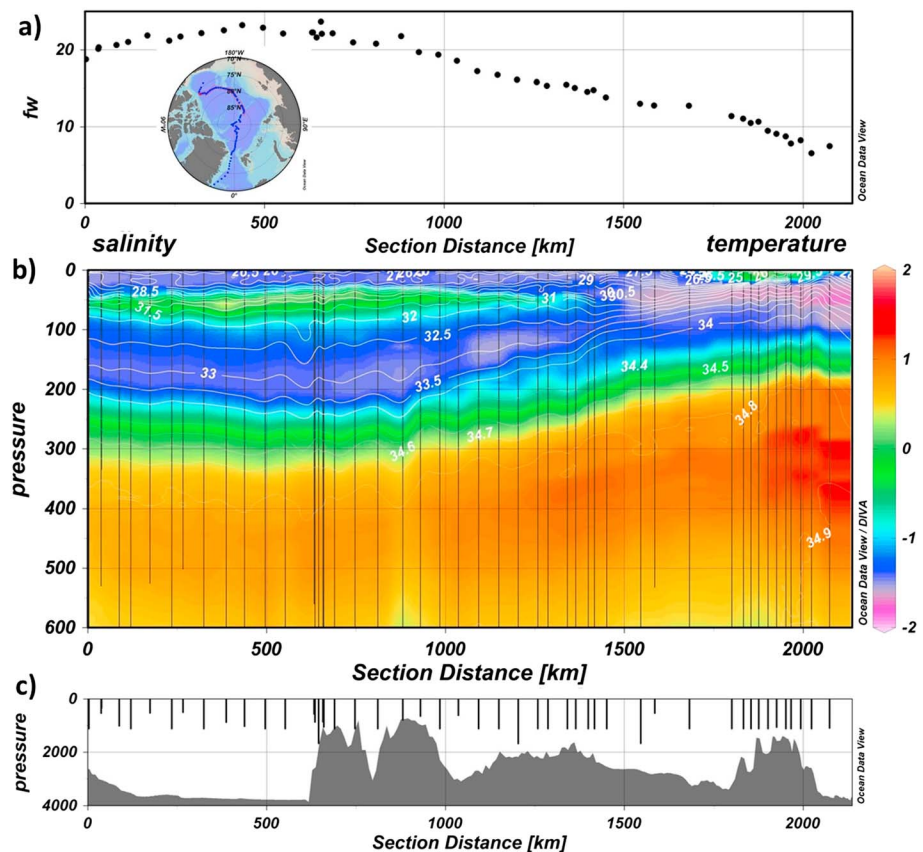
Figure 8. A transect from the Beaufort Gyre to the Lomonosov Ridge in August–September 2014 showing (a) the integrated freshwater content relative to a reference salinity of 34.80, (b) temperature (color shading) overlaid with salinity (white contours), and (c) bottom depth along the transect. The XCTD data used here were collected using expendable probes from the CCGS Louis S. St-Laurent as part of collaboration between T. Kikuchi and M. Itoh of the Japan Agency of Marine Science and Technology and Fisheries and Oceans Canada.

exceeded annual melt by about 2 m in the southeastern Beaufort Sea. Note that Beaufort Gyre has been changed to a region of net sea ice melt since 2006 at least until 2010 [*Krishfield et al.*, 2014]. The same phenomenon plays out on a larger scale in that about 10% of the ice area in the central Arctic drifts out to the North Atlantic each year [*Kwok et al.*, 2004].

The disparity in movement between sea ice and the upper ocean varies inversely with the diffusion rate of momentum within the ice/ocean boundary layer; this is linked in turn to measures of under ice roughness and boundary layer stability. Use of a constant ice-ocean drag coefficient precludes a feedback response between FW accumulation at the ocean surface and the differential velocity of ice drift [cf. *Tsamados et al.*, 2014]. Deep ice keels also have potential to extract heat from subsurface temperature maxima that shallow ice does not (although the importance of this and the associated feedbacks is not well known). Exceptional work includes that of *Mellor et al.* [1986] who studied drag variation with boundary layer stability and of *Steiner et al.* [1999] who explored its variation with ice roughness. However, the assumption of a flat-plate boundary layer flow is intrinsic to all this work; this requires that ice roughness elements are small relative to the thickness of the logarithmic sublayer which is only 1–2 m in the ocean. In reality, however, the roughness elements of sea ice (ridge keels) push not only through the logarithmic sublayer but frequently through the entire thickness (15–20 m) of the planetary boundary layer. Roughness elements cannot be incorporated into a friction velocity parameterization but must be treated explicitly when modeling ocean drag on drifting ice via consideration of internal hydraulic interactions between ridge keels and the two-layer Arctic hydrography established by surface FW accumulation. There is a range of flow-topography interactions determined by the value of the internal Froude number, based on keel draft, on upper layer depth, and on its buoyancy. Possibilities include entrapment of upper ocean water above keel depth (reduced drag) and energetic

Figure 9. Map of major river inflows to the Arctic Ocean and schematic representation of the Riverine Coastal Domain pathway. Reprinted from Progress in Oceanography, Carmack, E. C., P. Winsor, and W. Williams, The contiguous panarctic Riverine Coastal Domain: A unifying concept, 2015, copyright 2015, with permission from Elsevier.

internal wave generation (greatly increased drag or "dead water": [*Ekman*, 1904]). Detailed discussion is found in *Cummins et al.* [1994] and *Pite et al.* [1995].

2.5.6. The Riverine Coastal Domain

When a river enters the sea, the primary initial pathway in the transport of FW along coastal oceans is via the formation and propagation of coastal-trapped, buoyancy-boundary currents, with the exact (local) response determined by volume discharge, bathymetry, shelf width and slope, and winds [*Weingartner et al.*, 1999; *Bacon et al.*, 2002, 2014]. Such flows form when lower density water is discharged into a higher-density basin and is subsequently deflected to the right (in the Northern Hemisphere) by the Coriolis force [*Griffiths and Linden*, 1981; *Chapman and Lentz*, 1994; *Garvine*, 1995]. The merging of multiple sources of FW discharge from northern North America and northern Eurasia, including hundreds of rivers and glacial ice melt, may subsequently enable the formation of an aggregate or contiguous domain along the coastline, which *Carmack et al.* [2015a, 2015b] termed the Riverine Coastal Domain (RCD), that extends around the northern part of each continent (see Figure 9). The RCD, as defined, is neither stationary nor continuous; it is an initial and transient step in the complex set of mechanisms that ultimately govern the flux of buoyant waters across the shelf and into the offshore ocean [cf. *Carmack and McLaughlin*, 2001; *St-Laurent et al.*, 2011].

The RCD scales as a narrow (1–20 km), shallow (10–20 m) feature that is primarily forced driven by an aggregate of continental runoff sources. The RCD carries a terrestrial signal that affects light, nutrient, and carbon regimes and provides a coastal pathway for the dispersal and migration of marine biota [cf. *Craig*, 1984]. The physical and biogeochemical variables within the RCD yield a contiguous gradient of environmental conditions along and across the pan-Arctic coastal zone. The RCD acts as the initial connector between terrestrial and marine ecosystems and may become even more prominent as terrestrial runoff, permafrost thawing, and local ice melt are assumed to increase in the near-future climate.

2.6. Freshwater Volumes Outside the Classical (Gateway) Boundaries

The concept of a "Northern Ocean" distinct by virtue of FW content was introduced by *Carmack* [2007]. The defining characteristic of this northern ocean is a permanent pycnocline linked to lower salinity in the upper ocean in contrast to temperate oceans where it is linked to higher temperature. The boundary of this Northern Ocean lies far south of the Arctic Ocean, at about 45°N in the northeast Pacific, at 55°N in Hudson Bay and roughly extending diagonally from about 45°N in the northwest Atlantic to about 60°N in the northeast Atlantic (Figure 2b) [*Carmack et al.*, 2010]. When considering FW systems outside the classical boundaries but still within the Northern Ocean, it is again necessary to incorporate the role of shelf seas (where much FW resides) and the Nordic and Labrador Sea basins (where cyclonic gyres are conducive to deep convection, depending on the strength of regional stratification). Most discussions of FW in the marine Arctic, however, have positioned the boundaries much farther north, either across Bering Strait, along the western edge of the Canadian polar shelf and across Fram Strait and the Barents Sea opening [*Aagaard and Carmack*, 1989; *Serreze et al.*, 2006] or along the perimeter of the deep central basin of the Arctic [*Rabe et al.*, 2011, 2014]. The most recent by *Haine et al.* [2015] has included the Canadian polar shelf and Baffin Bay.

How significant are the FW volumes extant outside the classical boundaries? *Aagaard and Carmack* [1989] estimated that the deep Arctic Basins, with an area of 4.6 million km^2, contained about 58,000 km^3 of FW (referenced to $S_{ref} = 34.8$) and that the surrounding shelf with an area of 5.5 million km^2 (excluding the Canadian polar shelf) contained about 22,000 km^3, for a total of 80,000 km^3. These numbers are consistent within estimation error with *Serreze et al.* [2006] and *Haine et al.* [2015]. The area of shelves within the northern ocean that are not generally counted (e.g., the Bering, Canadian polar, East Greenland and Labrador shelves, and Hudson Bay) adds another 4.3 million km^2. These additional shelve areas accommodate almost 75,000 km^3 of FW, or 30% more than the Arctic Basin itself; two thirds of this volume is in Hudson Bay. Baffin Bay, also generally ignored, contains an estimated 13,000 km^3 above the sill depth of Davis Strait. Discharge of water from the Gulf of St. Lawrence also enters the Northern Ocean where it merges with the Labrador Current but has thus far been ignored in budget assessments even though it may retroflect back into the Nordic Seas.

To summarize, there are approximately 88,000 km^3 of FW outside the marine Arctic as usually defined by the gateways, about the same volume as within it when ice is included [*Serreze et al.*, 2006]. From a hypsometric perspective, there are approximately 102,000 km^3 of FW on the 9.8 million km^2 of northern polar shelf, to compare with 84,000 km^3 within the Arctic Basin, ice included.

The large volume of virtually unmonitored FW beyond the only region that is closely monitored (the Beaufort Gyre which contains about 23,500 km^3) dictates that a clear distinction exists between changes in the storage of FW in that gyre and changes in the storage of FW in the marine Arctic. It is plausible, though not yet studied, that FW recently added to the gyre might simply been collected from the vast shelf area of the marine Arctic and not necessarily indicative of an Arctic-wide anomaly relative to earlier times (section 3) [*Lique et al.*, 2011]. If the 5000 km^3 FW gained by the Beaufort gyre during the 2000s [*Proshutinsky et al.*, 2009] were to be drawn from Arctic shelves, their FW stock would have decreased by only 0.5 m, a change achievable via a small 3.5 m uplift of the halocline.

2.7. Arctic Glaciers and Greenland Ice Discharge

Discharge of FW from Arctic land ice is due to the sum of surface melt and ice flux into the ocean from glaciers and ice caps (henceforth termed "glaciers") and the Greenland ice sheet (GrIS). Most of this FW is discharged into shelf regions and marginal seas rather than directly into the central Arctic Ocean. The bulk of the Arctic glaciers, outside of Greenland, is concentrated in the CAA. The FW discharge from Arctic glaciers for the 1961–1992 period is estimated to be $146 \pm 38 \, km^3$/yr, and increasing to $202 \pm 48 \, km^3$/yr for the period 1993–2006 [*Dyurgerov et al.*, 2010]. More recently, Arctic glacier ice loss estimates for the 2003–2009 period (again excluding those around Greenland whose contributions are typically accounted for in GrIS estimates) was dominated by the Canadian Arctic ($60 \pm 8 \, km^3$/yr), Iceland ($10 \pm 2 \, km^3$/yr), and the Russian Arctic ($11 \pm 4 \, km^3$/yr) contributions [*Gardner et al.*, 2013]. Thus, the FW discharge from Arctic glaciers during the 2003–2009 period is on the order of 226 km^3/yr. The bulk of this discharge flows into the Arctic Ocean and Baffin Bay with smaller contributions from Baffin Island glaciers flowing into Hudson Bay and the Labrador Sea. While the discharge volumes from glaciers are relatively small, about 5% of that for rivers, it may be an important local source of both freshwater and material properties. The seasonal discharge of rivers originating from snowmelt in glacial catchments may also be delayed relative to those derived from melting snow on land.

The total FW discharge from the GrIS includes both a runoff contribution, R, due to surface melt, and ice discharge, D, due to icebergs or submarine melt of marine-terminating glaciers [*Straneo et al.*, 2013]. D is estimated as the ice flux through a "gate" near the glaciers' termini [e.g., *Enderlin et al.*, 2014] while R estimates rely on regional climate models (including an atmosphere and a snowpack) forced at its boundaries by reanalysis products [e.g., *van den Broeke et al.*, 2009]. For the GrIS, from 1961 to 1990, both D and R were largely stable, $D = 497 \pm 50$ km³/yr and $R = 416 \pm 57$ km³/yr, amounting to FW discharge of 913 ± 107 km³/yr [*Bamber et al.*, 2012]. Both these components have increased over the past two decades, and recent studies estimate that since 2005, the FW discharge is often above 1200 km³/yr [*Bamber et al.*, 2012] with a peak value of 1291 ± 50 km³/yr [*Enderlin et al.*, 2014].

These bulk estimates of ice loss, however, only provide a partial account of a FW discharge into the ocean that is characterized by large temporal and spatial variability. In summer, GrIS FW can peak at 0.1 sverdrup (Sv) [*Bamber et al.*, 2012]. Spatially, the FW discharge is concentrated at the outlet glaciers which, in turn, discharge at the head of glacial fjords. Here submarine melting, runoff injected at the base of glaciers, often hundreds of meters below sea level, and the presence of icebergs result in a complex transformation of water masses and ensuing FW export [*Straneo and Cenedese*, 2015].

2.8. Hudson Bay

The Hudson Bay System (HBS), including Hudson, James and Ungava Bays, Foxe Basin, and Hudson Strait, is a large, relatively shallow, inland sea connected to the Arctic Ocean via the narrow and shallow Fury and Hecla Strait and to the Labrador Sea via the 400 km long Hudson Strait. It is characterized by a large riverine input (~900 km³/yr from 1964 to 2000) [*Déry et al.*, 2005] and a seasonally complete sea ice cover. An additional FW input into the HBS is due to the exchange through Fury and Hecla Strait (200 km³/yr relative to a salinity of 34.8) [*Straneo and Saucier*, 2008a]. Assuming the system to be in steady state, the FW export from Hudson Strait is ~1200 km³/yr [*Straneo and Saucier*, 2008b]. This FW is a major contributor to the Labrador Current —a relatively fresh current that flows along the south Labrador coast contributing to maintaining a productive marine ecosystem [*Loder et al.*, 1998] and playing an integral role in the water mass transformation within the Labrador Sea [*Schmidt and Send*, 2007].

While no detectable trend was observed in the river discharge into the HBS during the 1964–2008 period, large interannual and decadal variability exists with minimum discharge in the 1980s and peak discharge in 2005 [*Déry et al.*, 2011]. Limited measurements of the FW flux through Hudson Strait make it challenging to determine how a variable riverine input translates into a variable FW export from Hudson Strait. Both a high-resolution numerical model and a conceptual model, however, suggest that storage and release of FW in Hudson Bay as a result of a variable wind stress over the HBS can filter the variable riverine input over timescales of several years [*St-Laurent et al.*, 2011, 2012]. Thus, even if on a smaller scale, the same FW storage and release mechanisms that are at play in the Arctic Ocean are at play in the Hudson Bay System.

2.9. The Ocean Biogeochemical System
2.9.1. Stratification, Nutrients, and Primary Production
Primary production and the associated biological pump are key process in the Arctic Ocean's ocean carbon cycle and are key factors that affect both ocean pH and atmospheric carbon dioxide (CO_2). Here it is important to distinguish between net community production (also called new or export) primary production, which is fixed by the rate of nutrient supply to the euphotic zone during the vegetative season and recycled primary production which is fueled by the remineralization of organic matter within the euphotic zone [cf. *Codispoti et al.*, 2013]. On the one hand, sea ice loss will increase light penetration, thus enhancing photosynthesis. On the other hand, meltwater capping may suppress nutrient supply, thus decreasing new production. A basic but still difficult challenge is to predict whether or not new primary production will increase or decrease under conditions of an enhanced hydrological cycle and reduced ice cover is regionally specific and linked to ocean circulation [*Nishino et al.*, 2011]. Here we suggest that there is no single answer and—recalling much of the Arctic Ocean, particularly the deep basins, is nitrate limited [*Carmack et al.*, 2004; *Tremblay and Gagnon*, 2009; *Bluhm et al.*, 2015]—that the response will depend on regional conditions [*Carmack and McLaughlin*, 2011].

The deep basins of the Arctic Ocean are decidedly oligotrophic so that new production there is mainly nutrient limited and characterized by a subsurface chlorophyll maximum [cf. *Bluhm et al.*, 2015]. For example, the biological pump is constrained within the Beaufort Gyre because freshwater accumulation within the gyre

limits nutrient supply from deep layers and shelves [*McLaughlin and Carmack*, 2010] and this also acts to inhibit the growth of large-bodied phytoplankton [*Li et al.*, 2009]. *Slagstad et al.* [2015] used results from a physical-biologically coupled model to explore future states of primary and secondary productivity and showed that in the central Arctic Ocean new production will not increase proportionately with increasing light availability due to increased stratification. The biological pump could be enhanced by sea ice loss in the central Arctic where uplifted isohaline surfaces associated with the Transpolar Drift may enhance the supply of nutrients from deep layers. On the interior shelves the removal of complete ice cover beyond the shelf break will enhance wind- and ice-forced shelf break upwelling; indeed, the transfer of momentum from the atmosphere to the ocean may be maximal at partial ice concentration [*Carmack and Chapman*, 2003; *Pickart et al.*, 2013; *Williams and Carmack*, 2015]. The resulting increases in both nutrient fluxes and solar radiation should thus increase new production, as discussed by *Slagstad et al.* [2015]. In many passages and channels within shelf archipelagos the resulting strong flows and tidal mixing will force nutrients into the surface layer, and combined with reduced ice cover and a longer growing season, new production should increase. In the relatively deep subbasins of the CAA increased ice melt and river discharge will increase surface layer stratification, and the resulting decrease in vertical nutrient flux should thus decrease new production. The above, highly simplified concepts admittedly ignore other regional processes (e.g., increased turbidity from river discharge and altered convective process) but at least serve as a starting point for discussion.

2.9.2. Role of Freshwater Inputs for Biological Communities and Biodiversity

In the Arctic, FW or low-salinity water shapes biological communities primarily by two pathways. The first pathway is through the direct consequences of low salinity on the physiological capacity of osmoregulation, and the second one is through riverine transport of terrestrial organic matter, inorganic particles, and micronutrients and macronutrients.

Brackish water tends to contain biological communities of lower biodiversity than either FW or fully marine water, with a well-documented minimum in species richness falling between freshwater and marine assemblages, as first noted by *Remane* [1958]. In the Arctic, multiple examples confirm this observation in all three realms, the sea ice, the water column, and at the seafloor. In sea ice, freshwater species assemblages tend to dominate closed, surface melt ponds [*Lee et al.*, 2011; *Kilias et al.*, 2014]. The low-salinity water layer immediately underneath melting sea ice also tends to be species-poor regarding multicellular fauna compared to other seasons, and sea ice ridges have been proposed as a refuge for such mobile fauna during the melt process [*Gradinger et al.*, 2010]. FW, through its effect on increasing stratification of the upper water column in the central Arctic (see sections 2.5.5 and 4.3), has also changed algal communities toward smaller cell sizes and difference production rates than the "typical" diatom blooms [*Li et al.*, 2009]. In the large Arctic river estuaries, different—often less diverse and/or less biomass-rich—pelagic and benthic communities are found near the river mouths than offshore in fully marine waters [*Parsons et al.*, 1988; *Dolotov et al.*, 2002; *Denisenko et al.*, 2003; *Deubel et al.*, 2003]. Here again, the low-salinity waters are dominated by euryhaline (low-salinity tolerant) crustaceans in the zooplankton, and relatively few euryhaline crustaceans, bristle worms, and bivalves at the seafloor [*Denisenko et al.*, 1999; *Ravelo et al.*, 2015]. Increased stratification and runoff, through its influence on community structure, can therefore, be expected to change biological production cycles in the future, although a budget on primary and secondary production changes with changing salinity is still outstanding.

Arctic rivers (along with coastal erosion) transport tons of both organic and inorganic material from upriver sources into the Arctic Ocean every year [*Rachold et al.*, 2004; *McClelland et al.*, 2012, 2014; *Goñi et al.*, 2013]. These materials can have both suppressing and enhancing effects on biological diversity, food webs, and production. On the one hand, the high turbidity results both in reduced light climate for primary production and the risk for clogging filtration apparatuses of filter-feeding fauna [*Thrush et al.*, 2004; *Konar*, 2013]. On the other hand, nutrient inflow can enhance primary production in otherwise oligotrophic areas of some interior shelves [*Pivovarov et al.*, 2003]. The large amounts of terrestrial organic matter are difficult for marine primary producers to assimilate directly [*Garneau et al.*, 2009; *Dunton et al.*, 2012]. Recent work, however, has demonstrated that microbial reworking of these hard-to-break-down materials render them a useful carbon subsidy for a broad range of marine fauna [*Garneau et al.*, 2009; *Goñi et al.*, 2013; *Divine et al.*, 2015]. The use of terrestrial organic carbon in marine food webs has been tracked by stable carbon isotope signatures in animal tissue in Arctic coastal lagoons [*Dunton et al.*, 2006, 2012; *Casper et al.*, 2014], but also way offshore in shelf and slope communities in the Beaufort Sea (L. E. Bell et al., The influence of terrestrial organic matter in

marine food webs of the Beaufort Sea shelf and slope, *Marine Ecology Progress Series*, in review, 2015). These findings may have predictive value for the character of Arctic food webs in light of climate change scenarios that show river runoff to be increasing [*Peterson et al.*, 2002; *McClelland et al.*, 2004].

2.9.3. Ocean Acidification

Ocean acidification by uptake of anthropogenic CO_2 is expected to have negative impacts on calcifying organisms such as pelagic snails (pteropods) and bivalves [e.g., *Comeau et al.*, 2012]. In the Arctic Ocean, ocean acidification is complicated by other effects of climate change, such as warming, melting of sea ice, surface freshening, and increased primary productivity. Here we focus on the impact of the Arctic FW system on the ocean acidification.

The input of FW makes the Arctic Ocean particularly vulnerable to ocean acidification. Mixing with FW lowers not only salinity but also alkalinity (buffer capacity) and calcium ion concentrations of Arctic surface waters [*AMAP*, 2013]. As a result, surface waters in the Arctic Ocean are characterized by a low calcium carbonate saturation state (Ω) and exhibit a greater decrease in pH with additional CO_2 uptake. Therefore, model simulations predict that the Arctic Ocean will be the first to experience basin-wide surface undersaturation with respect to calcium carbonate [*Steinacher et al.*, 2009]. In fact, waters undersaturated with respect to aragonite-type calcium carbonate have been observed at surface and subsurface layers of the Canada Basin as well as bottom waters of shelf seas with potential negative consequences on calcifying organisms and Arctic ecosystem [*Yamamoto-Kawai et al.*, 2013].

The degree of impact of FW on ocean acidification depends on the chemical property of the source FW. Runoff from North America has the highest alkalinity and calcium ion concentration, followed by runoff from Siberia, sea ice melt, and precipitation. Accordingly, mixing with precipitation or sea ice meltwater causes a greater decrease in buffering capacity and Ω than mixing with river runoff [*Azetsu-Scott et al.*, 2010]. Regional and seasonal variability in runoff properties [*Cooper et al.*, 2008] reflect differences in vegetation and hydrology within specific drainage basins. Such variability should directly influence on coastal ocean acidification and local ecosystem but not well studied yet. With changes in hydrology and ecosystems on land [*Wrona et al.*, 2016], future changes in alkalinity and calcium ion concentration in river water are also expected. Furthermore, an enhanced processing of terrestrial organic matter in warmer climate will act to lower pH and Ω by producing CO_2 in coastal and shelf waters. In shallow regions, an increase in FW flux can also increase stratification of water column to produce lower pH and lower Ω waters at the bottom than present with possible negative impacts on benthos. Because Arctic shelf seas are one of the most vulnerable areas to ocean acidification, simultaneous observations from land to ocean and experiments on river and shallow water chemistry are required to improve our understanding of the Arctic Ocean acidification.

The inflow from the Pacific has important implications in the Arctic Ocean acidification. Pacific origin water is preconditioned by the global-scale circulation to be low Ω source waters and as they move northward across the Bering and Chukchi seas they are modified by biological activity [*Yamamoto-Kawai et al.*, 2013]. The addition of anthropogenic CO_2 has already made the Pacific Winter Water to be corrosive to aragonite [*Jutterström and Anderson*, 2005; *Anderson et al.*, 2010; *Yamamoto-Kawai et al.*, 2013]. The enhanced upwelling of subsurface water in recent years brings this corrosive water onto shelves in the Pacific Arctic [*Mathis et al.*, 2012]. The flow of Pacific water carries low Ω signal to downstream regions into Canada Basin, the CAA, and Baffin Bay [*Azetsu-Scott et al.*, 2010; *Yamamoto-Kawai et al.*, 2013]. Other oceanic processes such as mixing, cooling/warming, upwelling/downwelling, photosynthesis, and remineralization alter pH and Ω in waters along advective pathways, but these are poorly quantified [*Yamamoto-Kawai et al.*, 2013; *Popova et al.*, 2014]. As described in the present paper, the Arctic FW system acts in all of these processes. Clearly, quantification of local and regional physical and biological effects on pH and Ω under the changing Arctic FW system is essential in order to predict the future ocean acidification.

2.9.4. Flux and Marginal Filtering of Terrestrial Materials

The extensive Arctic coastline is the gateway to the ocean for both organic and inorganic materials of terrestrial origin that subsequently affect marine biological production. In particular, dissolved organic carbon (DOC) concentrations in Arctic rivers are among the highest in the world's rivers, and the total flux accounts for about 10% of DOC discharged by global rivers [*Dittmar and Kattner*, 2003]. Nitrogen and phosphorus are also discharged mostly in organic compounds but in low concentrations. Arctic rivers discharge onto the vast continental shelves where active biological production and biogeochemical cycling occur. Recent

observations have revealed that terrigenous dissolved organic matter (DOM) during the spring freshet (runoff driven by rapid snowmelt) is more labile than in other seasons [*Letscher et al.*, 2011; *Holmes et al.*, 2008, 2012]. Therefore, terrigenous inputs of DOM by Arctic rivers are of more importance than previously thought in regional and also global CO_2 and biogeochemical cycles. Furthermore, less ice cover and higher temperature enhances processing of terrestrial organic matter on shelves [see *Schuur et al.*, 2015 for review]. Input of micronutrients such as iron from Arctic rivers and glaciers also supports regional primary production [*Klunder et al.*, 2012; *Bhatia et al.*, 2013].

It is expected that there will be important shifts in flux and timing in the river transport of organic matter and its lability, macronutrients and their ratios, and major and trace elements [e.g., *Pokrovsky et al.*, 2013]. Such changes may in turn have critical implications for primary production and carbon cycling on Arctic shelves, basins, and other oceans [*Frey and McClelland*, 2009]. However, it is recognized that our understanding of estuarine and coastal processes in the Arctic is far less developed than in other regions [*Holmes et al.*, 2012]. The river-sea mixing zone is the marginal filter which retains up to 95% of the sediment and up to 40% of dissolved mater of river discharge in the estuaries and deltas [*Lisitzyn*, 1995]. Cold temperatures and the presence of ice and snow on ocean and land surfaces has resulted in the sharp seasonality of these marginal filters [*Lisitzyn*, 1995], but these are changing now. Therefore, observation and monitoring of river inputs and removal processes in near shore are essential in order to understand the role of terrigenous fluxes in the current and future Arctic Ocean. Furthermore, future changes in properties, such as nutrient, $\delta^{18}O$, alkalinity, barium, and CDOM, in river water, and in marginal filtering will cause a bias in freshwater source identification in the Arctic seawater using these as geochemical tracers (section 2.5.1).

3. Past Changes and Key Drivers

3.1. Observed Changes in Storage on Interannual and Multidecadal Time Scales

The Arctic FW reservoirs described in section 2.4 are changing; in particular, there has been a rapid increase in liquid FW storage since 2000 over the basins and a rapid decline in summer sea ice. We discuss these observed changes here by contrasting the decade of the 2000s with earlier periods (see Table 1). Over the twentieth century the central Arctic Ocean—above the density surface $\sigma_\theta = 27.35$ or roughly the upper 150 m—became increasingly saltier with a rate of freshwater loss of 239 ± 270 km^3 decade^{-1}. For example, FWC anomalies averaged over 1950–1975 were estimated as 102 ± 20 km^3; this salinification led to a substantial decrease, 1478 ± 17 km^3, of FWC over 1976–1999. *Polyakov et al.* [2008] argued that ice production and sustained draining of freshwater from the Arctic Ocean in response to winds were the key contributors to the salinification of the upper Arctic Ocean during the twentieth century. However, the FWC anomalies extant in the 2000s and 2010s stand out: the freshening is dramatic, with no analogy in almost a century-long history of oceanographic observations [*Polyakov et al.*, 2013b].

The expansion of the liquid FW reservoir amounts to about 8000 km^3 for the 2000s compared to the 1980–2000 average [*Giles et al.*, 2012]. The increase is seen mainly in the western Arctic Ocean and in the Beaufort Gyre, specifically, which has increased its volume over the past two decades by about 5000 km^3. Relatedly, the upper ocean salinity in the Canada Basin was 1–3 practical salinity units fresher in 2008 than prior to 1990 [*Morison et al.*, 2012]. The main line of evidence comes from hydrographic observations from ships, ice camps, aircraft, and autonomous instruments. *Rabe et al.* [2014] performed the most recent analysis of hydrographic data. They find an annual increase in liquid FW of 600 ± 300 km^3 yr^{-1} between 1992 and 2012. Satellite measurements of sea level concur. For example, *Giles et al.* [2012] estimate that the inflated Beaufort Gyre contributed to 8000 ± 2000 km^3 more western Arctic FW in 2010 than in 1995.

The total liquid FW store is increasing, but not in all parts of the Arctic Ocean. *Morison et al.* [2012] used hydrography, geochemistry, satellite altimetry, and satellite bottom pressure data to show that the FW content of the Amerasian Basin increased while in the Eurasian Basin it decreased. Upper ocean salinity was 1–2 practical salinity units higher in the Makarov Basin in 2008 compared to before 1990, for instance. Therefore, at least some of the increased FW observed in the Beaufort Gyre has been redistributed from the Eurasian Basin.

The Arctic sea ice reservoir is losing volume, especially in summer. Sea ice extent is the best observed ice parameter, being monitored by passive microwave measurements from orbit since 1979. It is declining at

an average rate of $-3.8 \pm 0.3\%$ per decade between November 1979 and December 2012 [*Vaughan et al.*, 2013]. Most of the loss occurs in summer and autumn, for which the average rate is $-6.6 \pm 1.2\%$ per decade. Sea ice thickness is in decline too, although it is harder to measure than sea ice extent. For example, *Kwok and Rothrock* [2009] report submarine and satellite data that show that the average end-of-melt season thickness was 3.02 m in 1958–1976 but just 1.43 m in 2003–2007. Because both ice extent and thickness are declining, sea ice volume, the most useful metric of FW storage, is also declining; and faster than either ice extent or thickness individually. Probably, the best estimate of sea ice volume is from a numerical ice/ocean model that assimilates Arctic observations. The Pan-Arctic Ice Ocean Modeling and Assimilation System (PIOMAS) [*Zhang and Rothrock*, 2003] is a good choice of this type. The PIOMAS estimates of the FW stored in seasonal ice are nearly constant at 13,000 km^3 over the period 1980–2010. The volume of FW in multiyear ice declines, however; from 10,900 km^3 for 1980–2000 to 7400 km^3 for the 2000s. Over this period, the annual average volume of FW in sea ice declines from 17,800 km^3 to 14,300 km^3 (Table 1) [*Schweiger et al.*, 2011; *Haine et al.*, 2015]. This loss of FW from sea ice contributes together with the shift of fluxes toward Arctic freshening (section 2.4). Collectively, the loss of ice and increased flux convergence accounts for the greater volume of liquid FW observed in the 2000s [*Haine et al.*, 2015].

3.2. Observed Changes in Freshwater Trajectories and Pathways

The processes that store FW and export it from the Arctic are connected to the surface circulation and hence to winds. Figure 3 shows the 2000–2010 average sea ice drift trajectories which reflect ocean surface flows and in turn the sea level pressure. The average sea level pressure is relatively high over the Canada Basin (the Beaufort High) and low over the Eurasian Basin, Barents Sea, and Nordic Seas [*Serreze and Barrett*, 2011]. The associated sea level pressure gradients drive geostrophic flow around the Beaufort High and across the pole toward Greenland and the North Atlantic. The surface ocean responds to the average wind with a convergent Ekman flow under the Beaufort High which raises sea level and depresses the halocline (storing FW) [*Proshutinsky and Johnson*, 1997; *Morison et al.*, 2012]. The associated sea level slope acquires geostrophic balance with an anticyclonic surface flow parallel to the wind, namely, the Beaufort Gyre and Trans-Polar Drift.

Analysis of FWC anomalies observations suggests that sustained phases of freshening in the central Arctic Ocean are associated with salinification in the Barents and western Greenland seas (with much stronger anomalies in the Greenland Sea) and vice versa [*Polyakov et al.*, 2008]. These estimates strongly suggest that at decadal and longer time scales, the magnitudes of ice and FW exchanges through straits connecting the Arctic Ocean to the subarctic basins are of primary importance for stratification within the subarctic basins. *Polyakov et al.* [2008] concluded that in the past, changes in large-scale atmospheric and oceanic circulation had a greater effect on the freshwater flux to subarctic basins than variations of the Arctic Ocean FWC.

This set of linked processes has been documented to vary over the last 35 years. Specifically, the decade of the 2000s was a time of stronger than average Beaufort High sea level pressure (winter 2007 exemplifies this state). Hence, the Beaufort Gyre was stronger than normal with higher sea level, a deeper halocline, stronger anticyclonic flow, and greater FW storage [*Proshutinsky et al.*, 2009]. The Trans-Polar Drift was also stronger and more direct than normal; water and ice from the Eurasian shelves flowed toward the pole near the Lomonosov Ridge and then through Fram Strait to leave the Arctic [*Stewart and Haine*, 2013]. At those times, Eurasian runoff entering the Canada Basin decreased, and Pacific Water was absent in Fram Strait outflow [*Falck et al.*, 2005].

Prior to the 2000s the Beaufort High was weaker, the Beaufort Gyre sea level was lower, the halocline was shallower, the anticyclonic circulation was weaker (or absent), and less FW was stored in the Beaufort Gyre. Summer of 1989 exemplifies this state. The Trans-Polar Drift was weaker and penetrated farther into the Amerasian Basin. Eurasian shelf water and ice entered deep water farther east, near the Mendeleev Ridge [*Steele and Boyd*, 1998; *Ekwurzel et al.*, 2001].

This variability is coordinated by the atmospheric forcing of the ocean by the surface wind. The strength of the Beaufort High sea level pressure and the low sea level pressure in the Barents Sea are the main actors. These features are related to the Arctic Oscillation, among other atmospheric modes of variability, although they act independently too. Variations in the Arctic Oscillation mainly drive changes in the central and eastern Arctic, and Nordic Seas, rather than the western Arctic [*Serreze and Barrett*, 2011; *Morison et al.*, 2012]. The Beaufort High anticorrelates with the Arctic Oscillation in summer (that is, a negative Arctic Oscillation index is associated with a strong Beaufort High in summer).

Long-term variations in freshwater storage and export have been examined by *Proshutinsky et al.* [2015], who note that between 1948 and 1996 the mean annual environmental parameters in the Arctic experienced a well-defined decadal variability with two basic circulation regimes, cyclonic and anticyclonic, alternating at 5 to 7 year intervals [cf. *Proshutinsky and Johnson*, 1997; *Proshutinsky et al.*, 2002]. Since 1997, however, the Arctic system has been under the influence of the anticyclonic circulation regime, with an attendant increase in freshwater storage. *Proshutinsky et al.* [2015] then employ box model results to explain this and to demonstrate the importance of treating the Arctic Ocean and North Atlantic subarctic region as a coupled ocean/ice/ atmosphere system. They further suggest that additional freshwater arising from Greenland ice melt is altering system behavior.

The importance of the wind in controlling the FW storage and export suggests that our ability to predict future FW *pathways* is limited, as it is for the sea level pressure. Predictability of the FW *sources*, however, is distinct and greater, as discussed in section 4. Moreover, the changing sea ice cover discussed in section 3.1 likely impacts the way that the wind exerts stress on the surface ocean, irrespective of changes in the wind itself. This mechanism, which is still somewhat unknown, has been proposed by *Giles et al.* [2012] to account for FW accumulation in the western Arctic since 1995 and may become more important in the future (section 4.3) [*Nummelin et al.*, 2015].

3.3. Observed Changes in Sea Ice Volume and Transport

Ice draft from naval submarine sonar during the "old" Arctic regime (1960–1982) has been mapped by *Bourke and Garrett* [1987], revealing an average 3–8 m for the central Arctic pack ice of the time and an average 1–3 m for the peripheral areas of first-year ice. This average draft has declined greatly during the last quarter century. *Kwok and Rothrock* [2009] provide a recent perspective that combines the analysis of pre-2000 sonar data from submarines [*Rothrock et al.*, 1999] with post-2000 data from satellite altimetry [*Kwok et al.*, 2009]. Their Figure 1 shows a decrease by 40% or more in all subregions between 1958–1976 and 1993–1997; *Tucker et al.* [2001] using data from an often surveyed path northward along 150°W show that the change actually occurred within a few years of 1990. The subsequent change to the mid-2000s was smaller, about 6.5%.

Meanwhile, the expanse of decades-old ice has shrunk by 45%. *Rigor and Wallace* [2004] have argued that the impetus for multiyear ice loss was a change in wind-driven ice circulation—caused by an interval of high Arctic Oscillation conditions—that forced old ice out to the Atlantic. The substitutions of open water for almost half of the preexisting multiyear in summer and of much thinner first-year ice for the same multiyear ice in winter can explain much of the drop in average ice thickness. Moreover, loss of summer ice has exposed a larger area of water to insolation in summer, creating a warmer sea surface and accelerated melting of ice— the positive albedo feedback effect [*Perovich et al.*, 2011].

The ice inventory at summer's end reflects a balance between the recruitment and loss of multiyear ice. Recruitment begins with seasonal ice, some which melts in the summer, some which drifts out of the Arctic before it melts, and some which survives to become second-year ice; options are the same second-year and older ice. Recruitment occurs if ice is especially thick at winter's end and/or if the net absorption of radiation is relatively low [*Maykut and Untersteiner*, 1971]. Thickness at winter's end varies with ice type, snow accumulation, winter cloud, winter's severity, ocean heat flux, and accumulated ice deformation [see *Maykut and Untersteiner*, 1971; *Brown and Coté*, 1992; *Flato and Brown*, 1996; *Melling and Riedel*, 1996]. Radiation absorption is influenced by initial snow depth, local ice concentration, ice surface ponding, cloud cover, duration of the melt season, and geographic location [*Perovich et al.*, 2011].

It is possible to develop multiyear ice from second-year ice via a series of annual cycles during which ice growth during winter exceeds ice ablation during summer. However, there is a limit to the maximum attainable thickness (about 3 m after a decade) [*Maykut and Untersteiner*, 1971; *Flato and Brown*, 1996]. This maximum is not attained, however, if ice is swept from the Arctic in less time.

Ridging is critical to the formation of very thick ice; rubble 10–30 m in thickness can form from first-year ice in days not decades [*Amundrud et al.*, 2004]. In this manner it resembles multiyear ice relative to the rate of ablation, which is at most 2–3 m per year [*Amundrud et al.*, 2006]. However, its formation is spatially constrained, being most effective within the stamukhi zone at the ice-land interface.

It is instructive to examine individually the two populations of Arctic pack ice—first-year ice and multiyear pack—that mingle in the central Arctic. Long records of first-year ice have been acquired in the Beaufort Sea (since 1990) and the northern Chukchi Sea (since 2003). *Melling et al.* [2005, 2012] used data from the Beaufort to demonstrate negligible trend in thickness there during 1991–2003 and during 1991–2008; thickness measured over 10 years in the northern Chukchi is also trendless (Melling, unpublished data, 2015). Apparently, climate change has not strongly impacted the thickness of Arctic first-year pack. Thick multiyear ice floes are the second ice population within the central Arctic. Scientists seek such ice in the Canadian High Arctic, where it is found drifting southward from the region of thickest ice mapped by *Bourke and Garrett* [1987]. *Johnston* [2011] readily found and measured very thick multiyear and ridged floes (averaging 5–15 m) in this area even after two decades of thinning in the mixed population of the central Arctic. Continuous measurements of multiyear ice by subsea sonar in the same area since 2009 support this viewpoint (H. Melling, Sea-ice thickness on the north Canadian polar shelf: A second look after 40 years, *Journal of Geophysical Research*, manuscript in preparation, 2015). It is reasonable to conclude that thick multiyear ice continues to form via ridging in Canadian and Greenland waters.

3.4. Observed Changes in Duration and Thickness of Ice Cover Near the Coast

There are very few systematic long-term thickness observations for seasonal Arctic sea ice. The longest data series, built by Canadian and Russian weather services since the mid-1900s, document the annual growth-decay cycle of fast ice close to shore. End-of-winter data from both Siberia and Canada reveal only weak trends in thickness (a few centimeters/decade), with decrease at some sites and increase at others [*Brown and Coté*, 1992; *Polyakov et al.*, 2003]. Observations in the Canadian Arctic reveal that variation in snow depth strongly influences that in ice thickness variation [*Brown and Coté*, 1992; *Dumas et al.*, 2005; *Melling*, 2012]. *Polyakov et al.* [2013a] has prepared a 15-station composite of Siberian observations that began in the 1930s; this shows a 13 cm thickness decrease during 1960–2009 (2.2 cm/decade), which was, however, preceded by a 20 cm increase between 1934 and 1960; snow depth was not measured. Data, such as exist, suggest that the impact of climate change on the thickness of coastal fast ice has been much smaller than its impact on pack ice in the central Arctic.

3.5. Observed Changes in Sea Level Along the Arctic Coastlines

Observations of sea level at Arctic coastal stations began in the first half of the twentieth century. *Proshutinsky et al.* [2004] provided estimates of sea level trends from the 1950s to the 1990s. For the period 1954–1989 the sea level was generally rising at a spread of 0.185 cm/yr. Using atmospheric observations and reanalysis products and modeling, they inferred that approximately a third of this trend was due to steric effects. Another third of the trend may be explained by falling sea level pressure (the so-called effect of the reverse barometer). The rest of the trend may be explained by effects of winds and change of Arctic Ocean mass. In addition, *Danielson et al.* [2014] show that a recent increase in the polar easterlies was associated with a decline in sea surface height (SSH) along the Siberian Arctic coast (2006–2011 relative to 2000–2005), and they propose that the SSH fluctuations here contribute in part to variations of the Pacific-Arctic pressure head and the Bering Strait fluxes.

Analysis of more recent observations suggested a drastic change of sea level variability along the Siberian Arctic coast [*Ashik et al.*, 2015]. Starting from approximately 1985 a rapid increase of sea level began; this level rise may be characterized by a linear trend of 0.244 ± 0.097 cm/yr. The maximum trend (0.441 cm/yr) was observed in the southwestern part of the Kara Sea. *Ashik et al.* [2015] argued that this substantial increase of the rate of sea level rise may be explained by increased frequency and intensity of arctic cyclones which depress sea level off the shore at the same time building sea level at the coastal line. The authors noted also that there was a transformation of the seasonal cycle of sea level along the Arctic coast. Historical records demonstrated a well-pronounced seasonal cycle with maximum of sea level in fall (September–November) and minimum in spring (March–May). However, recent observations demonstrated most significant sea level seasonal rise in November–January which may be related to later onset of freezing in the Siberian seas (section 3.4).

3.6. Observed Changes in the Supply of Nutrients to Primary Producers

Two factors limit productivity in the Arctic Ocean: light (photosynthetically active radiation) and nutrients (primarily nitrate). With regards to the latter, the Arctic can be considered an advective ocean

[*Carmack and Wassmann*, 2006; *Wassmann et al.*, 2015; *Grebmeier et al.*, 2015], through which nutrients are transported and transformed between the Pacific and Atlantic Oceans [*Yamamoto-Kawai et al.*, 2006]. As noted in section 2.9.1, however, it is important to distinguish between new and recycled primary production, with the former fixed by the supply of nitrate to the euphotic zone during the vegetative season [cf. *Codispoti et al.*, 2013]. In turn, this supply has three seasonal modes of delivery: (1) replenishment by haline convection during the winter, nonvegetative season, (2) vertical mixing at the base of the mixed layer in summer, and (3) enhanced mixing by winds and convection in autumn when sufficient light is still available to support a fall bloom. As shown by *Codispoti et al.* [2013] winter replenishment is very small owing to robust freshwater stratification. The importance of vertical mixing at the base of the mixed layer in summer is confirmed by the ubiquitous presence of the subsurface chlorophyll maximum [*Martin et al.*, 2013; *Tremblay et al.*, 2015; *Bluhm et al.*, 2015]. The growing importance of the fall bloom, following sea ice retreat, is discussed by *Ardyna et al.* [2014]. At present, data are lacking to provide a quantitative, Arctic-wide assessment of temporal trends in nutrient supply. There is evidence, however, that freshwater capping is suppressing the supply of nutrients in the Canada Basin, as shown by the recent deepening of the chlorophyll maximum [*McLaughlin and Carmack*, 2010] and by the increased fraction of smaller phytoplankton in the upper ocean [*Li et al.*, 2009], whereas ice retreat beyond the shelf break may be increasing nutrient supply on shelves due to enhanced upwelling [*Williams and Carmack*, 2015; *Tremblay et al.*, 2015].

3.7. Observed Changes in Ocean Acidification

Changes in environmental parameters over the past two decades (increased river discharge, warming, melting of sea ice, and increased primary productivity) are affecting the rate of acidification in the Arctic Ocean. Time series observations have revealed significant decrease in pH and calcium carbonate saturation state (Ω) in Iceland and Nordic Seas from 1985 to 2008 [*Olafsson et al.*, 2009] and in Canada Basin from 1997 to 2008 [*Yamamoto-Kawai et al.*, 2009; *Miller et al.*, 2014]. In the former region, ocean acidification was enhanced by a surface ocean $p\mathrm{CO_2}$ increase slightly exceeding the atmospheric CO_2 growth rate, due probably to decadal timescale climate variability [*Thomas et al.*, 2008; *McKinley et al.*, 2011]. In the latter region, the increase in atmospheric CO_2 could account only for half of the decrease in Ω and the remnant half was due to the extensive melting of sea ice during the 2000s [*Yamamoto-Kawai et al.*, 2011]. Melting of sea ice has enhanced uptake of CO_2 by the surface water and meltwater diluted alkalinity and calcium ion. These effects combined resulted in a large decrease in Ω and undersaturation of surface water with respect to aragonite-type calcium carbonate the Canada Basin.

Aragonite undersaturation has also been observed in the low-salinity surface waters in coastal regions in Bering Sea [*Mathis et al.*, 2011], East Siberian Sea [*Anderson et al.*, 2011], the CAA [*Chierici and Fransson*, 2009; *Azetsu-Scott et al.*, 2010; *Chierici et al.*, 2011; *Yamamoto-Kawai et al.*, 2013], and Hudson Bay [*Azetsu-Scott et al.*, 2014]. These observations prove that FW input significantly exacerbated ocean acidification in surface waters. It should be noted that warming and primary productivity in the surface water can counteract to the decrease in surface Ω [e.g., *Chierici et al.*, 2011].

FW inputs also affect ocean acidification by stratifying the surface layer. A stronger and shallower halocline results in a higher temperature and lower biological productivity in surface waters and prevents transport of anthropogenic CO_2 into deeper layers [*Cai et al.*, 2010]. In shelf seas, stratification also makes low pH and low Ω bottom waters by accumulating remineralized CO_2 at the bottom. Aragonite-undersaturated shelf bottom waters have been observed in Bering [*Mathis et al.*, 2011], Chukchi [*Bates et al.*, 2009] and East Siberian [*Anderson et al.*, 2011] seas, the CAA [*Yamamoto-Kawai et al.*, 2013], and Hudson Bay as well in the intermediate layer of the Canada Basin where shelf-derived water exists [*Jutterström and Anderson*, 2005]. Of these, bottom waters were undersaturated even for calcite in East Siberian Sea and Hudson Bay [*Anderson et al.*, 2011; *Azetsu-Scott et al.*, 2014].

Although Arctic waters are originally characterized by low Ω, largely due to high FW inputs, calculations have shown that observed undersaturation is a recent phenomenon. In fact, *Yamamoto-Kawai et al.* [2013] show that most of Arctic Ocean would be oversaturated if there were no uptake of anthropogenic CO_2. An increase in FW supply to the ocean will act to further exacerbate ocean acidification by uptake of anthropogenic CO_2 and to expand the area of calcium carbonate undersaturation.

4. Projected Changes and Key Drivers

Coupled climate models provide information about future change to the Arctic FW system [*Lique et al.*, 2016]. They are inherently uncertain, however, and often in mutual contradiction. Nevertheless, there are some projected changes that are robust across current climate models. They derive from two well-accepted predictions, first, that the global hydrological cycle will accelerate in a warmer climate and, second, that Arctic warming will be (and has been) amplified compared to the global average. The implications for the Arctic FW system are as follows.

4.1. Projected Changes in Sea Ice

Arctic sea ice extent is predicted to shrink in all seasons in the 21st century [*Intergovernmental Panel on Climate Change*, 2013], and this has been linked to anthropogenic CO_2 forcing [*Notz and Marotzke*, 2012]. The fifth Coupled Model Intercomparison Project (CMIP5) assessment of the Intergovernmental Panel on Climate Change suggests that sea ice extent will diminish by 8–34% in February and 43–94% in September for 2081–2100 compared to 1986–2005, depending on choice of scenario for the 21st century. Models predict that it is likely that a nearly ice-free Arctic (defined to be a September ice extent of less than $10^6 \, km^2$ for five consecutive summers) will occur before 2050. There is large variability between CMIP5 models on the rate of decline of ice extent, however, and most models lose ice slower than observed [*Stroeve et al.*, 2012a, 2012b; *Overland and Wang*, 2013].

4.2. Projected Changes in Freshwater Delivery, Storage, and Export

The increasing hydrological cycle magnifies the atmospheric convergence of water vapor in the Arctic [*Zhang et al.*, 2012] and hence increases precipitation and runoff. For example, one CMIP5 model exhibits a 40% precipitation increase north of 70°N over the 21st century [*Vavrus et al.*, 2012; *Vihma et al.*, 2016]. Most of the precipitation increase is likely due to an increasing Arctic hydrological cycle (that is greater evaporation linked to sea ice retreat) and not to water vapor flux from lower latitudes [*Bintanja and Selten*, 2014]. *Haine et al.* [2015] conclude that the total *P-E* FW source to the ocean will increase by about 30% by 2100, and the total runoff will increase by about 14%. Bering Strait FW flux is projected to increase too but by an unknown amount.

The total volume of FW stored in the Arctic will probably increase due to these larger inflows. For example, *Haine et al.* [2015] speculate that an extra 50,000 km^3 will be stored by the end of the century, a growth of 50%, based on a selection of CMIP models, although there are significant differences between different models. Most of this increase will be in the liquid reservoir as the sea ice volume shrinks. Presumably, most of liquid reservoir increase will occur in the Canada Basin, although it is presently unknown if the Beaufort Gyre has, or is approaching, a maximum capacity.

For the outflow fluxes, Fram Strait will probably transition to more liquid export—perhaps doubling by 2100—and less ice export, which may shrink to become just a minor term in the budget [*Vavrus et al.*, 2012]. The flux through Davis Strait is uncertain; one model projects that it will increase to 2070 as the outflow freshens and then decrease as its volume flux drops [*Vavrus et al.*, 2012]. *Haine et al.* [2015] project that the total Arctic FW outflow will increase this century but maybe by less than the FW sources go up. On this basis, the Arctic Ocean would be freshening in 2100, perhaps at a somewhat faster rate even than in the decade of the 2000s.

4.3. Key Drivers With Declining Sea Ice Cover

In addition to a net loss of FW content, the decline in sea ice cover may have additional effect for the Arctic FW storage and exports. Recently, a few model studies have suggested that the ongoing changes affecting the Arctic sea ice conditions (e.g., thinner and weaker sea ice pack and retreat from coastlines) might alter the efficiency of momentum transfer from the wind to the ocean through sea ice [*Shimada et al.*, 2006; *Martin et al.*, 2014; *Tsamados et al.*, 2014]. In the future, as the sea ice pack will tend to retreat further and for longer each year, the amount of energy input to the ocean from the wind forcing will likely increase as less energy is lost to internal ice stress. This will affect the storage of FW within the upper layers of the Beaufort Gyre as well as the depth of the underlying nutricline [*McLaughlin and Carmack*, 2010]. Using a simple process model, *Davis et al.* [2016] have shown that this possible change in momentum input at the ocean

surface might affect the magnitude of Ekman pumping and the rate of FW accumulation in the Beaufort Gyre, with implications for the FW exports to the lower latitude.

Additionally, as the wind will tend to input more energy to the ocean surface, this might increase the generation of internal waves and amount of vertical mixing, with the consequence of weakening the stratification of the water column [*Rainville et al.*, 2011] and enhance the vertical diffusive heat flux with possible implication for the sea ice cover [*Carmack et al.*, 2015b]. However, results from climate models project that competing effects might likely occur, with additional projected input of FW from river runoff and precipitations [*Bintanja and Selten*, 2014], that will tend to enhance even more the stratification in the surface layer and isolate the heat contained in the Atlantic Water layer from the sea ice cover. Using a 1-D process model, *Davis et al.* [2016] suggest that as long as the elevated vertical mixing is too small to fully erode the cold halocline, the enhanced stratification is likely to play a dominant role in the future, and the projected enhanced liquid FW storage in the Arctic might represent a negative feedback for the stability of the sea ice cover.

4.4. Arctic-Subarctic Coupling

The predicted increase in liquid FW export from the Arctic to the North Atlantic might have implication for the AMOC in the future, through its influence on the salinity of the surface water and thus on the rate of dense water formation in the subarctic convective regions [*Proshutinsky et al.*, 2002]. As a result of the Arctic sea ice disappearance in summer in a climate model forced with the least conservative Intergovernmental Panel on Climate Change scenario, *Jahn and Holland* [2013] suggest that the increase of liquid FW export would result in a 72% decrease of the AMOC intensity. It should be noted, however, that the link between changes of FW exports and AMOC intensity appears to be strongly model dependent and in particular depends upon the ability of models to realistically represent deep convection, which is often biased in coupled climate models (see *Lique et al.*, 2016).

Additionally, the predicted Arctic sea ice decline might also have consequences for the global-scale atmospheric circulation. Studies using climate models have suggested that part of the predicted intensification of the Arctic hydrological cycle happens in response of the sea ice decline [e.g., *Deser et al.*, 2010]. Moreover, the predicted change of equator-to-pole surface temperature gradient resulting from the sea ice disappearance might lead to a shift of the latitudinal position and the intensity of the jet stream and storm tracks [*Francis and Vavrus*, 2012; *Francis and Skific*, 2015; *Overland et al.*, 2011, 2015; *Barnes and Screen*, 2015], although the signal is not robust across the different CMIP5 models [*Harvey et al.*; *Vihma et al.*, 2016].

5. Cross-System Effects

Changes that occur within the ocean's freshwater system are linked to other components of the system [cf. *Francis et al.*, 2009] and are discussed in other papers of this volume. Key impacts and feedbacks according to whether they are due to freshening, warming, decreased sea ice coverage, or intensified ocean circulation are shown schematically in Figure 10 and discussed below.

5.1. Ocean-Atmosphere Interactions

Ocean-atmosphere interactions are reviewed by *Vihma et al.* [2016]. The continuing trend of sea ice loss has potential implications for both Arctic and midlatitude systems [*Screen et al.*, 2014; *Vihma*, 2014; *Cohen et al.*, 2014]. More extensive areas of open water over the ocean are projected to increase evaporation and hence increase precipitation over land drainage surfaces [*Vihma et al.*, 2016]. Sea ice loss has been linked to colder winters and snowfall over Eurasia [*Honda et al.*, 2009; *Inoue et al.*, 2012; *Liu et al.*, 2012] and to extreme cold events over North America [*Overland et al.*, 2011]. Some studies have suggested that the Arctic amplification of climate warming favors a weaker and more meandering jet stream, and this may have contributed to the extreme snow fall events in recent winters in the U.S. East Coast [e.g., *Francis and Vavrus*, 2012; *Francis and Skific*, 2015]. This subject is of great importance and remains under debate [see, for example, *Wallace et al.*, 2014], and while linkages have been found, many are regional and individual events are likely due to a combination of forcing responses and internal variability [*Overland et al.*, 2015; *Francis and Skific*, 2015; *Barnes and Screen*, 2015].

Figure 10. Schematic summarizing some of the potential impacts of changes in Arctic marine freshwater system among other system components. Impacts are colored depending on whether they are primarily a result of warming (orange), freshening (blue), decreased sea ice coverage (purple), or intensified ocean circulation (grey). This is not intended to be comprehensive but rather to illustrate the multifaceted nature of change in the Arctic freshwater system.

5.2. Ocean-Terrestrial Interactions

Ocean-terrestrial interactions are reviewed by *Bring et al.* [2016]. Among the major effects of ice loss and a warmer ocean are increased precipitation over land surfaces and increased flow to coastal oceans arising from permafrost thaw [*McClelland et al.*, 2004, 2014; *Bring et al.*, 2016]. Increased precipitation will, in turn, support Arctic greening, thus altering drainage basin hydrology [*Bhatt et al.*, 2014]. Groundwater discharges are likely to increase, but little systematic analysis has been carried out [see *Bobba et al.*, 2012]. While the fluvial flux of sediments to the Arctic Ocean are low, only about 1% of the global flux, owing to the low precipitation, thin weathering crust, low temperatures, and underlying permafrost, a model-based analysis by *Gordeev* [2006] suggests that for every 2°C of atmospheric warming a 30% increase in sediment flux will occur, and for every 20% increase in water discharge a 10% increase in sediment flux could follow.

5.3. Ocean-Terrestrial Ecology Interactions

Ocean-terrestrial ecology interactions are reviewed by *Wrona et al.* [2016]. Across the range of increasing latitude within the drainage systems a range of vegetation zones (biomes) exists according to temperature, moisture supply, permafrost, total degree days available for growth, and the duration of snow and ice cover. At any given location temporal variations in the above parameters are governed by changes in air temperature, precipitation, and snow cover depth. As reviewed by *Vihma et al.* [2016] and *Bring et al.* [2016], the accelerated retreat of sea ice from the coastal margins has opened up a new moisture supply to the

surrounding terrestrial landscape. Both mean annual air temperature and the winter snow depth in the Arctic coastal areas are likely related to summer sea ice extent. As one example, the Arctic tundra biome owes its existence to cold summer air masses associated with sea ice that keeps coastal summer temperatures below that required for tree growth; the warming and increased moisture flux associated with sea ice retreat will thus impact biome boundaries [*Wrona et al.*, 2016].

6. Major Knowledge Gaps and Future Research Directions

Major advances have been made over the past two decades toward understanding the sources, storage, and release of FW to the Arctic Ocean, as reviewed by *Haine et al*. [2015]. It is clear from this synthesis, however, that fundamental knowledge gaps still exist, both internal to the ocean and to the other components of the system, and that central questions remain unanswered. Among these are the following:

1. What key processes control Arctic Ocean FW delivery, transport, storage, and subsequent export back to the lower latitudes, and how will the relative importance of these processes change in the future under scenarios of climate warming and sea ice decline?
2. What role will other components of the FW system (atmospheric and terrestrial) play in terms of two-way interactions and cross-system feedbacks within the Arctic Ocean?
3. Will the melting of glacial ice (including Greenland) and thawing of permafrost substantially alter the FW budget and flow regimes of the Arctic Ocean and surrounding subarctic seas?
4. What quantitative roles do FW discharge into and recirculation within the subarctic Atlantic play in constraining the global thermohaline circulation?
5. What quantitative roles do additional FW discharges outside the defined gateways (e.g., from Hudson Bay, Labrador, and Gulf of St. Lawrence) play in system recirculation and in constraining the global thermohaline circulation?
6. Will the joint effects of sea ice decline and altered (accelerated?) hydrological processes have a significant effect on Northern Hemisphere weather and global climate?

To address these questions, we make the following specific recommendations.

6.1. Mapping of System Components

One cannot quantify change without solid monitoring, and one cannot monitor what has not been adequately mapped. In this case, our fundamental knowledge of Arctic Ocean hydrography, both spatially and temporally, remains rudimentary. Of all components of the AMS, the Nordic, Barents, Chukchi, and Beaufort seas are the best mapped, while large portions of the Canadian Arctic Archipelago and the Siberian Shelves are deficient, albeit the latter gap is in part due to insufficient attention to the Russian literature. The deep basin domains have decent coverage, with the exception to the Makarov Basin and the Amerasian Basin north of the Canadian Arctic Archipelago, where major holes in our understanding of boundary current pathways exist. The inner coastal domain inside the 10–20 m isobaths, where FW is initially discharged, where river plumes initially spread, where unique ecosystems exist and where many important biogeochemical transformations take place, is a near *tabula rasa* (but see http://nsidc/dataggd629). Discharges from hundreds of smaller rivers remain ungauged, and their collective effects of the biogeochemistry and their FW system are ignored. Despite ongoing efforts, potential discharges to the ocean from groundwater and thawing permafrost remain poorly quantified owing to the scale and complexity of the problem and lack a firm basis for defining a benchmark for future comparisons.

Mapping efforts that focus specifically on freshwater disposition must take into account the anticipated time variability (seasonal and interannual) and bulk residence times of the main storage layers (surface, halocline, and upper Atlantic waters) when designing programs. Here a mixed or "nested" strategy is advised: for example, short-term variability in the seasonal mixed layer and across steep bathymetry will require more frequent sampling and closer station spacing (sub-Rossby scale) but perhaps shallower casts (upper 200–400 m). Longer-term mapping will benefit from the development of new geochemical tracers to quantify the various sources of FW into and through the marine system and to track changes over time.

Survey cruise are infrequently coordinated, and a one-time, full synoptic survey of the Arctic Ocean, combining shelf and deep basin work, has never been conducted: this is unacceptable for such a small ocean (3% of the global ocean surface area). Once such a benchmark is carried out, we will be in a better position to plan and

prioritize sustained observational programs. To be globally meaningful, such a mapping undertaking must be linked to other observational programs in the bordering subarctic seas, both in the subarctic Pacific and Bering Sea, from which preconditioned waters enter through Bering Strait and in the convective gyre domains of the subarctic Atlantic that couple Arctic Ocean exports to the global thermohaline circulation.

6.2. Monitoring and Sustained Observations

Detection of change requires sustained monitoring. Time series data throughout the Arctic Ocean are extremely sparse, and because of this, it remains near impossible to distinguish variability and trends at different time scales. Here remote sensing approaches such as the ICESat (Ice, Cloud, and land Elevation Satellite) program for the ice component, GRACE (Gravity Recovery and Climate Experiment) for bulk FW estimates, SMOS (Soil Moisture and Ocean Salinity) for sea surface salinity provide year-round, basin-wide information on density, and ice freeboard (which gives sea ice mass) can assist tremendously. Such methods cannot, however, detect subsurface structures and fronts nor identify the individual sources (e.g., meteoritic versus ice melt) which require in situ mapping by ships, aircraft, and snow machines of upper ocean hydrographic and biogeochemical properties, circulation, and FW and heat fluxes throughout both shelf and basin domains; and parallel information provided year-round by Ice-Tethered Profilers (ITPs) of velocity, temperature, and salinity in the upper kilometer, autonomous underwater vehicles, gliders, and Ice Mass Balance buoys. Flagship programs such as the ice-based North Pole Environmental Observatory and the ship-based Beaufort Gyre Observing System/Joint Ocean Ice Study (BGOS/JOIS) and the Nansen and Amundsen Basins Observational system (NABOS) should continue.

At present, only two programs conduct sustained, ship-based regional-scale monitoring on the deep basins: the BGES/JOIS program in the Canada Basin (since 2003) and the NABOS program in the Nansen and Amundsen basins (since 2002); of the two, only BGOS/JOIS has freshwater as its core objective, with NABOS focused more on the circumpolar boundary current and heat flux dynamics. While not planned as such, NABOS records the "signal sent" record while BGES/JOIS records the "signal received" record via the Arctic circumpolar boundary current. Both programs must be continued to provide the "pulse" of the two contrasting basins and changes within the two distinct halocline structures.

Other components of the AFS also demand sustained observation. There is an immediate need to begin assessing and then monitoring FW on the shelves and, specifically, to answer the question of how much of the observed variability in basin inventories is due to transfer both from shelves to basins and from basins to shelves. As noted earlier, both the basins and the shelves are of near-equal FW volume.

Essential monitoring also includes the maintenance and expansion of essential long-term monitoring of upper ocean state at key gateways within the Arctic Ocean through moored arrays, hydrographic and biogeochemical measurements, and autonomous probes to provide a complete and continuous record of Arctic FW and heat fluxes. In addition, new sustained monitoring programs are required that will unambiguously link variability in freshwater fluxes observed at gateways to their impacts on subarctic gyre domains. While the existence of events such as the "Great Salinity Anomaly" are well established [*Dickson et al.*, 1988], and while impacts on the convective gyres has been hypothesized [*Proshutinsky et al.*, 2002], their indisputable sources and pathways within the AMS are still poorly known. As one example, the large change in the Arctic Oscillation index observed in 1989 [*Thompson and Wallace*, 1980] coincided with the relocation of the Atlantic/Pacific halocline front from the Lomonosov to the Alpha-Mendeleyev Ridge in ~1989–1990 [cf. *McLaughlin et al.*, 1996]; the subsequent loss of roughly 10^5 km^3 of Pacific origin waters from the Makarov Bain was accompanied by the occurrence of anomalous cold, freshwater in Davis Strait [*Lobb*, 2004], and the well-known collapse in 1991 of Atlantic Cod (a subarctic species) off Newfoundland. No observational system was in place then to evaluate a possible link between these events then nor is there one in place now to link upstream and downstream processes.

6.3. Knowledge Gaps in Fundamental Concepts and Processes

We require improved understanding of processes that control FW delivery, transport, storage, and discharge back to the lower latitudes, the role that other components of the system (atmospheric and terrestrial) play in terms of two-way interactions and system feedbacks, and the joint effects of sea ice decline and the accelerated hydrological cycle will have Northern Hemisphere weather and global climate. A fundamental rule is that observation-based knowledge of important processes (including those involved in feedbacks) is required to validate models and reduce uncertainty. Better understanding of along-shelf and cross-shelf

transport of river plumes and currents in relation to ice and wind conditions is required as is a better understanding of FW transfer from one shelf domain to another and from individual shelves into the basins.

New freshwater sources and their associated geochemical fluxes are emerging in the warming Arctic. These include enhanced and prolonged thawing of permafrost [*Bring et al.*, 2016] and melting of the Greenland ice cap. While the discharges of the major Arctic rivers, which have their headwaters in the midlatitudes, are currently gauged, the discharges coming from the huge number of small, true "Arctic" rivers remain ungauged. This is not acceptable if we are to detect rearrangement of fluxes within the full system. Further, an obvious fact is that all rivers discharge into shallow waters, where comfortable ships and icebreakers are unable to sample. Given the vast coastline of the Arctic Ocean and the anticipated geochemical (carbon and nutrient fluxes) and biological (new production, benthic diversity, and sea grass expansion), this is likewise unacceptable. New ways must be found and applied to explore, map, and conduct process studies in the shallow (depths less than 20 m) waters of the Arctic Ocean.

In terms of FW sources that are external to the Arctic Ocean, Greenland's freshwater discharge is projected to increase in a warming climate but the rate of increase is largely unknown—especially the contribution from ice discharge. Likewise, changes in the export of FW from Hudson Bay and the Gulf of St. Lawrence will track river discharge variability on decadal or longer timescales, but storage and release of FW within these basins may contribute to year-to-year variations.

The importance of deep-injection processes is unexamined. It is generally thought that freshwater from principle sources are supplied to the upper ocean and halocline layers. For example, the depth of the 34.8 isohaline used in reference salinity budgets lies at depths of 200–400 m (Figure 6b), and thus, freshwater components that might be injected below this depth are not currently included in budget assessments. *Aagaard and Woodgate* [2001] noted, however, that the high-latitude freezing and melting cycle can support freshwater injection into the interior of the Arctic Ocean, resulting in a secondary salinity minimum at about 800 m depth. This is because Atlantic water transiting the Barents Sea is both freshened and cooled to become the Barents Sea Branch, with about one third of the freshening due to ice melt. The degree of freshening (buoyancy gain) is largely compensated by the degree of cooling (buoyancy loss) so that there is a small increase in the density of water leaving the Barents Sea, thus allowing it to sink to depths near 800 m. They note the curious feature that freshwater distilled at the surface by freezing is reinjected at depth following melting. Since the Barents Sea Branch Water extends to substantial depth (perhaps 1600 m) in both the Eurasian and Amerasian basins, and because it has salinities above the classical 34.8 psu reference salinity, its role in the Arctic Ocean's freshwater budget requires consideration in future works.

A similar argument could be advanced for the Arctic Ocean deep waters below the sill depth of the Lomonosov Ridge. In both the Eurasian and Amerasian basins the deep water salinities, 34.91 and 34.95 psu, respectively, are higher that the classical reference salinity of 34.8 psu [but see *Dickson et al.*, 2007] but lower than that of Atlantic Waters crossing Fram Strait and the Barents Sea Opening, about 35.0 psu. Hence some injection of freshwater must occur somewhere to full water column depth.

Considerations of thermobaric processes are required to advance our understanding of the role of freshwater in convective processes and deepwater renewal. For example, it is generally thought that a freshened upper ocean acts to suppress deep convection and thus constrain the meridional overturning circulation, as it increases the buoyance of surface waters [*Lique et al.*, 2016]. However, as described in *Aagaard et al.* [1985], some addition of FW to the surface is, in fact, a necessary requirement for full-depth convection.

The connectivity of the hundreds of thousands of lakes within the Arctic drainage system [*Prowse et al.*, 2015a, 2015b] to the coastal ocean is completely unexamined. Much is made of the altered albedo of sea ice under scenarios of global warming, but no attention is paid to the same phenomena in lakes, where impacts may be equally significant [*Prowse et al.*, 2015a, 2015b]. For example, some are so-called karst lakes, meaning that they overly permafrost. As such, during the ice-free period, they act as "thermal drills" to thaw the underlying permafrost and thus release carbon products to the atmosphere. Programs that link high-latitude lakes to their drainage systems and thus to the coastal and shelf oceans, in terms of phenology, radiative heat exchange, discharge and biogeochemical fluxes are herein endorsed.

Expanded knowledge of cross-component interactions, including those with the atmosphere (e.g., how the wind drives the near-surface Arctic circulation, how that is mediated by sea ice, and how it is changing), and those with surrounding terrestrial systems (e.g., an accelerated hydrological cycle and interactions within the coastal

domain) would benefit the continued development, validation, and application of numerical capabilities focusing on improved parameterization of FW and heat flux mechanisms in coupled, cross-component climate models.

6.4. Defining the Meaning of "Freshwater"

The pressing question, "What defines meaningful reference salinity and does meaningful reference salinity even exist?" requires debate. The value 34.8 psu selected by *Aagaard and Carmack* [1989] has thus far proved useful and practical. *Carmack et al.* [2008]; however, note that depending on the specific application or ocean domain under consideration, other values may be more appropriate. As argued by *Tsubouchi et al.* [2012], *Bacon et al.* [2015], and here (Appendix A), the reference salinity concept is regime specific and nonrigorous. The selection of 34.8 psu, roughly the mean salinity of the Arctic Ocean (as deduced from available data in 1989) omits deep injection processes, as noted by *Aagaard and Woodgate* [2001], and any outflow products that may be recycled within the Nordic seas and injected back into the Arctic Ocean, leading perhaps to a "downward spiraling" of freshwater components. It also omits the injection of deep waters formed by convection in the Greenland and Norwegian seas back into the Arctic Ocean, rather than supposing that the full volume of water convective overturn water exiting via the Greenland-Scotland overflow; in this case the role of the thermobaric instability in drawing freshwater to full ocean depth is important.

7. Summary and Conclusions

FW delivery to the Arctic Ocean arises as a consequence of the transport northward of FW, demanded by the climate system to transport heat (in this case as latent heat) from the low to the high latitudes. It is supplied to the Arctic Ocean by moisture flux convergence above the ocean and adjacent drainage basins and by low-salinity anomalies from the Pacific Ocean. Future conditions under warming scenarios are likely to include increased runoff as well as increased inputs from glacial melt and permafrost, and changes in the phenology of discharge are also almost certain to occur [*Bring et al.*, 2016; *Instanes et al.*, 2016]. In this synthesis paper, we also recognize that the FW supply into the south of the conventional Arctic Ocean gateways is significant and may recirculate back into the Arctic Ocean or influence the convective gyres in the subarctic North Atlantic to impact the AMOC together with the outflow from the Arctic. This requires an expanded geographical domain for understanding of the Arctic Freshwater system. The larger-scale perspective of marine FW system should also improve our understanding of the ocean-atmosphere coupling at oceanic boundaries between salt-stratified ocean and temperature stratified ocean, which constrain the pathway of storm tracks.

In the Arctic Ocean interior, FW is stored in distinct, water mass reservoirs with different depth ranges, biogeochemical characteristics, and residence times. Significant changes in FW reservoirs have been observed in the 2000s: an increase in liquid FW, mostly in the Beaufort Gyre, and a decrease in the solid FW phase. Future loss of sea ice and increases in net precipitation, runoff, and Bering Strait FW flux are expected. Export of FW from the Arctic Ocean will also increase but by less than the increase in FW inputs. Resulting increase of 50% in FW storage is projected by the end of this century [*Haine et al.*, 2015]. This implies that the Arctic Ocean becomes of increasing importance in global FW cycle as a reservoir and as a deliverer.

The upper layers of the Arctic Ocean are undergoing major increases in the seasonal inventories of freshwater associated with the freeze (brine rejection) and melt (freshwater capping) cycle, and increased storage within the Beaufort Gyre associated with increased Ekman convergence. Will this trend in water volume storage and associated biogeochemical consequences associated with seasonal phase change continue under scenarios of increased global warming? We are presently on a parabolic curve connecting two zero values of freshwater phase change volume. One zero value would occur in the case of extreme cold and ice thickness, as may have existed in glacial periods, and the other would occur in the case of no winter ice formation. In all likelihood, sea ice will continue to form in winter, but its thickness will continue to diminish. Thus, the area of seasonal ice may increase while its thickness will decrease: the volume of freshwater involved in the annual freeze-melt cycle, ignoring for now the advected components, is the product of the two, but it is uncertain if we are presently on the ascending or descending branch of this curve [but see *Holland et al.*, 2008, Figure 7]. Clearly, programs that focus on the joint roles of atmosphere and ocean on sea ice decline are needed to improve model predictions [*Carmack et al.*, 2015a].

Within the Arctic Ocean almost all physical, biological, and geochemical processes are influenced by the local quantities and geochemical qualities of FW. Observed changes with the increase in FW storage during the 2000s include faster circulation, altered water mass distributions, increased surface heat content, increased sea level along the Siberian coast, decreased nutrient supply, changed algal communities toward smaller cell sizes, and enhanced ocean acidification. However, most observations are from summer time only and in limited region. Given the fact that the distribution of FW and its consequences are not uniform across the Arctic, improved strategy in observation is required. Coordinated pan-Arctic survey for mapping of FW and related parameters, not only in water but also in sea ice and atmosphere, will provide a comprehensive baseline to detect future changes and information to evaluate model simulations. Application of physical, biological, and chemical sensors on floating or moored platforms and autonomous vehicles as well as satellite-based observations will be especially useful to increase observations in space and time.

Of areas that remain virtually unexplored, the coastal area is of central importance. The coastal area acts as the initial connector between terrestrial and marine systems and the contiguous flow of FW in this domain (RCD) provide a coastal pathway for the dispersal and migration of marine biota. Furthermore, changes in this domain can directly affect activity of local communities in transportation, fishing, and hunting. As described in *Bring et al.* [2016] and *Wrona et al.* [2016], changes and shifts are being observed in terrestrial hydrology and ecosystem. Consequent changes in FW and geochemical fluxes from the land will be received first by the RCD. Because most sediment and dissolved terrestrial matters are removed in the freshwater-seawater mixing zone, processes in the RCD have fundamental implications in the fate of terrestrial materials and thus in future biological productivity and ocean acidification in the shelf seas. To address this important but not well-quantified domain, simultaneous observation and monitoring at both sides of the land-ocean boundary are essential in future research.

Lique et al. [2016] have elegantly structured their synthesis to describe the hierarchy of models, from conceptual to process to component to fully coupled. One class builds upon the other: good process models require a strong underpinning of conceptual models, and so on up. Our integrated knowledge of Arctic systems is flawed, and much effort is still required to improve conceptual models. Such models should be based on sound hydrodynamics (e.g., geostrophy, Ekman dynamics, and vorticity conservation) and extend cross discipline to biogeochemistry (e.g., stoichiometry, stable, and time-dependent tracers) and biological (phenology, biodiversity, pelagic-benthic coupling, and advective ecology) systems. Such conceptual models must seek to identify and distinguish among variability (natural and anthropogenic), trends (their statistical validity), and potential system transition nodes (e.g., tipping points and system flips). Great efforts and resources are being placed in the end product of this model hierarchy (the fully coupled models), but little coordinated effort (and resources) are being directed to the starting point; this should change. Conceptual models require continual refreshing. Without this effort at step one, existing conceptual paradigms may propagate through the system without update when new evidence points toward a more complex system.

In closing we ask, "Are the current trends of change observed in the ocean, its ice cover, its contributing watersheds, and its atmospheric heat and moisture fluxes sufficient to push this complex, coupled system into a new stable mode of behavior, with altered gyre configurations, modal jet stream structures, and storm track arrangements?" The answer is, "probably not," but the risk posed to our existing infrastructures, economies, and life support systems is of sufficient magnitude to warrant very deep consideration."

Appendix A: Improved Methodologies for Budget Formulation Incorporating Observations and Modeling Approaches

When considering ice and ocean FW transports, it is worth drawing an analogy with the calculation of anthropogenic carbon concentrations. In both cases—carbon, or pure water—the aim is to separate a small fraction of a material signal from the bulk of the signal, when there is no difference in principle between the material comprising the fraction and the bulk. In the case of anthropogenic carbon, the difference lies in the source of the material, not in its nature. This suggests a way forward for FW calculation, by answering two related questions. First, what is the source of the FW? Second, is there a unique definition of a FW flux from which a rigorous derivation of the desired quantity can be obtained?

The conventional ice or ocean FW transport calculation invariably entails a search for criteria (or more commonly, precedent) whereby a "reference salinity" can be adduced. Then a calculation like this can be performed:

$$F = (\delta S / S_{ref}) V_O \qquad (A1)$$

where F is a FW volume flux, S_{ref} is a reference salinity, V_O is a (saline) seawater volume flux, and $\delta S = S - S_{ref}$ is the difference between the salinity of that seawater (S) and S_{ref}. Using example values of $V_O = 5$ Sv, $S_{ref} = 35$ and $\delta S = 1$, we obtain $F = 143$ mSv. This is a simple scaling, in order to assert that ~3% of the pure water in a seawater transport is something called a "FW transport," and the outcome is critically dependent on the choice (and it is a choice) of S_{ref}. In Appendix A of *Tsubouchi et al.* [2012], it is shown formally that in the special case of a closed volume when mass is conserved, the result of such a calculation is very little sensitive to this choice. The requirement of mass conservation causes any (arbitrary) reference value to drop out of the numerator in (A1), leaving the only sensitivity in the denominator. Thus, for this special case, the error introduced by choosing for S_{ref} (say) 35.0 instead of 34.8 is 0.6%—negligible in practice. However, *Tsubouchi et al.* [2012] also illustrate the impact of different values of S_{ref} on FW flux calculation when mass is not conserved (their Figure 20). The resulting uncertainty is of the same order of magnitude as the signal. This is unsatisfactory.

To return to the questions posed above, there is a simple answer: the surface flux of FW is defined as the surface mass exchange, conventionally considered as the sum of three atmospheric and terrestrial inputs (positive or negative) to the ocean: i.e., precipitation, evaporation, and runoff. This is a unique definition, and a source (the surface) is identified. A surface implies a surface area, which can then be used to define an ocean volume. Combining Gauss' theorem with time-varying mass (volume) and salinity conservation statements applied to a closed ocean volume defined by the sea surface and sea bed for the top and bottom, and land and (presumed measured) sea ice and ocean around the sides, a rigorous definition of FW fluxes results. See *Bacon et al.* [2015], who obtain the following expressions:

$$F_{vol}^{surf} + F_{vol}^{io} = \dot{V} \qquad (A2)$$

$$F_{vol}^{surf} = \frac{\iint v' S' ds dz}{\overline{S}} + \dot{V} - \frac{1}{\overline{S}}\left[\frac{\partial}{\partial t} \iiint S dV\right] \qquad (A3)$$

Equation (A2) is a statement of volume conservation. The left-hand side (LHS) is the sum of the surface FW volume flux (F_{vol}^{surf}) and the ice-ocean boundary volume flux (F_{vol}^{io}). The right-hand side (RHS) is then the rate of change of the volume within the defined boundary ($\dot{V}$). Equation (A3) has the practical application. Here the LHS is again F_{vol}^{surf}, which is the quantity to be calculated. The three terms on the RHS are as follows. The first term performs the role of the "regular" calculation illustrated in equation (A1). However, instead of a reference salinity, there is a well-defined quantity: the boundary mean salinity, $\overline{S}$. Then the salinity anomaly is given by $S' = S - \overline{S}$ (S' is similar to δS). The ice and ocean velocity anomaly field (v') is similarly defined ($v' = v - \overline{v}$), where v is velocity and $\overline{v}$ is boundary mean velocity; z is depth and s is the along-boundary coordinate. This is the ice-ocean FW flux in the stationary case (no variation with time), as calculated by *Tsubouchi et al.* [2012]. It expresses how (e.g.) a net saline inflow to the defined volume is transformed into a fresh outflow from the volume by the net input of FW at the surface, thereby enabling the surface FW flux to be calculated from ice and ocean measurements around the volume's boundary. For the second term, $\dot{V}$ is again the rate of change of the volume within the defined boundary. The third term is the rate of change of salinity (which is impacted by concentration or dilution by FW storage) contained within the boundary. Both of these terms can also be measured. The rate of change of total seawater mass is measurable from space by a satellite-detecting change in gravity, such as GRACE [*Peralta-Ferriz and Morison*, 2014]. The rate of change of volume is measurable by a satellite-detecting change in sea surface height, which, in combination with gravity measurements, can be used to infer changes in stored FW (*Giles et al.* [2012], who use Envisat). The rate of change of stored salinity is measurable via an in situ census: *Rabe et al.* [2014], but this does not include measurements on the shelves. These calculations are all illustrated using output from an ice-ocean general circulation model in *Bacon et al.* [2015].

This procedure is rigorous, but it may have uncomfortable conclusions: first, the boundary mean salinity can change, so there is no fixed "reference" and second, the same boundary mean salinity appears in the "salinity

storage" term, but for the "census" element of the calculation, reference values are irrelevant because any constant term is eliminated by the time derivative. Only rates of change are important.

Given that the simple procedure illustrated in equation (A1) is likely to endure for some time, however, it is still possible to make a practical recommendation to improve the presentation of FW fluxes. It is very probable that FW fluxes calculated in this way will vary monotonically with S_{ref}. Therefore, to enable other users to extract from such published results FW fluxes with any (plausible) value of S_{ref}—or $\overline{S}$, in terms of equation (A3)—at least three sensibly chosen values of S_{ref} should be employed. After *Tsubouchi et al.* [2012], they might be 34.6, 34.8, and 35.0, for the Arctic; then any value could be well approximated by interpolation.

This framework can be employed to clarify the indicative Arctic FW budget outlined in section 2.3. This budget is intended to represent the long-term mean, so we take the stationary case of equation (A3) by dropping the time-varying terms. For the Arctic Ocean domain (section 2.1 and *Tsubouchi et al.* [2012]), the continuous integral around the boundary of velocity and salinity anomalies can be separated into contributions from the four gateways, Fram, Davis, and Bering Straits and the Barents Sea Opening:

$$F_{vol}^{surf} = F_{FS}^{bdy} + F_{BSO}^{bdy} + F_{BS}^{bdy} + F_{DS}^{bdy} \tag{A4}$$

and where F_X^{bdy} is the portion of the first integral on the RHS of equation (A3) between the along-boundary limits for the contribution to the surface flux due to gateway X. Note that Gauss' theorem defines directions relative to the volume, so that fluxes into the volume are positive and out of the volume are negative. The surface flux elements of section 2.3 (precipitation minus evaporation plus runoff) then sum to 6400 ± 500 km^3/yr (although the RMS uncertainty appears low). If we proceed to treat an ocean inflow of relatively fresh seawater (i.e., the Bering Strait) as a freshwater input to the Arctic, then we transfer F_{BS}^{bdy} from the RHS to the LHS of equation (A4). Note that the sign convention "works": an inflow is signed positive, and anomalously freshwater is signed negative, so that F_{BS}^{bdy} is intrinsically negative. Transferring to the LHS of equation (A4) means that the equivalent FW flux due to the Bering Strait then *adds* to F_{vol}^{surf}, for a total of 12,800 km^3/yr. Equation (A4) expresses how *all* ocean inflows to the Arctic are diluted by the surface FW flux to be become the outflows. Separating out Bering Strait changes the interpretation: now we are stating how *Atlantic* inflows are diluted both by surface fluxes and by the Pacific inflow to become the outflows.

References

Aagaard, K. (1989), A synthesis of the Arctic Ocean circulation, *Rapp. P. V. Reun. Cons. Int. Explor. Mer*, *1188*, 11–22.

Aagaard, K., and E. C. Carmack (1989), The role of sea ice and other fresh water in the Arctic circulation, *J. Geophys. Res.*, *94*(C10), 14,485–14,498, doi:10.1029/JC094iC10p14485.

Aagaard, K., and E. C. Carmack (1994), The Arctic Ocean and climate: A perspective, in *The Polar Oceans and Their Role in Shaping the Global Environment*, *Geophys. Monogr. Ser.*, vol. 85, edited by O. M. Johannessen, R. D. Muench, and J. E. Overland, pp. 5–20, AGU, Washington, D. C., doi:10.1029/GM085p0005.

Aagaard, K., and R. A. Woodgate (2001), Some thoughts on the freezing and melting of sea ice and their effects on the ocean, *Ocean Modell.*, *3*, 127–135.

Aagaard, K., L. Coachman, and E. Carmack (1981), On the halocline of the Arctic Ocean, *Deep Sea Res.*, *28*, 529–547.

Aagaard, K., J. H. Swift, and E. C. Carmack (1985), Thermohaline circulation in the Arctic Mediterranean Seas, *J. Geophys. Res.*, *90*, 4833–4846, doi:10.1029/JC090iC03p04833.

Aagaard, K., T. Weingartner, S. L. Danielson, R. A. Woodgate, G. C. Johnson, and T. E. Whitledge (2006), Some controls on flow and salinity in Bering Strait, *Geophys. Res. Lett.*, *33*, L19602, doi:10.1029/2006GL026612.

Arctic Climate Impact Assessment (2005), *Arctic Climate Impact Assessment*, Cambridge Univ. Press, Cambridge, U. K.

Aksenov, Y., V. V. Ivanov, A. J. G. Nurser, S. Bacon, I. V. Polyakov, A. C. Coward, A. C. Naveira-Garabato, and A. Beszczynska-Moeller (2011), The Arctic circumpolar boundary current, *J. Geophys. Res.*, *116*, C09017, doi:10.1029/2010JC006637.

Alexeev, V. A., and C. H. Jackson (2013), Polar amplification: Is atmospheric heat transport important?, *Clim. Dyn.*, *41*, 533–547, doi:10.1007/s00382-012-160-z.

Alkire, M. B., K. K. Falkner, I. Rigor, M. Steele, and J. Morison (2007), The return of Pacific waters to the upper layers of the central Arctic Ocean, *Deep Sea Res., Part I*, doi:10.1016/j.dsr.2007.06.004.

Arctic Monitoring and Assessment Program (AMAP) (2013), *AMAP Assessment 2013: Arctic Ocean Acidification*, AMAP, Oslo, Norway.

Amundrud, T. L., H. Melling, and R. G. Ingram (2004), Geometrical constraints on the evolution of ridged sea ice, *J. Geophys. Res.*, *109*, C06005, doi:10.1029/2003JC002251.

Amundrud, T. L., H. Melling, R. G. Ingram, and S. E. Allen (2006), The effect of structural porosity on the ablation of sea ice ridges, *J. Geophys. Res.*, *111*, C06004, doi:10.1029/2005JC002895.

Anderson, L. G., S. Jutterström, S. Kaltin, E. P. Jones, and G. Björk (2004), Variability in river runoff distribution in the Eurasian Basin of the Arctic Ocean, *J. Geophys. Res.*, *109*, C01016, doi:10.1029/2003JC001773.

Anderson, L. G., T. Tanhua, G. Björk, S. Hjalmarsson, E. P. Jones, S. Jutterström, B. Rudels, J. H. Swift, and I. Wåhlstöm (2010), Arctic Ocean shelf–basin interaction: An active continental shelf CO_2 pump and its impact on the degree of calcium carbonate solubility, *Deep Sea Res.*, *57*(7), 869–879.

Anderson, L. G., G. Björk, S. Jutterström, I. Pipko, N. Shakhova, I. Semiletov, and I. Wåhlström (2011), East Siberian Sea, an Arctic region of very high biogeochemical activity, *Biogeosciences*, *8*(6), 1745–1754.

Ardyna, M., M. Babin, M. Gosselin, E. Devred, L. Rainville, and J.-É. Tremblay (2014), Recent Arctic Ocean sea ice loss triggers novel fall phytoplankton blooms, *Geophys. Res. Lett.*, *41*, 6207–6212, doi:10.1002/2014GL061047.

Arrigo, K. R., and G. L. van Dijken (2011), Secular trends in Arctic Ocean net primary production, *J. Geophys. Res.*, *116*, C09011, doi:10.1029/2011JC007151.

Arzel, O., T. Fichefet, and H. Goosse (2007), Causes and impacts of changes in the Arctic freshwater budget during the twentieth and twenty-first centuries in an AOGCM, *Clim. Dyn.*, doi:10.1007/s00382-007-0258-5.

Ashik, I. M., V. V. Ivanov, H. Kassens, M. S. Makhotin, I. V. Polyakov, L. A. Timokhov, I. E. Frolov, and J. Holemann (2015), Major results of oceanographic studies of the Arctic Ocean during the last decade: Problems of the Arctic and Antarctic [in Russian], *Prob. Arct. Antarct.*, *1*(103), 42–56.

Azetsu-Scott, K., A. Clarke, K. Falkner, J. Hamilton, E. P. Jones, C. Lee, B. Petrie, S. Prinsenberg, M. Starr, and P. Yeats (2010), Calcium carbonate saturation states in the waters of the Canadian Arctic Archipelago and the Labrador Sea, *J. Geophys. Res.*, *115*, C11021, doi:10.1029/2009JC005917.

Azetsu-Scott, K., M. Starr, Z. P. Mei, and M. Granskog (2014), Low calcium carbonate saturation state in an Arctic inland sea having large and varying fluvial inputs: The Hudson Bay system, *J. Geophys. Res. Oceans*, *119*, 6210–6220, doi:10.1002/2014JC009948.

Bacon, S., G. Reverdin, I. Rigor, and H. M. Snaith (2002), A freshwater jet on the East Greenland Shelf, *J. Geophys. Res.*, *107*(C7), 3068, doi:10.1029/2001JC000935.

Bacon, S., A. Marshall, N. P. Holliday, Y. Aksenov, and S. R. Dye (2014), Seasonal variability of the East Greenland Coastal Current, *J. Geophys. Res. Oceans*, *119*, 3967–3987, doi:10.1002/2013JC009279.

Bacon, S., Y. Aksenov, S. Fawcett, and G. Madec (2015), Arctic mass, freshwater and heat fluxes: Methods, and modelled seasonal variability, *Philos. Trans. R. Soc., A*, *373*, 20140169, doi:10.1098/rsta.2014.0169.

Bamber, J., M. van den Broeke, J. Ettema, J. Lenaerts, and E. Rignot (2012), Recent large increases in freshwater fluxes from Greenland into the North Atlantic, *Geophys. Res. Lett.*, *39*, L19501, doi:10.1029/2012GL052552.

Barber, D. G., R. Galley, M. G. Asplin, R. De Abreu, K.-A. Warner, M. Pucko, M. Gupta, S. Prinsenberg, and S. Julien (2009), Perennial pack ice in the southern Beaufort Sea was not as it appeared in the summer of 2009, *Geophys. Res. Lett.*, *36*, L24501, doi:10.1029/2009GL041434.

Barnes, E. A. (2013), Revisiting the evidence linking Arctic amplification to extreme weather in midlatitudes, *Geophys. Res. Lett.*, *40*, 4728–4733, doi:10.1002/grl.50788.

Barnes, E. A., and J. A. Screen (2015), The impact of Arctic warming on the midlatitude jet-stream: Can it? Has it? Will it?, *WIREs Clim. Change*, *6*, 277–286, doi:10.1002/wcc.337.

Bates, N. R., J. T. Mathis, and L. Cooper (2009), Ocean acidification and biologically induced seasonality of carbonate mineral saturation states in the western Arctic Ocean, *J. Geophys. Res.*, *114*, C11007, doi:10.1029/2008JC004862.

Bates, N. R., M. I Orchowska, R. Garley, and J. T. Mathis (2013), Summertime calcium carbonate undersaturation in shelf waters of the western Arctic Ocean—How biological processes exacerbate the impact of ocean acidification, *Biogeosciences*, *10*(8), 5281–5309.

Bekryaev, R. V., I. V. Polyakov, and V. A. Alexeev (2010), Role of polar amplification in long-term surface air temperature variations and modern arctic warming, *J. Clim.*, *23*(14), 3888–3906.

Beszczynska-Möller, A., R. A. Woodgate, C. Lee, H. Melling, and M. Karcher (2011), A synthesis of exchanges through the main oceanic gateways to the Arctic Ocean, *Oceanography*, *24*(3), 82–99, doi:10.5670/oceanog.2011.59.

Bhatia, M. P., E. B. Kujawinski, S. B. Das, C. F. Breier, P. B. Henderson, and M. A. Charette (2013), Greenland meltwater as a significant and potentially bioavailable source of iron to the ocean, *Nat. Geosci.*, *6*, 274–278, doi:10.1038/ngeo1746.

Bhatt, U. S., et al. (2014), Implications of Arctic sea ice decline for the Earth system, *Ann. Rev. Environ. Resour.*, *39*, 12.1–12.33, doi:10.1146/annurev-environ-122012-094357.

Bintanja, R., and F. M. Selten (2014), Future increases in Arctic precipitation linked to local evaporation and sea-ice retreat, *Nature*, *509*, 479–482, doi:10.1038/nature13259.

Bluhm, B. A., K. N. Kosobokoba, and E. C. Carmack (2015), A tale of two basins: An integrated physical and biological perspective of the deep Arctic Ocean, *Prog. Oceanogr.*, doi:10.1016/j.pocean.2015.07.011.

Bobba, A. G., P. A. Chambers, and F. J. Wrona (2012), Submarine groundwater discharge (SGWD): An unseen yet potentially important coastal phenomenon in Canada, *Nat. Hazards*, *60*, 991–1012, doi:10.1007/s11069-011-9884-7.

Bourke, R. H., and R. P. Garrett (1987), Sea ice thickness distribution in the Arctic Ocean, *Cold Reg. Sci. Technol.*, *13*(3), 259–280.

Bring, A., I. Fedorova, Y. Dibike, L. Hinzman, J. Mård, S. H. Mernild, T. Prowse, O. Semenova, S. L. Stuefer, and M.-K. Woo (2016), Arctic terrestrial hydrology: A synthesis of processes, regional effects, and research challenges, *J. Geophys. Res. Biogeosci.*, *121*, doi:10.1002/2015JG003131.

Brown, R. D., and P. Coté (1992), Inter-annual variability of land-fast ice thickness in the Canadian High Arctic, 1950–89, *Arctic*, *45*, 273–284.

Bulgakov, N. P. (1962), Determination of functional graphs of the time at which water reaches the freezing point and the depth of density mixing, *Probl. North*, *4*, 141–148.

Cai, W. J., et al. (2010), Decrease in the CO_2 uptake capacity in an ice-free Arctic Ocean basin, *Science*, *329*(5991), 556–559.

Carmack, E., and D. C. Chapman (2003), Wind-driven shelf/basin exchange on an Arctic shelf: The joint roles of ice cover extent and shelf-break bathymetry, *Geophys. Res. Lett.*, *30*(14), 1778, doi:10.1029/2003GL017526.

Carmack, E., et al. (2015a), Towards quantifying the increasing role of oceanic heat in sea ice loss in the new Arctic, *Bull. Am. Meteorol. Soc.*, doi:10.1175/BAMS-D-13-00177.1.

Carmack, E. C. (2000), The freshwater budget of the Arctic Ocean: Sources, storage and sinks, in *The Freshwater Budget of the Arctic Ocean*, *NATO Adv. Res. Ser.*, edited by E. L. Lewis, pp. 91–126, Kluwar Acad., Dordrecht, Netherlands.

Carmack, E. C. (2007), The alpha/beta ocean distinction: A perspective on freshwater fluxes, convection, nutrients and productivity in high-latitude seas, *Deep Sea Res., Part II*, *54*(23–26), 2578–2598, doi:10.1016/j.dsr2.2007.08.018.

Carmack, E. C., and E. A. Kulikov (1998), Wind-forced upwelling and internal Kelvin wave generation in Mackenzie Canyon, Beaufort Sea, *J. Geophys. Res.*, *103*(C9), 18,447–18,458, doi:10.1029/98JC00113.

Carmack, E. C., and F. A. McLaughlin (2001), Arctic Ocean change and consequences to biodiversity: A perspective on linkage and scale, *Mem. Natl. Inst. Polar Res.*, *54*, 365–375.

Carmack, E. C., and F. A. McLaughlin (2011), Towards recognition of physical and geochemical change in subarctic and arctic seas, *Progress Oceanogr.*, *90*, 90–104, doi:10.1016/j.pocean.2011.02.007.

Carmack, E. C., and P. Wassmann (2006), Food-webs and physical biological coupling on pan-arctic shelves: Perspectives, unifying concepts and future research, *Prog. Oceanogr.*, *71*, 446–477.

Carmack, E. C., K. Aagaard, J. H. Swift, R. W. MacDonald, F. A. McLaughlin, E. P. Jones, R. G. Perkin, J. N. Smith, K. M. Ellis, and L. R. Killius (1997), Changes in temperature and tracer distributions within the Arctic Ocean: Results from the 1994 Arctic Ocean section, *Deep Sea Res., Part II*, *44*(8), 1487–1502.

Carmack, E. C., R. W. Macdonald, and S. Jasper (2004), Phytoplankton productivity on the Canadian Shelf of the Beaufort Sea, *Mar. Ecol. Prog. Ser.*, *277*, 37–50.

Carmack, E. C., F. A. McLaughlin, M. Yamamoto-Kawai, M. Itoh, K. Shimada, R. Krishfield, and A. Proshutinsky (2008), Freshwater storage in the Northern Ocean and the special role of the Beaufort Gyre, in *Arctic–Subarctic Ocean Fluxes, Defining the Role of the Northern Seas in Climate*, edited by R. R. Dickson, J. Meincke, and P. Phines, pp. 145–169, Springer, Dordrecht, Netherlands.

Carmack, E. C., F. A. McLaughlin, S. Vagle, H. Melling, and W. J. Williams (2010), Structures and property distributions in the three oceans surrounding Canada in 2007: A basis for a long-term ocean climate monitoring strategy, *Atmos. Ocean*, *48*(4), 211–224.

Carmack, E. C., P. Winsor, and W. Williams (2015b), The contiguous panarctic Riverine Coastal Domain: A unifying concept, *Prog. Oceanogr.*, doi:10.1016/j.pocean.2015.07.014.

Casper, A. F., M. Rautio, C. Martineau, and W. F. Vincent (2014), Variation and assimilation of Arctic riverine seston in the pelagic food web of the Mackenzie River Delta and Beaufort Sea transition zone, *Estuaries Coasts*, doi:10.1007/s12237-014-9917-z.

Cavalieri, D. J., and C. L. Parkinson (2012), Arctic sea ice variability and trends, 1979–2010, *Cryosphere*, *6*, 881–889.

Chapman, D. C., and S. J. Lentz (1994), Trapping of a coastal density front by the bottom boundary layer, *J. Phys. Oceanogr.*, *24*, 1464–1479.

Chierici, M., and A. Fransson (2009), Calcium carbonate saturation in the surface water of the Arctic Ocean: Undersaturation in freshwater influenced shelves, *Biogeosciences*, *6*, 2421–2431.

Chierici, M., A. Fransson, B. Lansard, L. A. Miller, A. Mucci, E. Shadwick, H. Thomas, J.-E. Tremblay, and T. N. Papakyriakou (2011), Impact of biogeochemical processes and environmental factors on the calcium carbonate saturation state in the Circumpolar Flaw Lead in the Amundsen Gulf, Arctic Ocean, *J. Geophys. Res.*, *116*, C00G09, doi:10.1029/2011JC007184.

Codispoti, A., V. Kelly, A. Thessen, P. Matrai, S. Suttles, V. Hill, and B. Light (2013), Synthesis of primary production in the Arctic Ocean: III. Nitrate and phosphate based estimates of net community production, *Prog. Oceanogr.*, *110*, 126–150, doi:10.1016/j.pocean.2012.11.006.

Cohen, J., et al. (2014), Recent Arctic amplification and extreme mid-latitude weather, *Nat. Geosci.*, *7*, 627–637.

Comeau, S., S. Alliouane, and J. P. Gattuso (2012), Effects of ocean acidification on overwintering juvenile Arctic pteropods *Limacina helicina*, *Mar. Ecol. Prog. Ser.*, *456*, 279–284.

Comiso, J. C. (2012), The rapid decline of multiyear ice cover, *J. Clim.*, *25*, doi:10.1175/JCLI-D-11-00113.1.

Cooper, L. W., J. W. McClelland, R. M. Holmes, P. A. Raymond, J. J. Gibson, K. Guay, and B. J. Peterson (2008), Flow-weighted values of runoff tracers (δ^{18}O, DOC, Ba, alkalinity) from the six largest Arctic rivers, *Geophys. Res. Lett.*, *35*, L18606, doi:10.1029/2008GL035007.

Craig, P. (1984), Fish use of coastal waters of the Alaskan Beaufort Sea, *Trans. Am. Fish. Soc.*, *113*, 265–282.

Cummins, P. F., D. R. Topham, and H. D. Pite (1994), Simulated and experimental two-layer flows past isolated two-dimensional obstacles, *Fluid Dyn. Res.*, *14*, 105–119.

Curry, B., C. M. Lee, and B. Petrie (2011), Volume, freshwater, and heat fluxes through Davis Strait, 2004–05, *J. Phys. Oceanogr.*, *41*(3), 429–436.

Curry, B., C. M. Lee, B. Petrie, R. E. Moritz, and R. Kwok (2015), Multiyear volume, liquid freshwater, and sea ice transports through Davis Strait, 2004–10, *J. Phys. Oceanogr.*, *44*, 1244–1266, doi:10.1175/JPO-D-13-0177.1.

Curry, R. G., and C. Maurizen (2005), Dilution of the northern North Atlantic Ocean in recent decades, *Science*, *308*, 1772–1774.

Dai, A., and K. E. Trenberth (2002), Estimates of freshwater discharge from continents: Latitudinal and seasonal variations, *J. Hydrometeorol.*, *3*, 660–687.

Danielson, S. L., T. W. Weingartner, K. Hedstrom, K. Aagaard, R. Woodgate, E. Curchitser, and P. Stabeno (2014), Coupled wind-forced controls of the Bering–Chukchi shelf circulation and the Bering Strait through-flow: Ekman transport, continental shelf waves, and variations of the Pacific–Arctic sea surface height gradient, *Prog. Oceanogr.*, doi:10.1016/j.pocean.2014.04.006.

Davis, P.E.D., C. Lique, H. L. Johnson, and G. D. Guthrie (2016), Competing effects of elevated vertical mixing and increased freshwater input on the stratification and sea ice cover in a changing Arctic Ocean. *J. Phys. Oceanogr.*, doi:10.1175/JPO-D-15-0174.1.

Denisenko, N. V., E. Rachor, and S. G. Denisenko (2003), Benthic fauna of the southern Kara Sea, in *Siberian River Run-Off in the Kara Sea*, edited by R. Stein et al., pp. 213–236, Elsevier, Amsterdam.

Denisenko, S., H. Sandler, N. Denisenko, and E. Rachor (1999), Current state in two estuarine bays of the Barents and Kara Seas, *J. Mar. Syst.*, *56*, 187–193.

Déry, S. J., M. Stieglitz, E. C. McKenna, and E. F. Woods (2005), Characteristics and trends of river discharge into Hudson, James and Ungava Bays, 1964–200, *J. Clim.*, *18*, 2540–2557.

Déry, S. J., M. A. Hernández-Henríquez, J. E. Burford, and E. F. Wood (2009), Observational evidence of an intensifying hydrological cycle in northern Canada, *Geophys. Res. Lett.*, *36*, L13402, doi:10.1029/2009GL038852.

Déry, S. J., T. J. Mlynowksi, M. A. Hernandez-Henriquez, and F. Straneo (2011), Interannual variability and interdecadal trends in Hudson Bay streamflow, *J. Mar. Syst.*, *88*, 341–351.

Deser, C., R. Tomas, A. Alexander, and D. Lawrence (2010), The seasonal atmospheric response to projected Arctic sea ice loss in the late 21st century, *J. Clim.*, *23*, 333–351, doi:10.1175/2009JCLI3053.1.

Deubel, H., et al. (2003), The southern Kara Sea ecosystem: Phytoplankton, zooplankton and benthos communities influenced by river run-off, in *Siberian River Run-Off in the Kara Sea*, edited by R. Stein et al., pp. 237–275, Elsevier, Amsterdam, Netherlands.

Dickson, R. R., J. Meincke, S. A. Malmberg, and A. J. Lee (1988), The great salinity anomaly in the North Atlantic, *Nature*, *256*(5517), 479–482.

Dickson, R. R., S. Dye, M. Karcher, J. Meincke, B. Rudels, and I. Yashayaev (2007), Current estimates of freshwater flux through Arctic and Subarctic seas, *Prog. Oceanogr.*, *73*, 210–230, doi:10.1016/j.pocean.2006.12.003.

Dickson, R. R., J. Meincke, and P. Rhines (2008), Arctic–subarctic ocean fluxes: Defining the role of the northern seas in climate—A general introduction, in *Arctic–Subarctic Ocean Fluxes: Defining the Role of the Northern Seas in Climate*, edited by R. R. Dickson, J. Meincke, and P. Rhines, pp. 1–13, Springer, Dordrecht, Netherlands.

Dittmar, T., and G. Kattner (2003), The biogeochemistry of the river and shelf ecosystem of the Arctic Ocean: A review, *Mar. Chem.*, *83*, 103–120.

Divine, L. M., K. Iken, and B. A. Bluhm (2015), Regional benthic food web structure on the Alaska Beaufort Sea shelf, *Mar. Ecol. Prog. Ser.*, *531*, 15–32.

Dmitrenko, I. A., S. A. Kirillov, and L. B. Tremblay (2008), The long-term and interannual variability of summer freshwater storage over the eastern Siberian Shelf: Implication for climatic change, *J. Geophys. Res.*, *113*, C03007, doi:10.1029/2007JC004304.

Dmitrenko, I. A., V. V. Ivanov, S. A. Kirillov, E. L. Vinogradova, S. Torres-Valdes, and D. Bauch (2011), Properties of the Atlantic derived halocline waters over the Laptev Sea continental margin: Evidence from 2002 to 2009, *J. Geophys. Res.*, *116*, C10024, doi:10.1029/2011JC007269.

Dmitrenko, I. A., B. Rudels, S. A. Kirillov, Y. O. Aksenov, V. S. Lien, V. V. Ivanov, U. Schauer, I. V. Polyakov, A. Coward, and D. G. Barber (2015), Atlantic water flow into the Arctic Ocean through the St. Anna Trough in the northern Kara Sea, *J. Geophys. Res. Oceans*, *120*, 5158–5178, doi:10.1002/2015JC010804.

Dolotov, Y. S., V. N. Kovalenko, V. K. Lifshits, M. P. Petrov, A. V. Platonov, R. Prego, T. N. Rat'kova, N. N. Filatov, and V. P. Shevchenko (2002), On the dynamics of water and suspension in the Keret' River estuary, Karelian coast of the White Sea, *Oceanology*, *42*, 731–740.

Drinkwater, K. F., and G. C. Harding (2001), Effects of the Hudson Strait outflow on the biology of the Labrador shelf, *Can. J. Fish. Aquat. Sci.*, *58*, 171–184.

Dukhovskoy, D., M. Johnson, and A. Proshutinsky (2004), Arctic decadal variability: An auto-oscillatory system of heat and fresh water exchange, *Geophys. Res. Lett.*, *31*, L03302, doi:10.1029/2003GL019023.

Dumas, J., E. Carmack, and H. Melling (2005), Climate change impacts on the Beaufort shelf landfast ice, *Cold Reg. Sci. Technol.*, *42*(1), 41–51.

Dunton, K. H., T. Weingartner, and E. C. Carmack (2006), The nearshore western Beaufort Sea ecosystem: Circulation and importance of terrestrial carbon in Arctic coastal food webs, *Prog. Oceanogr.*, *71*(2–4), 362–378.

Dunton, K. H., S. V. Schonberg, and L. W. Cooper (2012), Food web structure of the Alaskan nearshore shelf and estuarine lagoons of the Beaufort Sea, *Estuaries Coasts*, *35*(2), 416–435.

Durack, P. J., and S. E. Wijffels (2010), Fifty year trends in global ocean salinities and their relationship to broad scale warming, *J. Clim.*, *23*, 4342–4362.

Dyurgerov, M., A. Bring, and G. Destouni (2010), Integrated assessment of changes in freshwater inflow to the Arctic Ocean, *J. Geophys. Res.*, *115*, D12116, doi:10.1029/2009JD013060.

Ekman, V. W. (1904), On Dead-water: Being a description of the so-called phenomenon often hindering the headway and navigation of ships in Norwegian fjords and elsewhere, and an experimental investigation of its causes etc. AW Brøgger, 152 p.

Ekwurzel, B., P. Schlosser, R. A. Mortlock, and R. G. Fairbanks (2001), River runoff, sea ice meltwater, and Pacific water distribution and mean residence times in the Arctic Ocean, *J. Geophys. Res.*, *106*(C5), 9075–9092, doi:10.1029/1999JC000024.

Enderlin, E. M., I. M. Howat, S. Jeong, M.-J. Noh, J. H. van Angelen, and M. R. van den Broeke (2014), An improved mass budget for the Greenland ice sheet, *Geophys. Res. Lett.*, *41*, 866–872, doi:10.1002/2013GL059010.

Falck, E., G. Kattner, and G. Budéus (2005), Disappearance of Pacific Water in the northwestern Fram Strait, *Geophys. Res. Lett.*, *32*, L14619, doi:10.1029/2005GL023400.

Fichot, G. G., K. Kaise, S. B. Hooker, R. M. W. Amon, M. Babin, S. Bélanger, S. A. Walker, and R. Benner (2013), Pan-Arctic distributions of continental runoff in the Arctic Ocean, *Sci. Rep.*, *3*, 1053, doi:10.1038/srep01053.

Flato, G. M., and R. D. Brown (1996), Variability and climate sensitivity of landfast Arctic sea ice, *J. Geophys. Res.*, *101*(C11), 25,767–25,777, doi:10.1029/96JC02431.

Fowler, C., W. Emery, and M. Tschudi (2013), Polar pathfinder daily 25 km EASE-grid sea ice motion vectors. Version 2. Tech. Rep., Natl. Snow and Ice Data Cent., Boulder, Colo.

Francis, J. A., and S. J. Vavrus (2012), Evidence linking Arctic amplification to extreme weather in mid-latitudes, *Geophys. Res. Lett.*, *39*, L06801, doi:10.1029/2012GL051000.

Francis, J. A., D. M. White, J. J. Cassano, W. J. Gutowski Jr., L. D. Hinzman, M. M. Holland, M. A. Steele, and C. J. Vorosmarty (2009), An arctic hydrologic system in transition: Feedbacks and impacts on terrestrial, marine, and human life, *J. Geophys. Res.*, *114*, G04019, doi:10.1029/2008JG000902.

Francis, J., and N. Skific (2015), Evidence linking rapid Arctic warming to mid-latitude weather patterns, *Philos. Trans. R. Soc., A*, *373*, doi:10.1098/rsta.2014.0170.

Frey, K. E., and J. W. McClelland (2009), Impacts of permafrost degradation on arctic river biogeochemistry, *Hydrol. Processes*, *23*(1), 169–182.

Gardner, A. S., et al. (2013), A reconciled estimate of glacier contributions to sea level rise: 2003 to 2009, *Science*, *340*, 852–857.

Garneau, M.-È., W. F. Vincent, R. Terrado, and C. Lovejoy (2009), Importance of particle-associated bacterial heterotrophy in a coastal Arctic ecosystem, *J. Mar. Syst.*, *75*(1–2), 185–197.

Garvine, R. W. (1995), A dynamical system for classifying buoyant coastal discharges, *Cont. Shelf Res.*, *15*(13), 1585–1596.

Giles, K. A. S., W. A. Laxon, L. Ridout, D. J. Wingham, and S. Bacon (2012), Western Arctic Ocean freshwater storage increased by wind-driven spin-up of the Beaufort Gyre, *Nat. Geosci.*, *5*, 194–197.

Gleick, P. H. (2000), *The World's Water 2000– 2001*, pp. 39–61, Island Press, Washington, D. C.

Goñi, M. A., A. E. O'Connor, Z. Z. Kuzyk, M. B. Yunker, C. Gobeil, and R. W. Macdonald (2013), Distribution and sources of organic matter in surface marine sediments across the North American Arctic margin, *J. Geophys. Res. Oceans*, *118*, 4017–4035, doi:10.1002/jgrc.20286.

Gordeev, V. V. (2006), Fluvial sediment flux to the Arctic Ocean, *Geomorphology*, *80*, 94–104, doi:10.1016/j.geomorph.2005.09.008.

Gradinger, R., B. Bluhm, and K. Iken (2010), Arctic sea ice ridges—Safe havens for sea ice fauna during periods of extreme ice melt?, *Deep Sea Res., Part II*, *57*, 86–95.

Grebmeier, J. M., et al. (2015), Ecosystem characteristics and processes facilitating persistent macrobenthic biomass hotspots and associated benthivory in the Pacific Arctic, *Prog. Oceanogr.*, *136*, 92–114.

Greene, C. H., and P. J. Pershing (2007), Climate drives sea change, *Science*, *315*, 1084–1085, doi:10.1126/science.1136495.

Griffiths, R. W., and P. F. Linden (1981), The stability of buoyancy driven currents, *Dyn. Atmos. Oceans*, *5*, 281–306.

Guay, C. K., and K. K. Falkner (1997), Barium as a tracer of Arctic halocline and river waters, *Deep Sea Res., Part II*, *44*(8), 1543–1569.

Guay, C. K., K. K. Falkner, R. D. Muench, M. Mensch, M. Frank, and R. Bayer (2001), Wind-driven transport pathways for Eurasian Arctic river discharge, *J. Geophys. Res.*, *106*, 11,469–11,480, doi:10.1029/2000JC000261.

Guay, C. K., F. A. McLaughlin, and M. Yamamoto-Kawai (2009), Differentiating fluvial components of upper Canada Basin waters on the basis of measurements of dissolved barium combined with other physical and chemical tracers, *J. Geophys. Res.*, *114*, C00A09, doi:10.1029/2008JC005099.

Guéguen, C., L. Guo, M. Yamamoto-Kawai, and N. Tanaka (2007), Colored dissolved organic matter dynamics across the shelf-basin interface in the western Arctic Ocean, *J. Geophys. Res.*, *112*, C05038, doi:10.1029/2006JC003584.

Haak, H., J. Jungclaus, U. Mikolajewicz, and M. Latif (2003), Formation and propagation of great salinity anomalies, *Geophys. Res. Lett.*, *30*(9), 1473–1476, doi:10.1029/2003GL017065.

Haine, T. W. N., et al. (2015), Arctic freshwater export: Status, mechanisms, and prospects, *Global Planet. Change*, *125*, 13–35, doi:10.1016/j.gloplacha.2014.11.013.

Harvey, B. J., L. C. Shaffrey, and T. J. Woolings (2014), Equator-to-pole temperature differences and the extra-tropical storm track responses of the CMIP5 climate models, *Clim. Dyn.*, *43*, 1171–1182.

Hinzman, L., C. Deal, A. D. McGuire, I. V. Polyakov, and J. E. Walsh (2013), Trajectory of the Arctic as an integrated system, *Ecol. Appl.*, *23*(8), 1837–1868.

Holland, M. M., M. C. Serreze, and J. Stroeve (2008), The sea ice mass budget of the Arctic and its future change as simulated by coupled climate models, *Clim. Dyn.*, doi:10.1007/s00382-008-0493-4.

Holmes, R. M., J. W. McClelland, P. A. Raymond, B. B. Frazer, B. J. Peterson, and M. Stieglitz (2008), Lability of DOC transported by Alaskan rivers to the Arctic Ocean, *Geophys. Res. Lett.*, *35*, L03402, doi:10.1029/02007GL032837.

Holmes, R. M., et al. (2012), Seasonal and annual fluxes of nutrients and organic matter from large rivers to the Arctic Ocean and surrounding seas, *Estuaries Coasts*, *35*, 369–382.

Honda, M., J. Inoue, and S. Yamane (2009), Influence of low Arctic sea-ice minima on anomalously cold Eurasian winters, *Geophys. Res. Lett.*, *36*, L08707, doi:10.1029/2008GL037079.

Huntington, T. (2006), Evidence for intensification of the global water cycle: Review and synthesis, *J. Hydrol.*, *319*(1–4), 83–95.

Inoue, J., M. E. Hori, and K. Takaya (2012), The role of Barents sea ice in the wintertime cyclone track and emergence of a warm-Arctic cold-Siberian anomaly, *J. Clim.*, *25*, 2561–2568.

Instanes, A., V. Kokorev, R. Janowicz, O. Bruland, K. Sand, and T. Prowse (2016), Changes to freshwater systems affecting Arctic infrastructure and natural resources, *J. Geophys. Res. Biogeosci.*, *121*, doi:10.1002/2015JG003125.

Intergovernmental Panel on Climate Change (2013), *Climate Change 2013: The Physical Science Basis. Contribution of Working Group I to the Fifth Assessment Report of the Intergovernmental Panel on Climate Change*, edited by T. F. Stocker et al., 1535 pp., Cambridge Univ. Press, Cambridge, U. K., and New York, doi:10.1017/CBO9781107415324.

Isachsen, P. E., J. H. LaCasce, C. Mauritzen, and S. Häkkinen (2003), Wind-driven variability of the large-scale recirculating flow in the Nordic Seas and Arctic Ocean, *J. Phys. Oceanogr.*, *33*(12), 2534–2550.

Jackson, J. M., E. C. Carmack, F. A. McLaughlin, S. E. Allen, and R. G. Ingram (2010), Identification, characterization and change of the near-surface temperature maximum in the Canada Basin, 1993–2008, *J. Geophys. Res.*, *115*, C05021, doi:10.1029/2009JC005265.

Jackson, J. M., W. J. Williams, and E. C. Carmack (2012), Winter sea-ice melt in the Canada Basin, Arctic Ocean, *Geophys. Res. Lett.*, *39*, L03603, doi:10.1029/2011GL050219.

Jahn, A., and M. M. Holland (2013), Implications of Arctic sea ice changes for North Atlantic deep convection and the meridional overturning circulation in CCSM4-CMIP5 simulations, *Geophys. Res. Lett.*, *40*, 1206–1211, doi:10.1002/grl.50183.

Jakobsson, M., et al. (2012), The International Bathymetric Chart of the Arctic Ocean (IBCAO) version 3.0, *Geophys. Res. Lett.*, *39*, L12609, doi:10.1029/2012GL052219.

Jeffries, M. O., J. E. Overland, and D. K. Perovich (2013), The Arctic shifts to a new normal, *Phys. Today*, *66*, 35–40, doi:10.1063/PT.3.2147.

Johnston, M. (2011), Results from field programs on multi-year ice August 2009 and May 2010. Technical Report # CHC-TR-082. Canadian Hydraulics Centre, National Research Council of Canada, Montreal Road, Ottawa, Canada K1A 0R6, 79 p.

Jones, E. P., and L. G. Anderson (1986), On the origin of chemical properties of the Arctic Ocean halocline, *J. Geophys. Res.*, *91*, 10,759–10,791, doi:10.1029/JC091iC09p10759.

Jones, E. P., J. H. Swift, L. G. Anderson, M. Lipizer, G. Civitarese, K. K. Falkner, G. Kattner, and F. McLaughlin (2003), Tracing Pacific water in the North Atlantic ocean, *J. Geophys. Res.*, *108*(C4), 3116, doi:10.1029/2001JC001141.

Jutterström, S., and L. G. Anderson (2005), The saturation of calcite and aragonite in the Arctic Ocean, *Mar. Chem.*, *94*, 101–110.

Kilias, E. S., I. Peeken, and K. Metfies (2014), Insight into protist diversity in Arctic sea ice and melt-pond aggregate obtained by pyrose-quencing, *Polar Res.*, *33*, doi:10.3402/polar.v33.23466.

Kinnard, C., C. M. Zdanowicz, D. A. Fisher, E. Isaksson, A. de Vernal, and L. G. Thompson (2011), Reconstructed changes in Arctic sea ice over the past 1,450 years, *Nature*, *479*(7374), 509–512.

Klunder, M. B., D. Bauch, P. Laan, H. J. W. de Barr, S. van Heuvan, and S. Ober (2012), Dissolved iron in the Arctic shelf seas and surface waters of the central Arctic Ocean: Impact of Arctic river water and ice-melt, *J. Geophys. Res.*, *117*, C01027, doi:10.1029/2011JC007133.

Konar, B. (2013), Lack of recovery from disturbance in high-arctic boulder communities, *Polar Biol.*, *36*(8), 1205–1214.

Krishfield, R. A., A. Proshutinsky, K. Tateyama, W. J. Williams, E. C. Carmack, F. A. McLaughlin, and M.-L. Timmermans (2014), Deterioration of perennial sea ice in the Beaufort Gyre from 2003 to 2012 and its impact on the oceanic freshwater cycle, *J. Geophys. Res. Oceans*, *119*, 1271–1305, doi:10.1002/2013JC008999.

Krishfield, R., J. Toole, A. Proshutinsky, and M. L. Timmermans (2008), Automated ice-tethered profilers for seawater observations under pack ice in all seasons, *J. Atmos. Oceanic Technol.*, *25*(11), 2091–2105.

Kwok, R., and D. A. Rothrock (2009), Decline in Arctic sea ice thickness from submarine and ICESat records: 1958–2008, *Geophys. Res. Lett.*, *36*, L15501, doi:10.1029/2009GL039035.

Kwok, R., and N. Untersteiner (2011), The thinning of Arctic sea ice, *Phys. Today*, *64*(4), 36–41.

Kwok, R., G. F. Cunningham, and S. S. Pang (2004), Fram Strait sea ice outflow, *J. Geophys. Res.*, *109*, C01009, doi:10.1029/2003JC001785.

Kwok, R., G. F. Cunningham, M. Wensnahan, I. Rigor, H. J. Zwally, and D. Yi (2009), Thinning and volume loss of Arctic sea ice: 2003–2008, *J. Geophys. Res.*, *114*, C07005, doi:10.1029/2009JC005312.

Kwok, R., G. Spreen, and S. Pang (2013), Arctic sea ice circulation and drift speed: Decadal trends and ocean currents, *J. Geophys. Res. Oceans*, *118*, 2408–2425, doi:10.1002/jgrc.20191.

Lee, S. H., et al. (2011), Holes in progressively thinning Arctic sea ice lead to new ice algae habitat, *Oceanography*, *24*(3), 302–308.

Letscher, R. T., D. A. Hansell, and D. Kadko (2011), Rapid removal of terrigenous dissolved organic carbon over the Eurasian shelves of the Arctic Ocean, *Mar. Chem.*, *123*, 78–87.

Li, W. K. W., F. A. McLaughlin, C. Lovejoy, and E. C. Carmack (2009), Smallest algae thrive as the Arctic Ocean freshens, *Science*, *326*(5952), 539, doi:10.1126/science.1179798.

Lindsay, R., M. Wensnahan, A. Schweiger, and J. Zhang (2014), Evaluation of seven different atmospheric reanalysis products in the Arctic, *J. Clim.*, *27*, 2588–2606, doi:10.1175/JCLI-D-13-00014.1.

Lique, C., G. Garric, A.-M. Treguier, B. Barnier, N. Ferry, C.-E. Testut, and F. Girard-Ardhuin (2011), Evolution of the Arctic Ocean salinity, 2007–08: Contrast between the Canadian and the Eurasian basins, *J. Clim.*, *24*, 1705–1717, doi:10.1175/2010JCLI3762.1.

Lique, C., M. M. Holland, Y. B. Dibike, D. M. Lawrence, and J. A. Screen (2016), Modeling the Arctic freshwater system and its integration in the global system: Lessons learned and future challenges, *J. Geophys. Res. Biogeosci.*, *121*, doi:10.1002/2015JG003120.

Lisitzyn, A. P. (1995), The marginal filter of the ocean, *Oceanology*, *34*, 671–682.

Liu, J., J. A. Curry, H. Wang, M. Song, and R. M. Horton (2012), Impact of declining Arctic sea ice on winter snowfall, *Proc. Natl. Acad. Sci. U.S.A.*, doi:10.1073/pnas.1114910109.

Lobb, J. (2004), Oceanography of Baffin Bay, Univ. of Victoria, PhD thesis.

Loder, J. W., G. Gawarkiewicz, and B. Petrie (1998), The coastal ocean of northeastern North America (Cape Hatteras to Hudson Strait), in *The Sea: Ideas and Observations on Progress in the Study of the Seas, The Global Coastal Ocean: Regional Studies and Syntheses*, vol. 11, edited by A. Robinson and K. Brink, 1062 pp., Wiley, Toronto.

Macdonald, R. W., E. C. Carmack, F. A. McLaughlin, K. K. Falkner, and J. H. Swift (1999), Connections among ice, runoff and atmospheric forcing in the Beaufort Gyre, *Geophys. Res. Lett.*, *26*, 2223–2226, doi:10.1029/1999GL900508.

MacGilchrist, G. A., A. C. Naveira Garabato, T. Tsubouchi, S. Bacon, S. Torres-Valdés, and K. Azetsu-Scott (2014), The Arctic Ocean carbon sink, *Deep Sea Res., Part I*, *86*, 39–55, doi:10.1016/j.dsr.2014.01.002.

Martin, J., D. Dumont, and J. E. Tremblay (2013), Contribution of subsurface chlorophyll maxima to primary production in the coastal Beaufort Sea (Canadian Arctic): A model assessment, *J. Geophys. Res. Oceans*, *118*, 5873–5886, doi:10.1002/2013JC008843.

Martin, T., M. Steele, and J. Zhang (2014), Seasonality and long- term trend of Arctic Ocean surface stress in a model, *J. Geophys. Res. Oceans*, *119*, 1723–1738, doi:10.1002/2013JC009425.

Mathis, J. T., J. N. Cross, and N. R. Bates (2011), Coupling primary production and terrestrial runoff to ocean acidification and carbonate mineral suppression in the eastern Bering Sea, *J. Geophys. Res.*, *116*, C02030, doi:10.1029/2010JC006453.

Mathis, J. T., et al. (2012), Storm-induced upwelling of high pCO$_2$ waters onto the continental shelf of the western Arctic Ocean and implications for carbonate mineral saturation states, *Geophys. Res. Lett.*, *39*, L07606, doi:10.1029/2012GL051574.

Mauritzen, C. (2012), Arctic freshwater, *Nat. Geosci.*, *5*, 162–164.

Maykut, G. A., and N. Untersteiner (1971), Some results from a time dependent thermodynamic model of sea ice, *J. Geophys. Res.*, *76*, 1550–1575, doi:10.1029/JC076i006p01550.

McClelland, J. W., R. M. Holmes, B. J. Peterson, and M. Stieglitz (2004), Increasing river discharge in the Eurasian Arctic: Consideration of dams, permafrost thaw, and fires as potential agents of change, *J. Geophys. Res.*, *109*, D18102, doi:10.1029/2004JD004583.

McClelland, J. W., S. J. Dery, J. Peterson, R. M. Holmes, and E. F. Woods (2006), A pan-arctic evaluation of changes in river discharge during the latter half of the 20th century, *Geophys. Res. Lett.*, *33*, L06715, doi:10.1029/02006GL025753.

McClelland, J. W., R. M. Holmes, K. H. Dunton, and R. W. Macdonald (2012), The Arctic Ocean estuary, *Estuaries Coasts*, *35*(2), 353–368.

McClelland, J. W., A. Townsend-Small, R. M. Holmes, F. Pan, M. Stieglitz, M. Khosh, and B. J. Peterson (2014), River export of nutrients and organic matter from the North Slope of Alaska to the Beaufort Sea, *Water Resour. Res.*, *50*, 1823–1839, doi:10.1002/2013WR014722.

McKinley, G. A., A. R. Fay, T. Takahashi, and N. Metzl (2011), Convergence of atmospheric and North Atlantic carbon dioxide trends on multidecadal timescales, *Nat. Geosci.*, *4*, 606–610.

McLaughlin, F., E. Carmack, R. Macdonald, A. J. Weaver, and J. Smith (2002), The Canada Basin, 1989–1995: Upstream events and far-field effects of the Barents Sea, *J. Geophys. Res.*, *107*(C7), 3082, doi:10.1029/2001JC000904.

McLaughlin, F., E. Carmack, R. Krishfield, C. Guay, M. Yamamoto-Kawai, J. Jackson, A. Proshutinsky, and W. Williams (2011), The rapid response of the Canada Basin to climate forcing: From Bellwether to Alarm Bells, *Oceanography*, *24*, 146–159.

McLaughlin, F. A., and E. C. Carmack (2010), Nutricline deepening in the Canada Basin, 2003–2009, *Geophys. Res. Lett.*, *37*, L24602, doi:10.1029/2010GL045459.

McLaughlin, F. A., E. C. Carmack, R. W. Macdonald, and J. K. B. Bishop (1996), Physical and geochemical properties across the Atlantic/Pacific water mass front in the southern Canadian Basin, *J. Geophys. Res.*, *101*(C1), 1183–1197, doi:10.1029/95JC02634.

McLaughlin, F. A., E. C. Carmack, W. J. Williams, S. Zimmerman, K. Shimada, and M. Itoh (2009), Joint effects of boundary currents and thermo-haline intrusions on the warming of Atlantic water in the Canada Basin, 1993–2007, *J. Geophys. Res.*, *114*, C00A12, doi:10.1029/2008JC005001.

McPhee, M. G. (2008), *Air-Ice-Ocean Interaction: Turbulent Ocean Boundary Layer Exchange Processes*, pp. 215, Springer, New York.

McPhee, M. G. (2013), Intensification of geostrophic currents in the Canada Basin, Arctic Ocean, *J. Clim.*, *26*, 3130–3138.

McPhee, M. G., A. Proshutinsky, J. H. Morison, M. Steele, and M. B. Alkire (2009), Rapid change in freshwater content of the Arctic Ocean, *Geophys. Res. Lett.*, *36*, L10602, doi:10.1029/2009GL037525.

Melling, H. (2012), Sea-ice observation: Advances and challenges, in *Arctic Climate Change*, edited by P. Lemke and H.-W. Jacobi, pp. 27–115, Springer, Netherlands.

Melling, H., and E. L. Lewis (1982), Shelf drainage flows in the Beaufort Sea and their effect on the Arctic pycnocline, *Deep Sea Res.*, *29*, 967–989.

Melling, H., and R. M. Moore (1995), Modification of halocline source waters during freezing on the Beaufort Sea shelf: Evidence from oxygen isotopes and dissolved nutrients, *Cont. Shelf Res.*, *15*(1), 89–113.

Melling, H., and D. A. Riedel (1996), Development of seasonal pack ice in the Beaufort Sea during the winter of 1991–1992: A view from below, *J. Geophys. Res.*, *101*(C5), 11,975–11,991, doi:10.1029/96JC00284.

Melling, H., Y. Gratton, and G. Ingram (2001), Ocean circulation within the North Water polynya of Baffin Bay, *Atmos. Ocean*, *39*(3), 301–325.

Melling, H., D. A. Riedel, and Z. E. Gedalof (2005), Trends in the draft and extent of seasonal pack ice, Canadian Beaufort Sea, *Geophys. Res. Lett.*, *32*, L24501, doi:10.1029/2005GL024483.

Melling, H., R. Francois, P. G. Myers, W. Perrie, A. Rochon, and R. L. Taylor (2012), The Arctic Ocean—A Canadian perspective, *Clim. Change*, *115*, 89–114, doi:10.1007/s10584-012-0576-4.

Mellor, G. L., M. G. McPhee, and M. Steele (1986), Ice-seawater turbulent boundary layer interaction with melting or freezing, *J. Phys. Oceanogr.*, *16*(11), 1829–1846.

Miller, L. A., R. W. Macdonald, F. McLaughlin, A. Mucci, M. Yamamoto-Kawai, K. E. Giesbrecht, and W. J. Williams (2014), Changes in the marine carbonate system of the western Arctic: Patterns in a rescued data set, *Polar Res.*, *33*, 20,577, doi:10.3402/polar.v33.20577.

Milliman, J. D., K. L. Farnsworth, P. D. Jones, K. H. Xu, and L. C. Smith (2008), Climatic and anthropogenic factors affecting river discharge to the global ocean, 1951–2000, *Global Planet. Change*, *62*(3–4), 187–194.

Morison, J., R. Kwok, C. Peralta-Ferriz, M. Alkire, I. Rigor, R. Andersen, and M. Steele (2012), Changing Arctic Ocean freshwater pathways, *Nature*, *481*, 66–70.

Nakayama, Y., S. Fujita, K. Kuma, and K. Shimada (2011), Iron and humic-type fluorescent dissolved organic matter in the Chukchi Sea and Canada Basin of the western Arctic Ocean, *J. Geophys. Res.*, *116*, C07031, doi:10.1029/2010JC006779.

Nishino, S., T. Kikuchi, M. Yamamoto-Kawai, Y. Kawaguchi, T. Hirawake, and M. Itoh (2011), Enhancement/reduction of biological pump depends on ocean circulation in the sea-ice reduction regions of the Arctic Ocean, *J. Oceanogr.*, doi:10.1007/s10872-011-0030-7.

Notz, D., and J. Marotzke (2012), Observations reveal external driver for Arctic sea-ice retreat, *Geophys. Res. Lett.*, *39*, L08502, doi:10.1029/2012GL051094.

Nummelin, A., C. Li, and L. H. Smedsrud (2015), Response of Arctic Ocean stratification to changing river runoff in a column model, *J. Geophys. Res. Oceans*, *120*, 2655–2675, doi:10.1002/2014JC010571.

Nürnberg, D., I. Wollenburg, D. Dethleff, H. Eicken, H. Kassens, T. Letzig, E. Reimnitz, and J. Thiede (1994), Sediments in Arctic sea ice: Implications for entrainment, transport and release, *Mar. Geol.*, *119*, 185–214.

Olafsson, J., S. R. Olafsdottir, A. Benoit-Cattin, M. Danielsen, T. S. Arnarson, and T. Takahashi (2009), Rate of Iceland Sea acidification from time series measurements, *Biogeosciences*, *6*(11), 2661–2668.

Overland, J., J. Francis, R. Hall, E. Hanna, S.-J. Kim, and T. Vihma (2015), The melting Arctic, the polar vortex and mid-latitude weird weather: Are they connected?, *J. Clim.*, doi:10.1175/JCLI-D-14-00822.1.

Overland, J. E., and M. Wang (2013), When will the Arctic be ice free?, *Geophys. Res. Lett.*, *40*, 2097–2101, doi:10.1002/grl50316.

Overland, J. E., K. R. Wood, and M. Wang (2011), Warm Arctic-cold continents: Climate impacts of the newly open, *Arctic Sea. Polar Res.*, *30*, doi:10.3402/polar.v30i0.15787.

Overpeck, J. T., et al. (2005), Arctic system on trajectory to new, seasonally ice-free state, *Eos Trans. AGU*, *86*(34), 309–313, doi:10.1029/2005EO340001.

Pabi, S., G. L. van Dijken, and K. R. Arrigo (2008), Primary production in the Arctic Ocean, 1998–2006, *J. Geophys. Res.*, *113*, C08005, doi:10.1029/2007JC004578.

Parsons, T. R., D. G. Webb, H. Dovery, R. Haigh, M. Lawrence, and G. E. Hopky (1988), Production studies in the Mackenzie River–Beaufort Sea estuary, *Polar Biol.*, *8*, 235–239.

Peralta-Ferriz, C., J. H. Morison, J. M. Wallace, J. A. Bonin, and J. Zhang (2014), Arctic ocean circulation patterns revealed by GRACE, *J. Clim.*, *27*, 1445–1468, doi:10.1175/JCLI-D-13-00013.1.

Perovich, D. K., J. A. Richter-Menge, K. F. Jones, B. Light, B. C. Elder, C. Polashenski, D. LaRoche, T. Markus, and R. Lindsay (2011), Arctic sea-ice melt in 2008 and the role of solar heating, *Ann. Glaciol.*, *52*(57), 355–359.

Peterson, B. J., R. M. Holmes, J. W. McClelland, C. J. Vörösmarty, R. B. Lammers, A. I. Shiklomanov, and S. Rahmstorf (2002), Increasing river discharge to the Arctic Ocean, *Science*, *298*, 2171–2173.

Peterson, B. J., J. McClelland, R. Curry, R. M. Holmes, J. E. Walsh, and K. Aagaard (2006), Trajectory shifts in the Arctic and subarctic freshwater cycle, *Science*, *313*, 1061–1066.

Petrenko, D., D. Pozdnyakov, J. Johannessen, F. Counillon, and V. Sychov (2013), Satellite-derived multi-year trend in primary production in the Arctic Ocean, *Int. J. Remote Sens.*, *34*(11), 3903–3937.

Pfirman, S. L., D. Bauch, and T. Gammelsrod (1994), The northern Barents Sea: Water mass distribution and modification, in *The Polar Oceans and Their Role in Shaping the Global Environment: The Nansen Centennial Volume*, Geophys. Monogr. Ser., vol. 85, edited by O. M. Johannessen, R. D. Muench, and J. E. Overland, pp. 77–94, AGU, Washington, D. C.

Pickart, R. S., J. T. Weingartner, L. J. Pratt, S. Zimmermann, and D. J. Torres (2005), Flow of winter-transformed Pacific water into the Western Arctic, *Deep Sea Res.*, *52*, 3175–3198.

Pickart, R. S., G. W. K. Moore, D. J. Torres, P. S. Fratantoni, R. A. Goldsmith, and J. Yang (2009), Upwelling on the continental slope of the Alaskan Beaufort Sea: Storms, ice, and oceanographic response, *J. Geophys. Res.*, *114*, C00A13, doi:10.1029/2008JC005009.

Pickart, R. S., M. A. Spall, and J. T. Mathis (2013), Dynamics of upwelling in the Alaskan Beaufort Sea and associated shelf–basin fluxes, *Deep Sea Res., Part I*, *176*, 35–51.

Pite, H. D., D. R. Topham, and B. J. Van Hardenberg (1995), Laboratory measurements of the drag force on a family of two-dimensional ice keel models in a two-layer flow, *J. Phys. Oceanogr.*, *25*(12), 3008–3031.

Pivovarov, S., R. Schlitzer, and A. Novikhin (2003), River runoff influence on the water mass formation in the Kara Sea, in *Siberian River Run-Off in the Kara Sea: Characterisation, Quantification, Variability, and Environmental Significance*, Proc. Mar. Sci., vol. 6, edited by R. Stein et al., pp. 9–26, Elsevier, Amsterdam.

Pnyushkov, A., I. V. Polyakov, V. Ivanov, Y. Aksenov, A. Coward, M. Janout, and B. Rabe (2015), Structure and variability of the boundary current in the Eurasian Basin of the Arctic Ocean, *Deep Sea Res.*, *101*, 80–97, doi:10.1016/j.dsr.2015.03.001.

Pokrovsky, O. S., et al. (2013), Transformation of organic carbon, trace element, and organo-mineral colloids in the mixing zone of the largest European Arctic river, *Ocean Science Discussions*, *10*(5), 1707–1764.

Polyakov, I. V., G. V. Alekseev, R. V. Bekryaev, U. S. Bhatt, R. Colony, M. A. Johnson, V. P. Karklin, D. Walsh, and A. V. Yulin (2003), Long-term ice variability in Arctic marginal seas, *J. Clim.*, *16*(12), 2078–2085.

Polyakov, I. V., et al. (2005), One more step toward a warmer Arctic, *Geophys. Res. Lett.*, *32*, LI7605, doi:10.1029/2005GL023740.

Polyakov, I. V., V. A. Alexeev, G. I. Belchansky, I. Dmitrenko, V. V. Ivanov, S. Kirillov, A. Korablev, M. Steele, L. Timokhov, and I. Yashayev (2008), Arctic Ocean freshwater changes over the past 100 years and their causes, *J. Clim.*, *21*, 364–384.

Polyakov, I. V., A. V. Pnyushkov, and T. A. Timokhov (2012), Warming of the intermediate Atlantic Water of the Arctic Ocean in the 2000s, *J. Clim.*, *25*(23), 8362–8370, doi:10.1175/JCLI-D-12-00266.1.

Polyakov, I. V., U. S. Bhatt, J. E. Walsh, E. P. Abrahamsen, A. V. Pnyushkov, and P. F. Wassmann (2013a), Recent oceanic changes in the Arctic in the context of long-term observations, *Ecol. Appl.*, *23*(8), 1745–1764.

Polyakov, I. V., A. V. Pnyushkov, R. Rember, L. Padman, E. C. Carmack, and J. M. Jackson (2013b), Winter convection transports Atlantic water heat to the surface layer in the eastern Arctic Ocean, *J. Phys. Oceanogr.*, *43*, 2142–2155.

Popova, E. E., A. Yool, Y. Aksenov, A. C. Coward, and T. R. Anderson (2014), Regional variability of acidification in the Arctic: A sea of contrasts, *Biogeosciences*, *11*, 293–308.

Proshutinsky, A., R. H. Bourke, and F. A. McLaughlin (2002), The role of the Beaufort Gyre in Arctic climate variability: Seasonal to decadal climate scales, *Geophys. Res. Lett.*, *29*(23), 2100, doi:10.1029/2002GL015847.

Proshutinsky, A., I. M. Ashik, E. N. Dvorkin, S. Häkkinen, R. A. Krishfield, and W. R. Peltier (2004), Secular sea level change in the Russian sector of the Arctic Ocean, *J. Geophys. Res.*, *109*, C03042, doi:10.1029/2003JC002007.

Proshutinsky, A., R. Krishfield, M.-L. Timmermans, J. Toole, E. Carmack, F. McLaughlin, W. J. Williams, S. Zimmermann, M. Itoh, and K. Shimada (2009), The Beaufort Gyre Fresh Water Reservoir: State and variability from observations, *J. Geophys. Res.*, *114*, C00A10, doi:10.1029/2008JC005104.

Proshutinsky, A., D. Dukhovskoy, M.-L. Timmermans, R. Krishfield, and J. Bamber (2015), Arctic circulation regimes, *Philos. Trans. R. Soc., A*, *373*, doi:10.1098/rsta.2014.0160.

Proshutinsky, A. Y., and M. A. Johnson (1997), Two circulation regimes of the wind driven Arctic Ocean, *J. Geophys. Res.*, *102*(C6), 12,493–12,514, doi:10.1029/97JC00738.

Prowse, T., A. Bring, J. Mård, and E. Carmack (2015a), Arctic Freshwater Synthesis: Introduction, *J. Geophys. Res. Biogeosci.*, *120*, 1887–1893, doi:10.1002/JG0033128.

Prowse, T., A. Bring, J. Mård, E. Carmack, M. Holland, A. Instanes, T. Vihma, and F. J. Wrona (2015b), Arctic Freshwater Synthesis: Summary of key emerging issues, *J. Geophys. Res. Biogeosci.*, *120*, 2121–2131, doi:10.1002/2015JG003128.

Prowse, T. D., and P. O. Flegg (2000), Arctic river flow: A review of contributing areas, in *The Freshwater Budget of the Arctic Ocean*, NATO Adv. Res. Ser., edited by E. L. Lewis, pp. 269–280, Kluwer Acad., Dordrecht, Netherlands.

Rabe, B., M. Karcher, U. Schauer, J. Toole, R. Krishfield, S. Pisarev, F. Kauker, R. Gerdes, and T. Kikuchi (2011), An assessment of Arctic Ocean freshwater content changes from the 1990s to 2006–2008, *Deep Sea Res., Part I*, *58*, 173–185, doi:10.1016/j.dsr.2010.12.002.

Rabe, B., M. Karcher, F. Kauker, U. Schauer, J. M. Toole, R. A. Krishfield, S. Pisarev, T. Kikuchi, and J. Su (2014), Arctic Ocean basin liquid freshwater storage trend 1992–2012, *Geophys. Res. Lett.*, *41*, 961–968, doi:10.1002/2013GL058121.

Rachold, V., H. Eicken, V. V. Gordeev, M. N. Grigoriev, H.-W. Hubberten, A. P. Lisitzin, V. P. Shevchenko, and L. Schirrmeister (2004), Modern terrigenous organic carbon input to the Arctic Ocean, in *The Organic Carbon Cycle in the Arctic Ocean*, edited by R. Stein and R. W. Macdonald, pp. 33–55, Springer, Heidelberg.

Rahmstorf, S., J. E. Box, G. Feulner, M. E. Mann, A. Robinson, S. Rutherford, and E. J. Chaffernicht (2015), Exceptional twentieth-century slowdown in Atlantic Ocean overturning circulation, *Nat. Clim. Change*, *5*, 475–480, doi:10.1038/nclimate2554.

Rainville, L., and P. Winsor (2008), Mixing across the Arctic Ocean: Microstructure observations during the Beringia 2005 expedition, *Geophys. Res. Lett.*, *35*, L08606, doi:10.1029/2008GL033532.

Rainville, L., C. M. Lee, and R. A. Woodgate (2011), Impact of wind-driven mixing in the Arctic Ocean, *Oceanography*, *24*, 136–145, doi:10.5670/oceanog.2011.65.

Rampal, P., J. Weiss, and D. Marsan (2009), Positive trend in the mean speed and deformation rate of Arctic sea ice, 1979–2007, *J. Geophys. Res.*, *114*, C05013, doi:10.1029/2008JC005066.

Rampal, P., J. Weiss, C. Dubois, and J. M. Campin (2011), IPCC climate models do not capture Arctic sea ice drift acceleration: Consequences in terms of projected sea ice thinning and decline, *J. Geophys. Res.*, *116*, C00D07, doi:10.1029/2011JC007110.

Ravelo, A. M., B. H. Konar, and B. A. Bluhm (2015), Spatial variability in epibenthic communities on the Alaskan Beaufort Sea shelf, *Polar Biol.*, doi:10.1007/s00300-015-1741-9.

Remane, A. (1958), Ökologie des Brackwassers, in *Die Biologie des Brackwassers*, edited by A. Remane and C. Schlieper, pp. 1–216, Schweizerbart'sche Verlagsbuchhandlung, Stuttgart, Germany.

Rennermalm, A. K., E. F. Wood, A. J. Weaver, M. Eby, and S. J. Déry (2007), Relative sensitivity of the Atlantic Meridional Overturning Circulation to river discharge into Hudson Bay and the Arctic Ocean, *J. Geophys. Res.*, *112*, G04S48, doi:10.1029/2006JG000330.

Rigor, I. G., and J. M. Wallace (2004), Variations in the age of Arctic sea-ice and summer sea-ice extent, *Geophys. Res. Lett.*, *31*, L09401, doi:10.1029/2004GL019492.

Rippeth, T. P., B. J. Lincoln, Y.-D. Lenn, J. A. M. Green, A. Sundfjord, and S. Bacon (2015), Tide-mediated warming of Arctic halocline by Atlantic heat fluxes over rough topography, *Nat. Geosci.*, doi:10.1038/ngeo2350.

Rothrock, D. A., Y. Yu, and G. A. Maykut (1999), Thinning of the Arctic sea-ice cover, *Geophys. Res. Lett.*, *26*(23), 3469–3472, doi:10.1029/1999GL010863.

Rudels, B., A. M. Larsson, and P. I. Sehlstedt (1991), Stratification and water mass formation in the Arctic Ocean: Some implications for the nutrient distribution, *Polar Res.*, *10*(1), 19–32.

Rudels, B., E. P. Jones, L. G. Anderson, and G. Kattner (1994), On the intermediate depth waters of the Arctic Ocean, in *The Polar Oceans and Their Role in Shaping the Global Environment: The Nansen Centennial Volume*, *Geophys. Monogr. Ser.*, vol. 85, edited by O. M. Johannessen, R. D. Muench, and J. E. Overland, pp. 33–46, AGU, Washington, D. C.

Rudels, B., L. G. Anderson, and E. P. Jones (1996), Formation and evolution of the surface mixed layer and halocline of the Arctic Ocean, *J. Geophys. Res.*, *101*, 8807–8821, doi:10.1029/96JC00143.

Rudels, B., H. J. Friedrich, and D. Quadfasel (1999), The Arctic circumpolar boundary current, *Deep Sea Res., Part II*, *46*, 1023–1062.

Rudels, B., L. Anderson, P. Eriksson, E. Fahrbach, M. Jakobsson, E. P. Jones, H. Melling, S. Prinsenberg, U. Schauer, and T. Yao (2012), Observations in the ocean, in *Arctic Climate Change: The ACSYS Decade and Beyond*, *Atmospheric and Oceanographic Sciences Library*, vol. 43, chap. 4, edited by P. Lemke and H.-W. Jacobi, pp. 117–198, Springer, Dordrecht, Netherlands.

Schauer, U., A. Beszczynska-Möller, W. Walczowski, E. Fahrbach, J. Piechura, and E. Hansen (2008), Variation of flow through the Fram Strait to the Arctic Ocean between 1997 and 2006, in *Arctic–Subarctic Ocean Fluxes*, edited by B. Dickson, J. Meincke, and P. Rhines, pp. 65–85, Springer, Dordrecht.

Schlosser, P., R. Newton, B. Ekwurzel, S. Khatiwala, R. Mortlock, and R. Fairbanks (2002), Decrease of river runoff in the upper waters of the Eurasian Basin, Arctic Ocean, between 1991 and 1996: Evidence from δ^{18}O data, *Geophys. Res. Lett.*, *29*(9), 1289, doi:10.1029/2001GL013135.

Schuur, E. A. G., et al. (2015), Climate change and the permafrost carbon feedback, *Nature*, *520*, doi:10.1038/nature14338.

Schweiger, A., R. Lindsay, J. Zhang, M. Steele, H. Stern, and R. Kwok (2011), Uncertainty in modeled Arctic sea ice volume, *J. Geophys. Res.*, *116*, C00D06, doi:10.1029/2011JC007084.

Screen, J. A., I. Simmonds, C. Deser, and R. Tomas (2013), The atmospheric response to three decades of observed Arctic sea ice loss, *J. Clim.*, *26*(4), 1230–1248.

Screen, J. A., C. Deser, I. Simmonds, and R. Tomas (2014), Atmospheric impacts of Arctic sea-ice loss, 1979–2009: Separating forced change from atmospheric internal variability, *Clim. Dyn.*, *43*, 333–344.

Serreze, M. C., and A. P. Barrett (2011), Characteristics of the Beaufort Sea High, *J. Clim.*, *24*, doi:10.1175/2010JCLI3636.1.

Serreze, M. C., and R. G. Barry (2011), Processes and impacts of Arctic amplification: A research synthesis, *Global Planet. Change*, *77*(1–2), 85–96.

Serreze, M. C., A. P. Barrett, A. G. Slater, R. A. Woodgate, K. Aagaard, R. B. Lammers, M. Steele, R. Moritz, M. Meredith, and C. M. Lee (2006), The large-scale freshwater cycle of the Arctic, *J. Geophys. Res.*, *111*, C11010, doi:10.1029/2005JC003424.

Serreze, M. C., A. P. Barrett, J. C. Stroeve, D. N. Knidig, and M. M. Holland (2009), The emergence of surface-based Arctic amplification, *Cryosphere*, *3*, 11–19.

Serreze, M., and J. Francis (2006), The Arctic amplification debate, *Clim. Change*, *76*, 241–264, doi:10.1007/s10584-005-9017/y.

Shiklomanov, A. I., and R. B. Lammers (2011), River discharge, in NOAA Arctic Report Card: Update for 2011. [Available at http://www.arctic.noaa.gov/report11/river_discharge.html.]

Shimada, K., T. Kamoshida, M. Itoh, S. Nishino, E. Carmack, F. McLaughlin, S. Zimmermann, and A. Proshutinsky (2006), Pacific Ocean inflow: Influence on catastrophic reduction of sea ice cover in the Arctic Ocean, *Geophys. Res. Lett.*, *33*, L08605, doi:10.1029/2005GL025624.

Slagstad, D., P. F. J. Wassmann, and I. Ellingsen (2015), Physical constraints and productivity in the future Arctic Ocean, *Front. Mar. Sci.*, *2*, 85, doi:10.3389/fmars.2015.00085.

Spielhagen, R. F., K. Werner, S. A. Sørensen, K. Zamelczyk, E. Kandiano, G. Budeus, K. Husum, T. M. Marchitto, and M. Hald (2011), Enhanced modern heat transfer to the Arctic by Warm Atlantic Water, *Science*, *331*, 450, doi:10.1126/science.1197397.

Steele, M., and T. Boyd (1998), Retreat of the cold halocline layer in the Arctic Ocean, *J. Geophys. Res.*, *103*, 10,419–10,435, doi:10.1029/98JC00580.

Steele, M., J. H. Morison, and T. B. Curtin (1995), Halocline water formation in the Barents Sea, *J. Geophys. Res.*, *100*(C1), 881–894, doi:10.1029/94JC02310.

Steele, M., R. Morley, and W. Ermold (2001), A global ocean hydrography with a high quality Arctic Ocean, *J. Clim.*, *14*, 2079–2087.

Steele, M., J. Morison, W. Ermold, I. Rigor, and M. Ortmeyer (2004), Circulation of summer Pacific halocline water in the Arctic Ocean, *J. Geophys. Res.*, *109*, C02027, doi:10.1029/2003JC002009.

Steinacher, M., F. Joos, T. L. Frölicher, G.-K. Plattner, and S. C. Doney (2009), Imminent ocean acidification in the Arctic projected with the NCAR global coupled carbon cycle-climate model, *Biogeosciences*, *6*, 515–533.

Steiner, N., M. Harder, and P. Lemke (1999), Sea-ice roughness and drag coefficients in a dynamic–thermodynamic sea-ice model for the Arctic, *Tellus A*, *51*(5), 964–978.

Stewart, K. D., and T. W. N. Haine (2013), Wind-driven Arctic freshwater anomalies, *Geophys. Res. Lett.*, *40*, 6196–6201, doi:10.1002/2013GL058247.

Stigebrandt, A. (1981), A model for the thickness and salinity of the upper layer in the Arctic Ocean and the relationship between the ice thickness and some external parameters, *J. Phys. Oceanogr.*, *11*, 1407–1422.

St-Laurent, P., F. Straneo, J.-F. Dumais, and D. G. Barber (2011), What is the fate of the river waters of Hudson Bay?, *J. Mar. Syst.*, *88*(3), 352–361.

St-Laurent, P., F. Straneo, and D. Barber (2012), A conceptual model of an Arctic sea, *J. Geophys. Res.*, *117*, C06010, doi:10.1029/2011JC007652.

Straneo, F., and C. Cenedese (2015), The dynamics of Greenland's glacial fjords and their role in climate, *Annu. Rev. Mar. Sci.*, *7*, 89–112.

Straneo, F., and F. Saucier (2008a), The outflow from Hudson Strait and its contribution to the Labrador Current, *Deep Sea Res., Part I*, *55*, 926–946.

Straneo, F., and F. Saucier (2008b), The Arctic-subarctic exchange through Hudson Strait, in *Arctic-Subarctic Ocean Fluxes: Defining the Role of the Northern Seas in Climate*, edited by R. Dickson, J. Meincke, and P. Rhines, pp. 740, Springer, New York.

Straneo, F., et al. (2013), Challenges to understand the dynamic response of Greenland's marine terminating glaciers to oceanic and atmospheric forcing, *Bull. Am. Meteorol. Soc.*, *94*(8), 1131–1144, doi:10.1175/BAMS-D-12-00100.1.

Stroeve, J. C., V. Kattsov, A. P. Barrett, M. C. Serreze, T. Pavlova, M. M. Holland, and W. N. Meier (2012a), Trends in Arctic sea ice extent from CMIP5, CMIP3 and observations, *Geophys. Res. Lett.*, *39*, L16502, doi:10.1029/2012GL052676.

Stroeve, J. C., M. C. Serreze, M. M. Holland, J. E. Kay, J. Masklanik, and A. P. Barrett (2012b), The Arctic's rapidly shrinking sea ice cover: A research synthesis, *Clim. Change*, *110*, 1005–1027.

Schmidt, S., and U. Send (2007), Origin and composition of seasonal labrador sea Freshwater, *J. Phys. Oceanogr.*, *37*, 1445–1454.

Swift, J. H., E. P. Jones, K. Aagaard, E. C. Carmack, M. Hingston, R. W. Macdonald, F. A. McLaughlin, and R. G. Perkin (1997), Waters of the Makarov and Canada basins, *Deep Sea Res., Part II*, *44*(8), 1503–1529.

Syed, T. H., J. S. Famiglietti, D. P. Chambers, J. K. Willis, and K. Hilburn (2010), Satellite-based global-ocean mass balance estimates of inter-annual variability and emerging trends in continental freshwater discharge, *Proc. Natl. Acad. Sci. U.S.A.*, doi:10.1073/pnas.1003292107.

Thompson, D. W. J., and J. M. Wallace (1980), The Arctic Oscillation signature in the wintertime geopotential height and temperature fields, *Geophys. Res. Lett.*, *25*, 1297–300.

Thomas, H., A. E. F. Prowe, I. D. Lima, S. C. Doney, R. Wanninkhof, R. J. Greatbatch, U. Schuster, and A. Corbière (2008), Changes in the North Atlantic Oscillation influence CO_2 uptake in the North Atlantic over the past 2 decades, *Global Biogeochem. Cycles*, *22*, GB4027, doi:10.1029/2007GB003167.

Thrush, S. F., J. E. Hewitt, V. J. Cummings, J. I. Ellis, C. Haton, A. Lohrer, and A. Norkko (2004), Muddy waters: Elevating sediment input to coastal and estuarine habitats, *Front. Ecol. Environ.*, *2*, 299–306.

Timmermans, M. L., A. Proshutinsky, R. A. Krishfield, D. K. Perovich, J. A. Richter-Menge, T. P. Stanton, and J. M. Toole (2011), Surface fresh-ening in the Arctic Ocean's Eurasian Basin: An apparent consequence of recent change in the wind-driven circulation, *J. Geophys. Res.*, *116*, C00D03, doi:10.1029/2011JC006975.

Timmermans, M. L., S. Cole, and J. Toole (2012), Horizontal density structure and restratification of the Arctic Ocean Surface Layer, *J. Phys. Oceanogr.*, *42*(4), 659–668, doi:10.1175/JPO-D-11-0125.1.

Timmermans, M.-. L., A. Proshutinsky, E. Golubeva, J. M. Jackson, R. Krishfield, M. McCall, and G. Platov (2014), Mechanisms of Pacific Summer Water variability in the Arctic's central Canada Basin, *J. Geophys. Res. Oceans*, *119*, 7523–7548, doi:10.1002/2014JC010273.

Toole, J. M., M. L. Timmermans, D. K. Perovich, R. A. Krishfield, A. Proshutinsky, and J. A. Richter-Menge (2010), Influences of the ocean surface mixed layer and thermohaline stratification on Arctic Sea ice in the central Canada Basin, *J. Geophys. Res.*, *115*, C10018, doi:10.1029/2009JC005660.

Toole, J. M., R. A. Krishfield, M.-L. Timmermans, and A. Proshutinsky (2011), The ice-tethered profiler: Argo of the Arctic, *Oceanography*, *24*(3), 126–135.

Torres-Valdés, S., T. Tsubouchi, S. Bacon, A. C. Naveira-Garabato, R. Sanders, F. A. McLaughlin, B. Petrie, G. Kattner, K. Azetsu-Scott, and T. E. Whitledge (2013), Export of nutrients from the Arctic Ocean, *J. Geophys. Res. Oceans*, *118*, 1625–1644, doi:10.1002/jgrc.20063.

Tremblay, J. E., and J. Gagnon (2009), The effects of irradiance and nutrient supply on the productivity of Arctic waters: A perspective on climate change, in *Influence of Climate Change on the Changing Arctic and Subarctic Conditions*, edited by C. J. Nihoul and A. G. Kostianoy, pp. 73–92, Springer Science, Berlin.

Tremblay, J. É., L. G. Anderson, P. Matrai, P. Coupel, S. Bélanger, C. Michel, and M. Reigstad (2015), Global and regional drivers of nutrient supply, primary production and CO_2 drawdown in the changing Arctic Ocean, *Prog. Oceanogr.*, doi:10.1016/j.pocean.2015.08.009.

Tsamados, M., D. L. Feltham, D. Schroeder, D. Flocco, S. L. Farrell, N. T. Kurtz, S. W. Laxon, and S. Bacon (2014), Impact of variable atmospheric and oceanic form drag on simulations of Arctic sea ice, *J. Phys. Oceanogr.*, *44*, 1329–1353, doi:10.1175/JPO-D-13-0215.1.

Tsubouchi, T., S. Bacon, A. C. Naveira Garabato, Y. Aksenov, S. W. Laxon, E. Fahrbach, A. Beszczynska-Möller, E. Hansen, C. M. Lee, and R. B. Ingvaldsen (2012), The Arctic Ocean in summer: A quasi-synoptic inverse estimate of boundary fluxes and water mass transformation, *J. Geophys. Res.*, *117*, C01024, doi:10.1029/2011JC007174.

Tucker, W. B. J. W., D. T. Weatherly, L. D. F. Eppler, and D. L. Bentley (2001), Evidence for rapid thinning of sea ice in the western Arctic Ocean at the end of the 1980s, *Geophys. Res. Lett.*, *28*(14), 2851–2854.

van den Broeke, M., J. Bamber, J. Ettema, E. Rignot, E. Schrama, W. J. van de Berg, E. van Meijgaard, I. Velicogna, and B. Wouters (2009), Partitioning recent Greenland mass loss, *Science*, *326*(5955), 984–986, doi:10.1126/science.1178160.

Vaughan, D. G., et al. (2013), Observations: Cryosphere, in *Climate Change 2013: The Physical Science Basis. Contribution of Working Group I to the Fifth Assessment Report of the Intergovernmental Panel on Climate Change*, edited by T. F. Stocker et al., pp. 102, Cambridge Univ. Press, Cambridge, U. K., and New York.

Vavrus, S. J., M. M. Holland, A. Jahn, D. Bailey, and B. A. Blazey (2012), Twenty-first-century Arctic climate change in CCSM4, *J. Clim.*, *25*, 2696–2710.

Vellinga, M., and R. A. Wood (2002), Global climatic impacts of a collapse of the Atlantic thermohaline circulation, *Clim. Change*, *54*, 251–267, doi:10.1023/A:1016168827653.

Vihma, T. (2014), Effects of Arctic sea ice decline on weather and climate: A review, *Surv. Geophys.*, *35*, 1175–1214, doi:10.1007/s10712-014-9284-0.

von Appen, W.-J., and R. S. Pickart (2012), Two configurations of the western Arctic shelfbreak current in summer, *J. Phys. Oceanogr.*, *42*, 329–351, doi:10.1175/JPO-D-11-026.1.

Vösömarty, C. J., A. D. McGuire, and J. E. Hobbie (Eds.) (2011), *Scaling Studies in Arctic Systems Science*; A Call to Research, pp. 76, USARC (Report to the United States Arctic Research Commission).

Wagner, A., G. Lohmann, and M. Prange (2011), Arctic river discharge trends since 7 ka BP, *Global Planet. Change*, *79*, 48–60.

Wallace, J. M., I. M. Held, D. W. J. Thompson, K. E. Trenberth, and J. E. Walsh (2014), Global warming and winter weather, *Science*, *343*, 739–730.

Wassmann, P., and T. Lenton (2012), Arctic tipping points in the Earth System perspective, *AMBIO*, *41*(1), 1–9.

Wassmann, P., et al. (2015), The contiguous domains of Arctic Ocean advection: trails of life and death, *Prog. Ocean.*, doi:10.1016/j.pocean.2015.06.011.

Watanabe, E., and H. Hasumi (2009), Pacific water transport in the western Arctic Ocean simulated by an eddy-resolving coupled sea ice-ocean model, *J. Phys. Oceanogr.*, *39*(9), 2194–2211, doi:10.1175/2009JPO4010.1.

Weingartner, T. J., S. Danielson, S. Yasunori, V. Pavlov, and M. Kulakov (1999), The Siberian Coastal Current: A wind- and buoyancy-forced Arctic coastal current, *J. Geophys. Res.*, *104*(12), 29,697–29,713, doi:10.1029/1999JC900161.

White, D., et al. (2007), The Arctic freshwater system: Changes and impacts, *J. Geophys. Res.*, *112*, G04S54, doi:10.1029/2006JG000353.

Williams, W. J., and E. C. Carmack (2015), The 'interior' shelves of the Arctic Ocean: Physical oceanographic setting, climatology and effects of sea-ice retreat on cross-shelf exchange, *Prog. Oceanogr.*, doi:10.1016/j.pocean.2015.07.008.

Williams, W. J., H. Melling, E. C. Carmack, and R. G. Ingram (2008), Kugmallit Valley as a conduit for cross-shelf exchange on the Mackenzie Shelf in the Beaufort Sea, *J. Geophys. Res.*, *113*, C02007, doi:10.1029/2006JC003591.

Wood, K. R., J. E. Overland, S. A. Salo, N. A. Bond, W. J. Williams, and X. Dong (2013), Is there a new normal in the Beaufort Sea?, *Polar Res.*, *32*, 19,552.

Woodgate, R. A., K. Aagaard, and T. J. Weingartner (2006), Interannual changes in the Bering Strait fluxes of volume, heat and freshwater between 1991 and 2004, *Geophys. Res. Lett.*, *33*, L15609, doi:10.1029/2006GL026931.

Woodgate, R. A., T. J. Weingartner, and R. Lindsay (2012), Observed increases in Bering Strait oceanic fluxes from the Pacific to the Arctic from 2001 to 2011 and their impacts on the Arctic Ocean water column, *Geophys. Res. Lett.*, *39*, L24603, doi:10.1029/2012GL054092.

Woodgate, R., K. Aagaard, R. Muench, J. Gunn, G. Björk, B. Rudels, A. T. Roach, and U. Schauer (2001), The Arctic Ocean boundary current along the Eurasian slope and the adjacent Lomonosov Ridge: Water mass properties, transports and transformations from moored instruments, *Deep Sea Res., Part I*, *48*, 1757–1792.

Woollings, T., J. M. Gregory, J. G. Pinto, M. Reyers, and D. J. Brayshaw (2012), Response of the North Atlantic storm track to climate change shaped by ocean–atmosphere coupling, *Nat. Geosci.*, *5*, 313–317, doi:10.1038/ngeo1438.

Wrona, F. J., M. Johansson, J. M. Culp, A. Jenkins, J. Mård, I. H. Myers-Smith, T. D. Prowse, W. F. Vincent, and P. A. Wookey (2016), Transitions in Arctic ecosystems: Ecological implications of a changing hydrological regime. *J. Geophys. Res. Biogeosci.*, *121*, doi:10.1002/2015JG003133.

Yamamoto-Kawai, M., N. Tanaka, and S. Pivovarov (2005), Freshwater and brine behaviors in the Arctic Ocean deduced from historical data of δ^{18}O and alkalinity (1929–2002 A.D.), *J. Geophys. Res.*, *110*, C10003, doi:10.1029/2004JC002793.

Yamamoto-Kawai, M., E. C. Carmack, and F. A. McLaughlin (2006), Nitrogen balance and Arctic throughflow, *Nature*, *443*, 43.

Yamamoto-Kawai, M., F. A. McLaughlin, E. C. Carmack, S. Nishino, and K. Shimada (2008), Freshwater budget of the Canada Basin, Arctic Ocean, from salinity, δ^{18}O, and nutrients, *J. Geophys. Res.*, *113*, C01007, doi:10.1029/2006JC003858.

Yamamoto-Kawai, M., F. A. McLaughlin, E. C. Carmack, S. Nishino, K. Shimada, and N. Kurita (2009), Surface freshening of the Canada Basin, 2003–2007: River runoff versus sea ice meltwater, *J. Geophys. Res.*, *114*, C00A05, doi:10.1029/2008JC005000.

Yamamoto-Kawai, M., F. A. McLaughlin, and E. C. Carmack (2011), Effects of ocean acidification, warming and melting of sea ice on aragonite saturation of the Canada Basin surface water, *Geophys. Res. Lett.*, *38*, L03601, doi:10.1029/2010GL045501.

Yamamoto-Kawai, M., F. McLaughlin, and E. Carmack (2013), Ocean acidification in the three oceans surrounding northern North America, *J. Geophys. Res. Oceans*, *118*, 6274–6284, doi:10.1002/2013JC009157.

Zhang, J., and D. A. Rothrock (2003), Modeling global sea ice with a thickness and enthalpy distribution model in generalized curvilinear coordinates, *Mon. Weather Rev.*, *131*, 845–861.

Zhang, X., J. He, J. Zhang, I. Polyakov, R. Gerdes, J. Inoue and P. Wu (2012), Enhanced poleward moisture transport and amplified northern high-latitude wetting trend, *Nat. Clim. Change*, doi:10.1038/NCLIMATE1631.

Zhao, M., M. L. Timmermans, S. Cole, R. Krishfield, A. Proshutinsky, and J. Toole (2014), Characterizing the eddy field in the Arctic Ocean halocline, *J. Geophys. Res. Oceans*, *119*, 8800–8817, doi:10.1002/2014JC010488.